

ESTIMATING SYMMETRY/ASYMMETRY IN  
THE HUMAN TORSO:  
A NOVEL COMPUTATIONAL METHOD

By

MAHENDRAN BALASUBRAMANIAN

Bachelor of Technology in Fashion Technology  
Anna University, Tamilnadu, India  
2007

Master of Science in Apparel design  
Auburn University  
Auburn, Alabama  
2009

Submitted to the Faculty of the  
Graduate College of the  
Oklahoma State University  
in partial fulfillment of  
the requirements for  
the Degree of  
DOCTOR OF PHILOSOPHY  
July, 2016

ESTIMATING SYMMETRY/ASYMMETRY IN  
THE HUMAN TORSO:  
A NOVEL COMPUTATIONAL METHOD

Dissertation Approved:

Dr. Kathleen Robinette

---

Dissertation Adviser

Dr. Semra Peksoz

---

Dr. Adriana Petrova

---

Dr. Bruce Benjamin

---

Dedicated to my parents  
T. Balasubramanian & K. Santha

Name: Mahendran Balasubramanian

Date of Degree: July, 2016

Title of Study: ESTIMATING SYMMETRY/ASYMMETRY IN THE HUMAN  
TORSO: A NOVEL COMPUTATIONAL METHOD

Major Field: Apparel Design and Production

Abstract: Asymmetry in human body has largely been based on bilateral traits and/or subjective estimates, with potential usage in fields such as medicine, rehabilitation and apparel product design. In case of apparel, asymmetry in human body has been measured primarily by estimating differential linear measurement of bilateral traits. However, the characteristics of asymmetry can be better understood and be useful for clinicians and designers if it is quantified by considering the whole 3D surface. To address the prevailing issues in measuring asymmetry objectively, this research attempts to develop a novel method to quantify asymmetry that is robust, effective and non-invasive in operation. The method discussed here uses 3D scans of human torso to estimate asymmetry as a numerical index. Furthermore, using skeletal landmarks, twist and tilt measurements of the torsos are computed numerically. Together, these three measures can characterize the asymmetric/symmetric nature of a human torso. The approach taken in this research uses cross sections of torso to estimate local plane of symmetry that equi-divides a given cross section on the basis of its area, and connecting those planes to form a global surface that divides the torso volumetrically. The computational approach in estimating the area of cross section is based on the Green's theorem. The developed method was validated by both testing it on a known geometric model and by comparing the estimated index with subjective ratings by experts. This method has potential applications in various fields requiring characterizing asymmetry i.e., in case of scoliosis patients as diagnostic tool or an evaluation metric for rehabilitation efficiency, for body builders, and fashion models as an evaluation tool.

## ABSTRACT [IN TAMIL]

### ஆய்வுச்சுருக்கம்

மனித உடல் பரிணாம வளர்ச்சியில் முன்னேற்றம் அடைந்த ஒரு உருவமாக அறியப்படுகிறது. அதன் வலது மற்றும் இடது புற தோற்றமானது காண்பதற்கு ஏறத்தாழ ஒரே மாதிரியாக உள்ளது. மனித உடலினை வலது இடதாக இரு கூறாக்கினால் அவை தோராயமாக ஒன்று மற்றொன்றின் பிம்பமாக இருக்கும். ஆயினும், அவைகளின் பிம்பங்கள் எந்த அளவுக்கு ஒத்திருக்கின்றன என்பதனை அளவீடு செய்ய துல்லியமான கணக்கீட்டு முறைகள் தற்போது இல்லை. மேலும், நோய் தாக்குதலினால் ஏற்படும் தண்டுவட முறுக்கம் காரணமாக உடலில் தோன்றும் சமமற்ற தன்மையினை அளவீடு செய்வதற்கும் கூட துல்லியமான மற்றும் எளிமையான முறைகள் ஏதும் பயன்பாட்டில் இல்லை.

இந்த ஆய்வில், முப்பரிமாண மனித உருவத்தினை இரு சமமான கூறாக பிரிப்பதற்கு தேவையான கணித மற்றும் கணினி தொழில்நுட்ப முறைகளை உருவாக்கி உள்ளோம். இம்முறைகளை பயன்படுத்தி மனித உருவங்களில் உள்ள வலது-இடது சமச்சீர்/சமச்சீற்ற தன்மை, உடல் பகுதியில் உள்ள வளைவுத்தன்மை மற்றும் திருகுத்தன்மை ஆகியவற்றினை அளவீடு செய்துள்ளோம்.

மனித உருவங்கள் முப்பரிமாண வருடியின் துணைகொண்டு கணினிசார் வடிவங்களாக உள்வாங்கப்பட்டன. பின்னர், அவற்றின் உடம்புப்பகுதிகள் மட்டும் தனியாக கொணரப்பட்டு ஆய்விற்கு உட்படுத்தப்பட்டன. ஒவ்வொரு உடம்புப்பகுதியும் கீழிருந்து மேலாக பல குறுக்குவெட்டு தோற்றமாக பகுக்கப்பட்டன. பின்னர் குறுக்குவெட்டு பகுதிகளின் பரப்பளவினை ஒரு பகுப்புக்கோட்டின் மூலம் இடம்-வலமாக இரு சமபாகங்களாக பிரிக்கப்பட்டன. இவ்வாறாக ஒவ்வொரு குறுக்கு வெட்டு தோற்றத்திற்கும் உள்ள பகுப்புக்கோடுகளை இணைப்பதன் மூலமாக மொத்த உடலினையும் இரு சமமான கொள்ளளவாக பிரிக்க இயலும்.

அடுத்ததாக இவ்விரு பாகங்களும் பரப்பளவில் ஒத்திருந்தாலும் வடிவத்தில் ஒத்துப்போகாமல் இருக்கக்கூடும். இந்த வடிவ வித்தியாசங்களை அளவீடு செய்ய ஒவ்வொரு குறுக்குவெட்டு தோற்றத்தின் இடது மற்றும் வலது வடிவங்கள் ஒன்றின் மேல் மற்றொன்றாக பிரதிபலிக்கப்பட்டன. அவ்வாறாக செய்யும் போது வடிவ ஒற்றுமை இல்லாத பரப்பளவுகளை எளிதாக அளவிட முடியும். மாறுபட்ட உருவ அமைப்பினை கொண்ட 30 மனித உருவங்களை இந்த ஆய்வில் பயன்படுத்தி அவைகளின் உருவ குணங்களை அளவிட்டுள்ளோம்.

இந்த ஆய்வில் உருவாக்கப்பட்டுள்ள கணக்கீட்டு முறைகள் மருத்துவம், ஆயத்த ஆடை வடிவமைத்தல் மற்றும் உடற்பயிற்சி மேம்பாடு ஆகிய துறைகளுக்கு மிகவும் பயனுள்ளதாக அமையும்.

## TABLE OF CONTENTS

| Chapter  | Page |
|--|------|
| I. INTRODUCTION.....   | 1    |
| Purpose Statement.....   | 4    |
| Significance of the Work .....                                     | 4    |
| Research Questions.....  | 6    |
| II. LITERATURE REVIEW.....   | 7    |
| Classes of Symmetry.....   | 7    |
| Bilateral Symmetry .....   | 9    |
| Measuring matched symmetry .....                                   | 10   |
| One or two dimensional approaches for asymmetry estimation.....    | 10   |
| Three dimensional approaches for asymmetry estimation.....         | 17   |
| Measuring object symmetry.....                                     | 23   |
| Estimating symmetry in geometrical space .....                     | 27   |
| Estimating symmetry in a transformed space .....                   | 29   |
| Asymmetry Measurement in Clinical and Pathological Studies.....    | 33   |
| Summary of Limitations in the Existing Techniques/Approaches ..... | 36   |
| III. METHODOLOGY .....   | 37   |
| Data sampling .....  | 38   |
| Data Characteristics .....   | 39   |
| Pre-processing of the Data Models.....                             | 40   |
| Defining Orientation of the Torso.....                             | 41   |
| Determining the Line of Symmetry .....                             | 47   |
| Computing the Area of Closed Surface .....                         | 48   |
| Estimating the Plane of Symmetry .....                             | 49   |
| Estimating the Asymmetry Index .....                               | 49   |
| Estimating Deviance from the Principal Axis .....                  | 50   |
| Estimating the Degree of Twist and Tilt in Torso .....             | 51   |
| Validation of the Developed Method.....                            | 53   |
| Known Geometry Validation.....                                     | 53   |
| Subjective Evaluation .....  | 54   |

| Chapter   | Page |
|---|------|
| IV. RESULTS .....   | 57   |
| Descriptive Statistics of the Sample Population .....         | 57   |
| Preprocessing of the Torso.....                               | 58   |
| Optimization of Cross-sections Extracted Per Torso .....      | 58   |
| Estimation of Asymmetry Index .....                           | 61   |
| Estimating the local and global lines of symmetry .....       | 61   |
| Estimation of Asymmetry Index .....                           | 67   |
| Estimation of Torso Twist and Tilt.....                       | 68   |
| Estimation of Deviance from the Principal Axis .....          | 71   |
| Validation of the Developed Method.....                       | 72   |
| Known Geometry Validation.....                                | 73   |
| Validation by Comparison With Subjective Expert Ratings ..... | 74   |
| Relationship between Variables.....                           | 76   |
| V. DISCUSSIONS .....  | 78   |
| Generalizability of the Method .....                          | 80   |
| Characteristics of the Findings.....                          | 81   |
| Findings of the Objective measure .....                       | 81   |
| Findings on the Validation.....                               | 83   |
| Applicability of the Method.....                              | 84   |
| Application to Apparel Field .....                            | 84   |
| Application to Medicine/Rehabilitation.....                   | 86   |
| V. CONCLUSIONS.....   | 89   |
| Summary .....   | 90   |
| Future Recommendations .....                                  | 91   |
| REFERENCES .....  | 92   |
| APPENDICES .....  | 104  |

## LIST OF TABLES

| Table   | Page |
|---|------|
| 2.1. Metrics for Object Symmetry and definition .....                                 | 25   |
| 4.1. Asymmetry Indices of Male and Female Sample Population.....                      | 67   |
| 4.2. Torso Twist and Tilt of Male Sample Population.....                              | 68   |
| 4.3. Torso Twist and Tilt of Female Sample Population .....                           | 70   |
| 4.4. Deviance from the principal axis .....   | 71   |
| 4.5. Mean Asymmetry and twist ratings of three experts (Likert scale of 1 to 4) ..... | 72   |



## LIST OF FIGURES

| Figure  | Page |
|---|------|
| 2.1. Bilateral symmetry.....  | 8    |
| 2.2. Rotational symmetry.....   | 8    |
| 2.3. Translational symmetry.....  | 9    |
| 2.4. Matching and Object Symmetry.....  | 9    |
| 2.5. Widely used landmarks for facial asymmetry.....  | 17   |
| 2.6. Plane and landmark representation used to estimate facial symmetry.....  | 19   |
| 2.7. Facial soft tissue asymmetry indices in normal adults plotted as 2D areal plot for each facial landmark.....   | 19   |
| 2.8. Semi-transparent 3D CT images showing facial surface and landmarks.....  | 20   |
| 2.9. Facial asymmetry index chart.....  | 21   |
| 2.10. Landmarks defining the breast location and the mirror plane.....  | 23   |
| 2.11. Symmetry detection for curved boundaries using polygonal approximation. Using the segment, local axes of symmetry were formed to estimate the global axes of symmetry.....            | 27   |
| 2.12. Cephalometric landmarks.....  | 31   |
| 2.13. Symmetry estimation on a 3D surface using stochastic clustering.....  | 32   |
| 2.14. Estimating symmetry using rigid geometry and extrapolating regions of matched symmetry.....   | 32   |
| 3.1. Schematic representation of the sample selection.....  | 40   |
| 3.2. Schematic representation of the processes of orientation of the torso, extraction of the cross sections, estimating the local plane of symmetry and computing the asymmetry index..... | 43   |
| 3.3. Location of the key anatomical landmarks used in this research.....  | 45   |
| 3.4. a) Planes depicting the location of dissections and torso extraction;b) Sample torso models.....   | 46   |
| 3.5. Schematic of the process of axes orientation and alignment. The local coordinate axes are rotated to align them with the global axes shown on the most left.....                       | 47   |
| 3.6. Computing the ROI. A typical Cross-section (left) was mirrored (middle), and the area corresponding to the region of interest (right) was computed.....                                | 50   |

|  |    |
|--|----|
| 3.7. Torso landmarks for Twist and Tilt computation; Top row: Definition of upper and lower torso; Middle row: Top view of torso with connected landmark lines; Bottom row: Angle calculation for torso and tilt.....  | 52 |
| 3.8. Cross-section of a 3d cylinder CAD model.....   | 54 |
| 3.9. Sample Images of a female subject presented for subjective ratings by apparel experts.....  | 56 |
| 4.1. Illustration of the rotation and aligning process. The torso on the top panel was subjected to rotation in all the three principal axes such that the final orientation is in alignment with the global reference frames. The oriented torso was used to define the sides (front, back, right and left).....  | 59 |
| 4.2. Plot shows the number of slices per torso and the improvement in the values of the estimated AI. Top panel was for the male torso models and the bottom panel corresponds to the female torso models.....   | 60 |
| 4.3. Typical cross sections and the local line of symmetry is shown. The left panel was from a male subject torso with less asymmetry and the right panel shows a cross section from a female subject model affected by scoliosis. It is visibly distinguishable and the shapes are not evenly distributed.....  | 61 |
| 4.4. Schematic representation of the sliding plane on a typical cross section is shown. The area of the closed contour formed by the sliding plane in conjunction with the surface contour was computed at each step and compared with the overall area of the cross section to determine the local plane of symmetry. The progression is shown with a coarse resolution here..... | 62 |
| 4.5. Top) shows the global line of symmetry overlaid on the torso model for a male subject with minimal asymmetry (AI of 5.55). (Bottom) shows the same for a female subject affected by scoliosis (AI of 24.92). The middle panels show the top view, and the spread of the plane of symmetry is higher for the scoliosis subject compared to the healthy subject.....            | 63 |
| 4.6. The global line of symmetry overlaid with the torso cross sections for the fifteen male subjects are shown here.....  | 64 |
| 4.7. The global line of symmetry overlaid with the torso cross sections for the fifteen female subjects are shown here.....  | 65 |
| 4.8. Schematic of the process of mirroring and the computation of ROI is shown here. The top panels show mirrored layout of chosen cross sections extracted from a single torso. The bottom panels show the ROI in square inches for those.....  | 66 |
| 4.9. The global plane of asymmetry on the known geometry is a single plane that runs through the centroid of the object.....   | 74 |
| 4.10. Relationship between the six variables – Weight, AI-obj, AI-sub, TT-obj, TT-sub and Tilt. The numbers within each panel shows the corresponding correlation values (red colored numbers are significant at an alpha of 0.05).....  | 77 |
| 5.1. (Left) shows the principal axes obtained from an individual cross section and (right) shows the principal axes estimated for the entire 3D object.....  | 79 |

## LIST OF TERMS AND ABBREVIATIONS

**Asymmetry:** lack of similarity between right and left side of the human torso, specifically in the sagittal plane.

**3D Scan/ 3D digital representation:** 3D data point of real human scanned using 3D body scanner.

**Torso:** 3D scan of the upper part of the body from the Cervicale to the Crotch-level, and with hands removed at Axilla point posterior left and right

**Twist:** Rotation of the torso along the transverse plane

**Tilt:** Lateral bending of the torso along the coronal plane

**ROI** - Region of Interest

**CAESAR** - Civilian American and European Surface Anthropometric Resource

**AI** - Asymmetry index in percentage by the developed method

**ISPR** - Iliac Spine posterior right

**ISPL** - Iliac Spine posterior left

**ACR** - Acromion right

**ACL** - Acromion left

**RTR** - Right tenth rib

**LTR** - Left tenth rib

## CHAPTER I

### Introduction

Symmetry is often defined as “*the quality of something that has two sides or halves that are the same or very close in size, shape, and position: the quality of having symmetrical parts*” (Merriam-Webster’s online dictionary, n.d.). In biological entities, symmetry is considered a prevalent feature, and an essential characteristic for navigational and other survival mechanisms. Humans are considered, more-or-less, bilaterally symmetric. However, several micro and macro factors perturb the symmetric nature in humans and other living organisms. Factors that could contribute to departure from symmetry includes, habitats with high population density, noise, nutritional stress (Gary and Marlowe, 2002), handedness, biomechanical pressure (Ruff, Holt & Trinkaus, 2006), high temperature (Zakharov, 1989), infections (Moller, 1996) and genetic issues (Townsend, 1987). The degree of symmetry, or asymmetry *per se*, varies from visually non-distinguishable (i.e, highly symmetric) to extremely noticeable (or, highly asymmetric as in the cases of Scoliosis). Quantification of the degree of symmetry is needed in several clinical and pathological analyses, in addition to developmental and genetic theorizations.

Characterizing the symmetric nature of human body is typically performed by (a) comparing individual components on either sides of a virtual plane, i.e., length of right vs left arm and (b) comparing the area or volume on either sides of a plane, i.e., volume of right vs left brain hemispheres. The former is often referred as match symmetry, while the latter is called object symmetry. Several techniques exist to characterize the degree of symmetry in both the categories. However, they are limited in terms of their applicability measuring symmetry in three-dimensional (3D) torso objects. The match symmetry methods rely on specific landmarks and componentized measurements, and are not suitable to measure symmetry in a 3D volume. The object symmetry techniques exist for two dimensional (2D) images and 3D volumes, but are landmark-dependent. Most of the studies rely on anatomical landmark to determine the mid-sagittal plane, and the process of estimating the mid-sagittal plane is often debated (Willing, Roumeliotis, Jenkyn, & Yazdani, 2013). Furthermore, there is no existing method that can quantify the degree of symmetry on a digital 3D torso that is also independent of anatomical landmarks.

In this study, a novel characterization technique was developed to detect and quantify symmetry/asymmetry of male and female 3D torsos. The developed method determines a plane/surface of symmetry using an iterative process along the sagittal orientation (see Chapter-3). Essentially, the 3D space was segmented in the transverse plane, and each cross-sectional slice was computationally analyzed to determine the local line of symmetry. This line marks the local sagittal plane that equi-divides the given slice based on its cross-sectional area. The estimated plane of symmetry for multiple slices chosen from the torso provides the global line of symmetry. The equi-divided slices despite having equal areas on both sides can vary highly in their shapes. In the subsequent

process, the difference in the shape (expressed as non-matching areas between the two halves) was computed numerically, and this forms the basis to quantify the degree of asymmetry. Furthermore, this study also calculated the twist and tilt present in the 3D torsos.

The key advantages of the developed method in comparison to the existing techniques are,

- (i) the asymmetry line and the asymmetry index are independent of anatomical landmark, and is applicable for natural posture and orientation,
- (ii) it is generalizable enough such that it can estimate symmetry in any of the three major axes, i.e., sagittal, coronal and transverse planes,
- (iii) the method does not require exposure to radiations like X-ray or computerized tomography (CT) scan and
- (iv) the indices derived are combination of both surface based (Asymmetry Index) and skeletal based (Torso twist and tilt) characteristics. In this work, torso twist is defined as the axial rotation of the torso along the transverse plane and the torso tilt is defined as the lateral deviation in the torso along the coronal plane.

The developed method was validated using two approaches, (i) by estimating the asymmetry for a perfectly known symmetrical geometry and (ii) by comparing the developed measure with subjective ratings of apparel experts. The former would validate whether the measure is capable of classifying a symmetric body as “Symmetric”, and the

latter approach would validate whether the measure is capable of detecting asymmetry comparable to or better than expert ratings.

### **1.1 Purpose Statement**

The main objectives of this research are,

1. To develop a novel method to estimate the degree of asymmetry in human body that can primarily serve as a characterization and an evaluation tool
  - To develop a computational algorithm for estimating a plane/surface of symmetry for a 3D human torso
  - To objectively quantify the degree of asymmetry and develop an asymmetry index (AI)
2. To develop a method to quantify the twist and tilt in human torso
3. To determine the degree of asymmetry and torso twist using visual ratings of field experts
4. Validate the developed method by comparing the estimated measures with the visual ratings of field experts

### **1.2 Significance of the Work**

Symmetry is an important factor in several fields, i.e., attractiveness, biomechanics modeling, body building, evolution science, functional clothing, growth developmental theory, physical therapy and rehabilitation, and physiology. Apparel field can benefit from this information towards evaluating the functional clothing systems such as physical therapy braces, exo-skeletons and other assistive devices that offer better fit and embodiment. Influence of constant load-bearing activities such as school backpack on

spinal deformation (Drzał-Grabiec, Snela, Rachwał, Podgórska & Rykała, 2014) can be quantified and design suggestions can be provided for optimal encumbrance. Symmetry characterization can help develop a database that establishes distribution of symmetry/asymmetry across different populations based on geophysical location, clinical conditions and economic backgrounds. Clinically, asymmetry of the torso serves as a strongest indicator for further investigation regarding scoliosis among school children (Bunnell, 1984). The proposed method is computationally efficient and can be used for rapid symmetry characterizations needed for the above-said applications. Besides, this method can be used to make planning on pre-operative procedure and for following up the progress post-operatively. It is possible to include this method as a component in virtual fit evaluating software utilities, and can serve as a coefficient in customizing the product.

This research will provide metrics (a.k.a, index) that can potentially serve for any study or design where symmetry is critical. A typical application for functional clothing would be the evaluation of support braces for patients with curved spine, i.e., idiopathic scoliosis. The primary applications of the asymmetry measure are as follows,

- The natural asymmetry of a given digital human torso can be estimated
- The lower and upper bounds of asymmetry in a given sample population can be objectively measured



- Effect of asymmetry on biomechanical movements can provide additional dimension to human factors applied in bio-model development and ergonomic product development
- The indices can serve as a basis in developing anthropometric digital human models for a given degree of asymmetry
- The indices can be used to measure the degree of success in scoliosis surgery
- The indices can be used to measure the rate of rehabilitation on spine deformation
- The indices can be used to evaluate the efficiency of physical therapy braces and other exoskeleton products
- The indices can be used as an evaluation metric for body building competitions

### **1.3 Research Questions**

1. Can a method be developed to characterize asymmetry in the 3D human torso using surface topography?
2. Can a plane/surface be derived for a human torso without using anatomical landmarks?
3. Is it possible to define an objective metric that can quantify the degree of asymmetry in human torso?
4. Is it possible to quantify the degree of twist and tilt in human torso?
5. Is there a significant relationship between the asymmetry index by the developed method and the subjective or perceived asymmetry index provided by experts?

## CHAPTER II

### Literature Review

This section comprises survey of the existing body of literature pertaining to symmetry and its quantification methods. The topics being discussed here include symmetry and its classes, bilateral Symmetry, matching and object symmetry, manual and computational methods of asymmetry estimation, and clinical and pathological applications of symmetry.

#### 2.1 Classes of Symmetry

Symmetry is often defined by a virtual plane or axis that provides an estimate of spatial, angular or volumetric bifurcation measure. Various aspects of symmetry are studied in art, biology, crystallography and physics. In a two/three-dimensional space, symmetry can be classified into three major classes, i.e., (i) bilateral or reflection, (ii) radial and (iii) translational symmetry.

*Bilateral Symmetry:* If an object or spatial configuration can be bisected on a virtual midline and have equal/mirror sides then it is bilaterally symmetric. This is

the most common type of symmetry. Examples for bilateral symmetry are butterfly, scorpion, human, cube, etc.

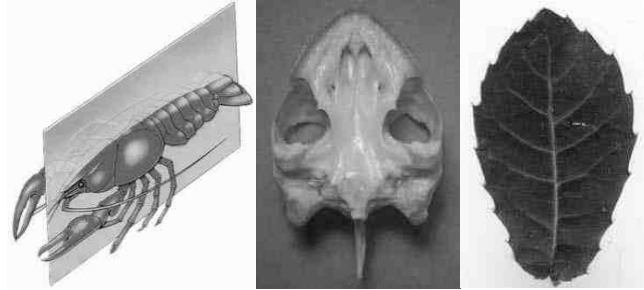


*Figure 2.1. Bilateral symmetry*

*Radial or Rotational Symmetry:* A set of pattern repeats itself in a circular configuration.

Examples include flowers and star fish.



*Figure 2.2. Rotational symmetry*

*Translational Symmetry:* If the shape or object maintains its original configuration after displacement, it is considered translational symmetry. For example, strip patterns are translational symmetric objects. (Weyl, 1952).

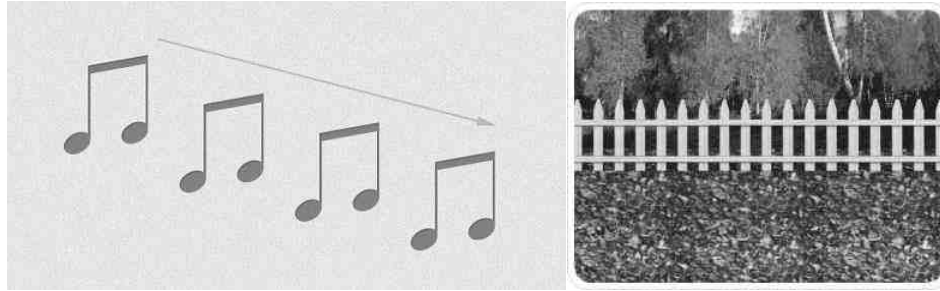


*Figure 2.3.* Translational symmetry

## **2.2 Bilateral Symmetry**

Bilateral symmetry is the most common class of symmetry. In general, a plane or line divides the object into two equal parts, i.e., one side is often the mirror image of the other side. Bilateral symmetry is further classified into object symmetry and matched symmetry. Object symmetry deals with the symmetry of single entity or object in whole, like the face or torso, whereas, matched symmetry refers to two landmarks on both sides of the plane, such as left hand and right hand. Object symmetry is considered more complex than matching symmetry (Mardia, Bookstein, & Moreton, 2000; Savriama & Klingenberg, 2011).

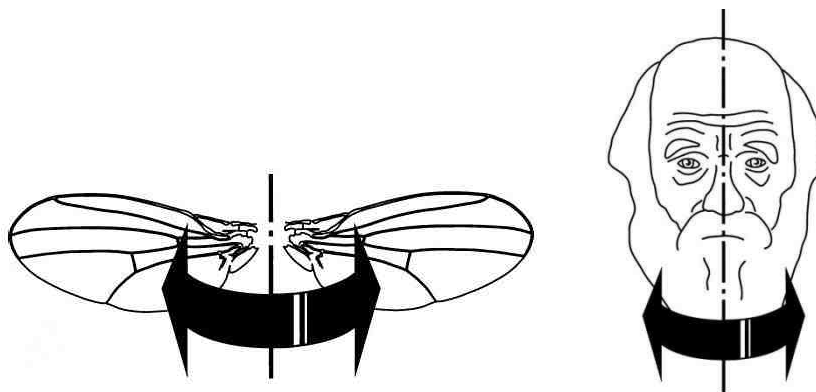


*Figure 2.4.* Matching and Object Symmetry

### **2.2.1 Measuring matched symmetry.**

Human body structure falls under the category of bilateral symmetry/asymmetry. It could be assessed for both object and matched symmetry. In case of matched symmetry, the established metrics to estimate symmetry/asymmetry are (i) fluctuating symmetry, (ii) directional asymmetry and (iii) antisymmetry. These metrics are primarily used in developmental symmetry.

*Fluctuating Symmetry:* When a population is assessed for the differences between the right and the left sides of the body for a set of traits, the distribution of the differences have a mean of zero and the variance is normally distributed.

*Directional Asymmetry:* If the differences are predominant on one side, skewing the distribution either to the right or the left, directional asymmetry is observed.

*Antisymmetry:* When the population is bimodal, meaning that there are subpopulations exhibiting both right and left asymmetry, it is referred as antisymmetry (Palmer, 1994).

Several studies have reported symmetric/asymmetric characteristics on human body using object-based measurements. Based on the method of estimation, asymmetry evaluation can be classified as (i) One or two dimensional and (ii) Three dimensional.

#### ***2.2.1.1 One or two dimensional approaches for asymmetry estimation.***

A study by Rikowski and Grammer (1999) attempted to understand the relationship between body and facial symmetry towards human body odour and attractiveness. To measure the body symmetry seven bilateral traits – hand breadth, elbow width, ear breadth, ear length, ankle width, wrist breadth and foot breadth measurement were

calculated for 16 male and 19 female subjects. They found significant difference in the between-subject variations. Fluctuating asymmetry were found for measurements ear breadth, ear length and foot breadth. The study concluded that there was no significant relationship between body asymmetry and facial attractiveness.

Anthropometric study with Kenyan distance runners by Kong and De Heer (2008) measured the leg length, calf circumference, ankle circumference for six elite athletes and found no matched bilateral difference. Additionally, they tested the strength characteristics of both legs using isometric torque and isokinetic torque ratio. Results showed no significant difference between the legs on the strength variable. Similarly, body parts asymmetry was studied on patients with partial seizure. Out of the 282 patients analyzed, 88 showed body asymmetry. Toes sizes, size of thumbs, levels of popliteal creases, levels of cubital creases, sized of forehead, temporal and maziillofacial bones and sizes of gastrocnemii were examined to analyze the body asymmetry. Body asymmetry noted in this study ranged from hemiatrophy of limbs (difference in the leg length) to atrophy involving thumb or big toe (Fong, Mak, Swartz, Walsh, & Delgado-Escueta, 2003). Similarly, asymmetry of body among white adults was examined by Schell, Johnston, Smith, and Paolone (1985). Measurements such as triceps skinfold, biepicondylar breadth, upper arm circumference, subscapular skinfold, calf circumference and bicondylar breadth-femur were measured on both right and left of the 94 males and 22 females. Significant levels of asymmetry were observed for biepicondylar breadth, upper arm circumference and triceps skinfold. Leg measurements and subscapular skinfold showed no significant differences.

Bilateral symmetry of Australian soccer and basketball players were measured by Tomkinson, Popović, and Martin (2003). Bilateral traits were recorded and analyzed for matched symmetry from a total of 52 subjects (26 basketball players and 26 soccer players). Measurements taken were categorized under skinfolds, girths, lengths and breadths. In skinfolds, triceps, subscapular, biceps, iliac crest, suprespinale, abdominal, front thigh, medial calf and mid axilla were grouped. Girth measurements taken were arm (relaxed and flexed), forearm, wrist, thigh, mid-thigh, calf and ankle. Acromiale-radiale, Radiale-styilion, Midstyilion-dactylion, Iliospinale height, Trochanterion height, Trochanterion-tibiale, laterale, Tibiale, laterale to floor, Tibiale mediale-sphyrion tibiale, Foot length, Humerus, Femur were the length and breadth measurements. Significant directional asymmetry were noted for triceps skinfold, arm-relaxed, arm-flexed, forearm, trochanterion height and humerus. However, no significant differences in asymmetry were observed between the two sport groups. Manning and Pickup (1998) explored the relationship between symmetry and running speeds among middle distance runners. For a total of 50 male subjects, measurements like 2<sup>nd</sup>, 3<sup>rd</sup>, 4<sup>th</sup>, 5<sup>th</sup> digit, wrists, nostrils and ears were recorded. Significant between-individual differences were noted for all the traits. Furthermore, they found that symmetric runners were faster than their asymmetric counterpart. Research on a tennis player population showed that the dominant hand had thick humerus for both men and women (Jones, Priest, Hayes, Tichenor, & Nagel, 1977). Likewise, another research on tennis players by Haapasalo et al . (2000) showed that the nine bilateral traits measured on the humerus had high asymmetry compared to the control group.

Significant relationship between fluctuating asymmetry and body weights were reported by Manning (1995). Bilateral traits such as ear height, wrist, length of second digit and length of fifth digit were measured for 31 adult males and 39 adult females and also for 110 children (50 males and 60 females). Results showed that there was a positive relationship between mean fluctuating asymmetry and body weight for female adults meaning that light females were more symmetric than heavy females. On the contrary, males showed negative relationship between fluctuating asymmetry and body weight meaning that heavy males were more symmetric than light males. No significant relationships between fluctuating asymmetry and body weight were found for male and female children.

Asymmetry/symmetry was examined on the body bones and skeleton as well and been observed over centuries (Arnold, 1844). In a study, adult femurs of 20 subjects (19 males and 1 female) were measured and analyzed for bilateral symmetry. Physical measurements taken on the femur were femoral length, mid-diaphysis outer diameter, neck length, neck width, intertrochanteric length. Though there were few anthropometric differences between the left and the right, no significant difference were observed between left and right femurs (Pierre, Zurakowski, Nazarian, Hauser-Kara, & Snyder, 2010).

Likewise, bilateral asymmetry was studied in the humerus and tibia bones. Both right and left humeri and tibiae of 30 males and 39 females were radiographed and then bone breadth, bone length, and bone areas were calculated. In tibia, asymmetry was small and the left tibiae were larger than the right tibiae, particularly for female. In humerus,



asymmetry was noted for both bone area and bone length. Right humeral bone area was larger than left for both sexes. However, the bilateral asymmetry decreases with increase in age for both humerus and tibia (Ruff & Jones, 1981).

A study by Hume and Montgomerie (2001) showed the relationship between facial attractiveness and the overall body asymmetry. Twenty-two traits and face photographs were taken on 94 females and 95 males. And, facial landmarks were located on the outer eye, inner eye, eye width, face, nose, cheek, mouth and jaw. The plane of symmetry for the face was calculated by the mean of the midpoints for all the width traits on face. For the body landmarks, six traits were measured at ankle, ear, elbow, foot, hand, wrist, ear length, length of index and little finger. Results showed that there was a negative relationship between facial attractiveness and overall body asymmetry for both males and females. Furthermore, attractive score was negatively related to BMI (body-mass index) for females and positively related to socioeconomic status for males.

Ozener (2010) explored the effect of heavy working conditions and socioeconomic status on the asymmetry of young males. It was reported that people living under poor conditions showed more fluctuating asymmetry than their peers living in better conditions. A total of 309 subjects were grouped into three categories based on age and socioeconomic status. Hand length, hand width, elbow width, wrist width, knee width, ankle width, foot length, foot width, ear length and ear width were measured for the subjects using digital calipers. Results showed that for all the three groups, few traits showed ideal fluctuating asymmetry. Significant directional asymmetry was reported for all the traits on upper extremities for Group-1. Group-3 showed statistically significant

directional asymmetry on foot width. Also, fluctuating asymmetry was found for the following traits in all three groups - knee width, ankle width, foot length, ear length, and ear width. In conclusion, they reported that body fluctuating asymmetry was greater for individuals with low socioeconomic status and high environmental stress.

Health complications such as low-back pain were related to asymmetry in humans. Al-Eisa, Egan, and Wassersug (2004) explored the relationship between low-back pain and asymmetry by measuring eight traits on control group (51 subjects) and back pain group (44 subjects). Bilateral traits measured were 3<sup>rd</sup> digit length, hand length, ulnar length, bistyloid breadth, tibial length, femur length, foot length, bimalleolar breadth and pelvic asymmetry. Statistical analysis showed that asymmetry of ulnar length and bistyloid breadth was significantly higher for back pain group than the control group. Also, the pelvic asymmetry was significantly higher for the back-pain group. Another study conducted by Milne et al . (2003) explored the relationship between fluctuating asymmetry and physical health of young males. The variables measured to determine the health were BMI, waist/hip ratio, systolic blood pressure, blood cholesterol, cardiorespiratory fitness and periodontal disease. Bilateral traits measured were ear breadth, ear length, wrist breadth, elbow breadth, ankle breadth and foot breadth. Results showed that the absolute asymmetry were larger for all traits and significant for ear breadth and length for males. Significant directional asymmetry was noted for all traits except wrist breadth. Regarding the relationship between fluctuating asymmetry and BMI, significant association was found for females but not for males. Further, fluctuating asymmetry is not associated with waist to hip ratio, BP, cholesterol, fitness and periodontal disease.

Some of the researches have focused on the body asymmetry of children. Study by Livshits and Kobylansky (1989) compared the fluctuating asymmetry of Israeli infants, children and adults. They reported that infants showed higher fluctuating asymmetry whereas adults showed least asymmetry. Similarly, a study on 680 English children by Wilson and Manning (1996) reported a strong negative association between fluctuating asymmetry and age. In another study on 6000 Polish children, Wolanski (1972) noted asymmetry on joint movement, hand strength and shoulder height. Research on Jamaican children by Trivers, Manning, Thornhill, Singh, and McGuire (1999) measured ten bilateral traits - 3<sup>rd</sup>, 4<sup>th</sup> and 5<sup>th</sup> digit lengths, ear size, elbow width, hand width, ankle width, wrist diameter, foot length and knee width. Results showed significant fluctuating asymmetry on all traits except hand width. Further, boys showed less fluctuating asymmetry than girls and positive relationships between fluctuating asymmetry and age, height and weight were reported.

Facial symmetry has been considered an important attractive factor and criteria for mate selection. More importantly, facial symmetry and restoration of symmetry is an important process in maxillofacial surgery. Investigations on symmetry play an important role in planning of operations and evaluation of different surgical procedures like cleft lip and palate (Bashour, 2006). Typically, facial symmetry analysis uses identification of landmarks on the face and the linear/angular measurements measured bilaterally. The most widely used landmarks are shown in the figure 2.5 (Berlin et al., 2014).

Relationship between facial and body fluctuating asymmetry and facial masculinity/femininity in men and women was examined by Koehler, Simmons, Rhodes, and Peters (2004). Photographs of males were rated by female for masculinity and vice

versa. Linear measurements taken on the face to measure the fluctuating asymmetry were eyebrow height, cheekbone width, jaw width and lower face length. Seven bilateral traits measured on the body were ear length, ear width, ankle width, wrist width, elbow width, foot width and foot length. They found no significant correlation between facial masculinity and asymmetry for males whereas facial femininity was associated with body asymmetry.

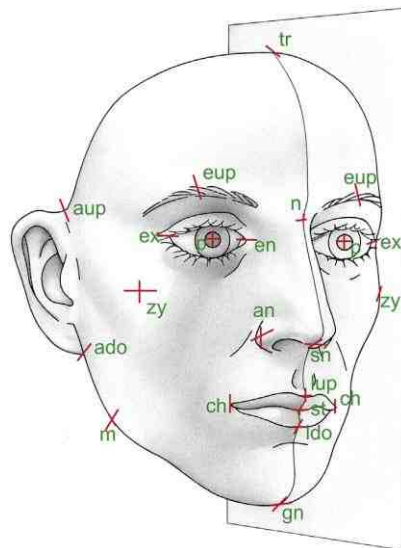


*Figure 2.5. Widely used landmarks for facial asymmetry*

The methods relied on the bilateral traits or paired landmarks. None of the methods discussed so far are landmark-independent and applicable for torso asymmetry.

### ***2.2.1.2 Three dimensional approaches for asymmetry estimation.***

A 3D analysis of bilateral directional asymmetry was performed on human clavicle bone. A statistical bone atlas was created using the CT scans of clavicle bones from 285 males

and 220 females. Cross-sectional analysis and contour analysis were conducted to determine bilateral asymmetry. Results showed that left clavicle bones were longer than the right ones. In the muscle attachment sites, males showed significant asymmetry than females. Also, for both sexes the area with no muscle on posterior mid-shaft was significantly asymmetric (Abdel Fatah, Shirley, Mahfouz, & Auerbach, 2012).

Huang, Liu, & Chen (2013) developed a quantitative method to measure facial asymmetry, and delineate the degree of asymmetry using facial landmarks. Sixty (60) healthy Chinese subjects (30 men and 30 women) were selected and 3D scans of their facial images were obtained to derive the facial symmetry index. The subjects were qualified based on the following criteria, (1) dental occlusion angle class I, (2) no craniofacial deformity (3) no facial trauma history (4) no prior orthodontic or orthognathic surgery and (5) face classified as symmetry by an orthodontist, a plastic surgeon and a nurse. The scanned and digitized heads were fitted with three orthogonal planes and 16 landmarks were denoted (ref Figure-2.6). Eight landmarks out of the 16 were located bilaterally and the rest fell on the sagittal plane. An experienced human operator defined the planes and subsequently identified the landmarks on the digitized images. For each landmark, the asymmetry index (the Euclidean distance) was calculated with reference to the three planes. A plot was generated based on the mean and standard deviations of the asymmetry Index (AI) calculated for each landmark (ref Figure-2.7). This diagram, which is the primary outcome of this study, serves as the basis footprint for symmetric faces. Using the diagram, normal symmetry was defined by the region covering  $\text{mean} \pm 1 \text{ standard deviation (SD)}$ , asymmetry was defined as regions covering  $1 \text{ SD} < \text{AI} \leq 2 \text{ SD}$ , and any deviation  $> 2 \text{ SD}$  was defined as marked asymmetry. The

results showed that landmarks located on the upper face had smaller AI than those of the lower face landmarks. The study has thus provided a criterion to classify facial symmetry versus asymmetry based on the spatial locations of the facial landmarks.

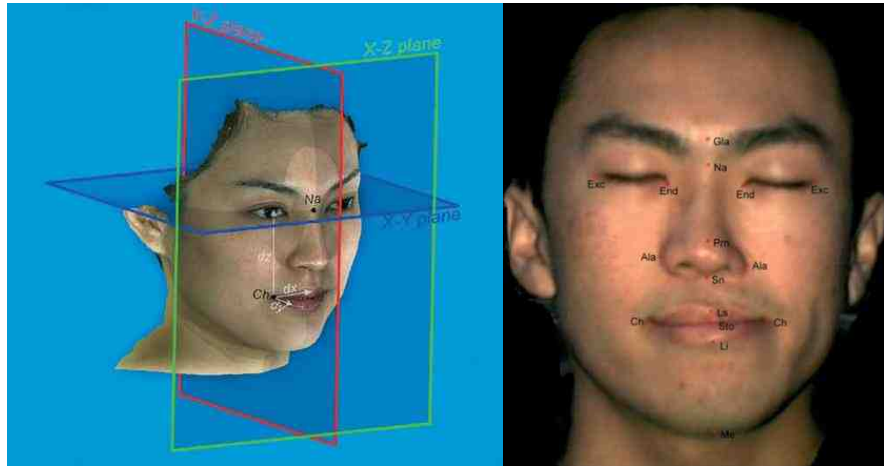


Figure 2.6. Plane and landmark representation used to estimate facial symmetry

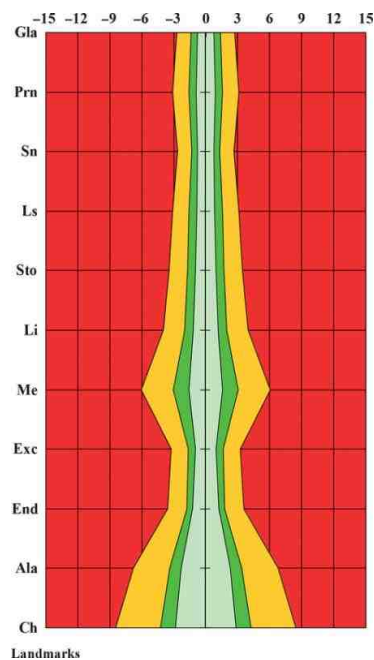
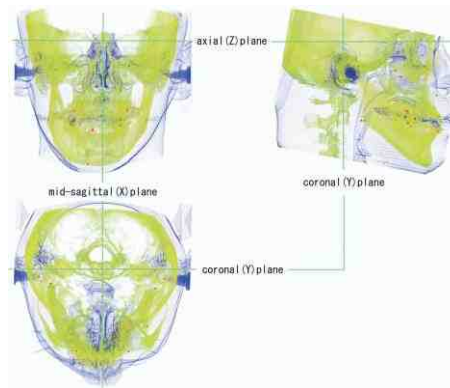
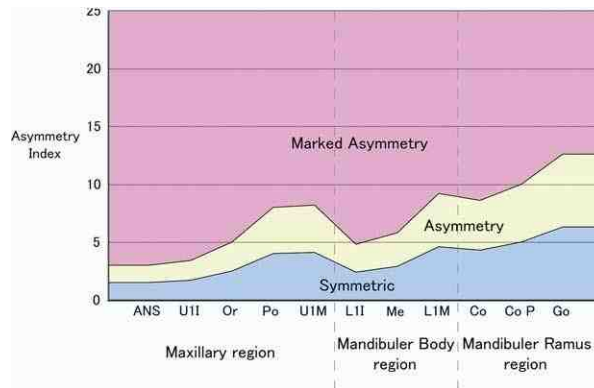


Figure 2.7. Facial soft tissue asymmetry indices in normal adults plotted as 2D areal plot for each facial landmark.

A new approach of measuring facial asymmetry using 3D computerized tomography (CT) images was developed by Maeda et al. (2006). Patients with facial deformities were compared with normal subjects. Landmarks such as sella, dent, orbitale, porion, anterior nasal spine, UII, U1M, LII, L1M, menton, condyle, gonion and superior point of coronoid were located manually on the CT images. Subsequently, semi-transparent 3D images showing facial surface, hard tissue and landmark points were generated using imaging software (ref Figure-2.8). Asymmetry index for bilateral and solitary landmarks were computed for both normal subjects and patients. A chart (ref Figure-2.9) was created comparing normal and facially asymmetric subjects. It was claimed that this new approach provided more detailed evaluation on facial asymmetry than the traditional cephalogram method.



*Figure 2.8.* Semi-transparent 3D CT images showing facial surface and landmarks



*Figure 2.9.* Facial asymmetry index chart

Breast asymmetry and its relationship to body size and fertility were studied among 500 British women. Mammograms of women breast were taken to measure the breast asymmetry. Breast volume and breast height were derived and calculated from the images. Results showed that left breasts were larger than right. Furthermore, breast volume, height and weight were positively associated with breast fluctuating asymmetry, and women with large breasts had least asymmetry (Manning, Scutt, Whitehouse, & Leinster, 1997). Similarly, Ramsay et al. (2014) studied the breast asymmetry of girls with significant adolescent idiopathic scoliosis (AIS) using magnetic resonance imaging. Breast volume of both sides was calculated for 30 patients with AIS. They reported that the mean left breast volume was larger than mean right breast volume, and also the mean breast asymmetry was significant. More than 67% of the patients showed breast asymmetry greater than 5%. Also, they have reported positive association between breast asymmetry and thoracic Cobb angle and between breast asymmetry and thoracic rib hump.



Another study by Denoel et al. (2009) evaluated the breast asymmetry of 24 women with right idiopathic scoliosis. Out of the 24 subjects, 23 were treated using brace therapy and one with brace and spine surgery. Five anthropomorphic measurements, i.e., suprasternal notch-to-nipple distance, inframammary crease length, nipple-to-inframammary crease, the horizontal comparative position of the left and right inframammary fold and the hemithoracic circumference at the level of the most inferior point of the inframammary crease were measured on both sides and differences were calculated. 3D surface scan was used to measure the breast volume. They reported that right breast was smaller for 20 women. Anthropomorphic analysis showed that right breast was higher for 19 subjects and smaller for 18 cases. Similarly, the volume of right breast calculated from the 3D scan was smaller for 19 women.

Eder et al. (2012) developed a new method to objectively quantify breast asymmetry. The author used 3D surface images and evaluated the mean 3D contour differences between the right and the left side by superimposing the mirror image of left breast over right breast. Eight landmarks were used in defining the breast locations (ref Figure-2.10). Results obtained using the new method was compared with the conventional 2D breast asymmetry measuring method (BCCT. Core). It was reported that the 3D method was superior in terms of the observed differences and the error caused by inter-observer variations.

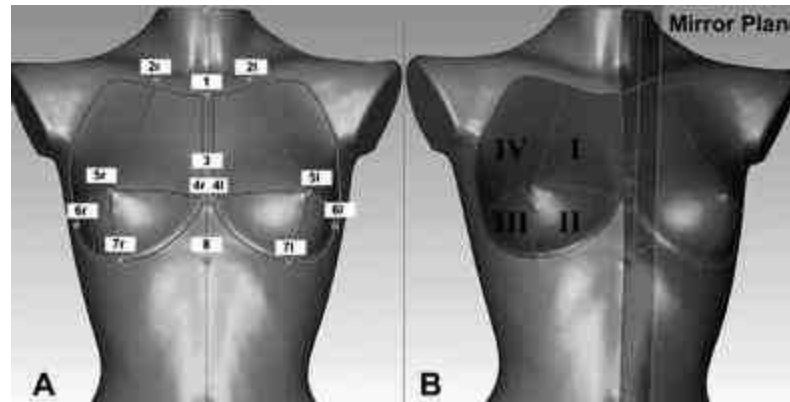


*Figure 2.10.* Landmarks defining the breast location and the mirror plane

In these 3D approaches, determination of planes are based on the researchers' assumptions that cross-sections of certain landmarks divides the face into two halves and a line passing through certain landmarks divides the body into two parts. Similar to the studies discussed in preceding sections, these approaches are also landmark-dependent and needs manual input to determine the landmarks and plane.

### **2.2.2 Measuring object symmetry**

Detecting the plane of symmetry is one of the complicated processes in measuring object symmetry. Vast majority of the biological structures exhibits high level of bi-fold or bilateral symmetry at normal conditions, whereas the presence of pathological conditions violates symmetry. Several researchers have focused on symmetry-based models to study the systematic correlation between asymmetry and pathologies (Liu, 2009). The framework of this methodology created interest in Computer-Aided Diagnostic (CAD) system integrating asymmetry analysis and knowledge of anatomy and pathology. Furthermore, the advancements in digital imaging techniques have revolutionized the 2D and 3D image visualization and have led to development of specialized software for

image display and processing. However, encoding symmetry information is often challenged by posture variations, image distortions, incomplete dataset and limitations of available intelligent systems. Though some methods were developed to detect the symmetry plane, the best method for calculating the mid-sagittal or symmetry plane is still under debate (Willing et al., 2013). The common characteristics of algorithms used for symmetry detection are 1) considering symmetry as either binary or continuous feature, 2) type of symmetry to be detected, 3) assumptions of symmetry feature exists in the center of image, 4) algorithms works in either image domain or transformed to other domain like Fourier domain and 5) robustness to noise and the complexity of the algorithms (Keller & Shkolnisky, 2004). Most of the algorithms were developed to measure the mid-plane or symmetry plane of 2d images.

In case of object symmetry, the measurement metrics are defined differently depending on assessment methods and applications. The following table provides some of the symmetry definitions as it is applied in the respective field of study.

Table 2.1

*Metrics for Object Symmetry and definition*

| Application    | Spatial Field | Symmetry Definitions  |
|----------------|---------------|---|
| Neuroradiology | 2D            | “Symmetry axis is defined as the axis best separating a planar brain image into two halves” (Liu, 2009)   |
| Neuroradiology | 3D            | “An ideal symmetry plane (a.k.a. mid-sagittal plane) has been defined as a 3D anatomical structure about which the given volumetric neuro-image presents maximum mirror symmetry” (Liu, 2009)   |
| Visual Stimuli | 2D            | <p>“Points <math>I(x, y)</math> and <math>I(-x, y)</math> are symmetrically placed with respect to the y axis and an image possesses the property of bilateral symmetry about the y axis if <math>\forall(x, y)I(x, y) = I(-x, y)</math>” (Mancini, Sally, &amp; Gurnsey, 2005)</p> <p>“Anti-symmetry is defined as <math>\forall(x, y)I(x, y) = -I(-x, y)</math> where there is a perfect negative correlation between the intensities of symmetrically placed points.” (Mancini et al., 2005)</p> |
| Biology        | 2D            | “Measure of symmetry of a structure is defined as the minimal amount of energy required to deform it into a symmetric structure” (Milner, Raz, Hel-Or,  |

---

|                                    |       |   |
|------------------------------------|-------|---|
|                                    |       | Keren, & Nevo, 2007)  |
| Symmetry and facial attractiveness | 2D    | “Asymmetry is defined as the Euclidean distance from each original version to the mirror-reversed version” (Komori, Kawamura, & Ishihara, 2009)                           |
| Solid Mechanics                    | 2D/3D | Cyclic symmetry is defined as “N-fold rotational symmetry about a central point in a plane figure (or an axis through the central point in a solid)” (Tate & Jared, 2003) |
|                                    |       | “Exact reflective symmetry is applied to prismatic solids where bilateral reflective symmetry is exhibited in one or more planes.” (Tate & Jared, 2003)                   |
|                                    |       | “Partial symmetry describes parts whereby portion of the boundary can be identified as symmetric.” (Tate & Jared, 2003)   |
|                                    |       | “Scale and skew symmetries, which change the geometry of an object, are considered as asymmetries in the context of assembly” (Tate & Jared, 2003)                        |

---

Detecting, analyzing, measuring and applying symmetry has been approached through different methods and practiced in several fields. Methods of object symmetry detection can be classified as (i) shape-based vs content-based and (ii) 2D based vs 3D based.

### 2.2.2.1 Estimating symmetry in geometrical space

This section discusses some of the research works where symmetry was assessed on objects in the geometric or Euclidean space, without any transform. Depending on the dimensionality of the objects, several criteria were applied to detect symmetry of an object such as volume/area, perimeter length/surface area, and centroid. A topological method quantifying asymmetry in bifurcating structures such as leaf vein structures used an indirect approach where the degree of symmetry was defined by the cost of the minimum energy needed to incorporate or restore symmetry on an object. Two estimates were reported, i.e., local and global symmetry (Milner et al., 2007). Capturing the global symmetry of the brain is not achievable in the slice-by-slice approach and led to meaningless results in analysis of as brain image obtained from positron emission tomography (PET). Compared to 2D based methods, 3D methods take significant computation time and cost, and are less sensitive to variability of the posture and orientation.

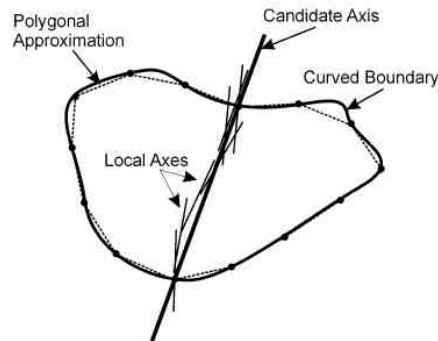


*Figure 2.11.* Symmetry detection for curved boundaries using polygonal approximation. Using the segment, local axes of symmetry were formed to estimate the global axes of symmetry

For curved boundaries, Parui's method (ref Figure-2.11) used a segmentation approach, where the contour of a given object is approximated using straight-line segments forming a polygon. Using paired segments on opposite sides of the contour, local candidate axes were formed that were then regressed to find a global axes of symmetry. A cost estimate was given to quantify the degree of symmetry, where '0' represents perfect symmetry. The accuracy of the algorithm can be improved by increasing the resolution of the polygonal segments. This method had been applied to planar curves (Parui & Majumder,1983). Cornelius and Loy (2006) proposed another method to determine the symmetry axis on perspective images. Their approach was to detect symmetric pairs of features and then grouping them to form quadruplets. For each quadruplet an axis of symmetry was calculated and then the quadruplets were grouped to find the common axis of symmetry. It was mentioned that the algorithm worked for any orientation and location.

The internal features of matter such as texture, gray level, etc. are also used to perform symmetry analysis, and are often referred as content-based methods. They are most popular in brain research where the head is treated as two halves of gray-level volumes and the intensities of chosen feature of one-half are matched to the other half. 3D volumetric texture analysis based on multi-sort co-occurrence matrices use intensities, gradient and anisotropy image features to find asymmetry information. Image segmentation techniques based on region, boundary and hybrid are often employed with these medical image analysis (Liu, 2009).

### *2.2.2.2. Estimating symmetry in a transformed space.*

Researchers have used several mathematical techniques to detect matching patterns and symmetry axes in objects that were non-geometric and were distorted through non-isometric transforms. Yip (2000) used Hough Transform (HT) to estimate reflection symmetry of a skewed image. Skewness is a class of distortion to the original image, but, preserves the pairs of parallel lines within the image. The HT method takes advantage of this preservation to detect skew-symmetry axis and skew-transverse angle. Another technique proposed by Zabrodsky, Peleg, and Avnir (1992) estimated symmetry of a given object by calculating a coefficient of symmetry. This technique used a symmetry transform (ST), which rearranges the data points on a given object to form a symmetric shape, and estimates the Euclidean distance involved for the rearrangement. If the object/image is close to symmetry, the coefficient will be close to '0'. This technique has limitations with truncated or occluded images. The method defined by O'Mara and Owens (1996) used a numerical approximation technique to determine the centroid and the eigen vectors of the covariance matrix of the data cloud. Each eigen vector and centroid pair defined a unique plane of symmetry for each dimension of a given object. Thus, accordingly, there can be  $n$  unique planes of symmetry for an  $n$ -dimensional object. Their method needs a data cloud to represent the object, and is not accurate to operate with contour points alone. To measure the rotational asymmetry of biological structures, a vector based geometric method was developed by Frey, Robertson, and Bukoski (2007). The authors estimated the center of mass for the shape and projects vectors to convert them into polygons. The angles between the vectors were measured and if the angles were same then the asymmetry of the shape was considered zero. Based on this



technique, flowers rotational symmetry was evaluated and the results were more consistent with the visual analysis. Another approach to detect reflection and rotational symmetry using features in the frequency domain was proposed by Keller et al., (2004). In this approach, a pseudo-polar Fourier Transform was estimated on (a) the original image and (b) rotated by  $2\pi/n$  version of the original image. A distance measure defined in the transformed space was used to determine the axes of symmetry. This method is robust to noise, but computationally intensive, as redundant transforms are needed for the same image to estimate symmetry. In another method that operates on the Principal Component space, a given 3D dataset of a rigid body was structured with three distinctive principal axes that were orthogonal to each other and the moments of inertia with respect to these axes was a function of the degree of symmetry. These axes represent the spatial distribution of masses and were used to characterize 3D body structures. They indicate that any hyperplane of symmetry passes was orthogonal to one of the principal axes of a given object. (Minovic, Ishikawa, & Kato, 1993).

Li, Zhang, and Kleeman (2008) developed a method to measure the bilateral symmetry plane for real time robotics applications. Their technique used an edge detection algorithm to define the contour of an object. Using a voting method, pairs of data points from the edges were identified and a plane dividing the pairs was estimated to determine the plane of symmetry. This method was rapid, but involves large amount of approximations and were not applicable for deformable objects such as human body. In another method, using the gradient information, a generalized symmetry transformation technique was developed by Reisfeld, Wolfson, and Yeshurun (1995) and was able to detect bilateral and radial symmetry at different scales. Similarly, Willing et al.( 2013)

developed a semi-automatic method to detect the bilateral symmetry plane on 3D CT images of face. Cephalometric landmarks such as FZS, po, or, CG, N, pr, ANS, sub, La, and Fm were manually marked on the skeleton image (ref Figure-2.12) and then the symmetry plane was calculated using principal component analysis and further refined with iterative closest point algorithm.

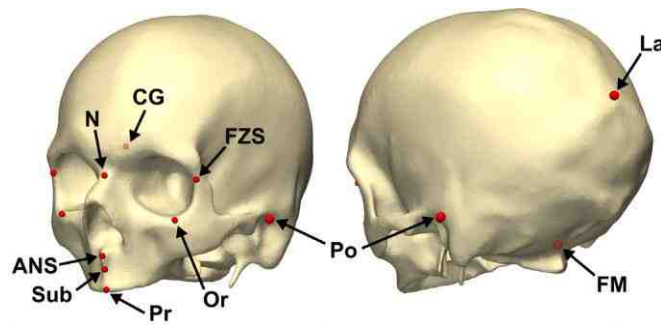


*Figure 2.12. Cephalometric landmarks*

Using the phase domain approach Kakarala, Kaliamoorthi, and Premachandran (2013) developed a way to detect the symmetry plane on 3D shape objects. They measured the spherical harmonic coefficients of 3D shapes, which were the linear phase structure to detect the symmetry plane. Similarly, research by Mitra, Guibas and Pauly (2006) showed a method to detect the partial and approximate symmetry detection for 3D shapes and objects. Samples data points were assessed for mathematical signatures and subjected to basic Euclidean transformations. The transformed data was then stochastically clustered to identify regions of symmetry. Their method was not developed to estimate the plane of symmetry, rather to estimate regions of symmetry that are spatially distributed on a 3D object (ref Figure-2.13).

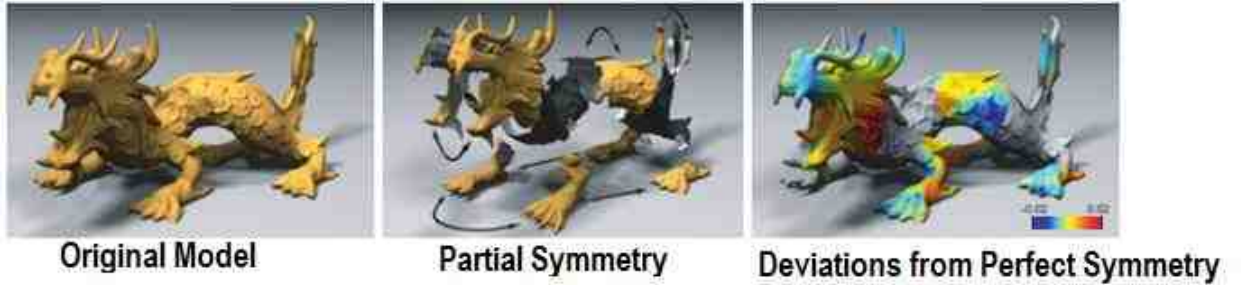


*Figure 2.13.* Symmetry estimation on a 3D surface using stochastic clustering

Another technique proposed by Bokeloh, Berner, Wand, Seidel, and Schilling (2009) detected the structural symmetry in 3D geometric data (ref Figure-2.14). Specifically, their algorithm calculated the rigid symmetry on the surface 3D model. The process involved extraction of line features from the input model and detects the pairs to define the local coordinate system. Using the iterative closest line algorithm the line features are aligned and compared. In the subsequent stage, geometric validation was carried out by comparing the extracted features with actual model which finally yielded symmetric parts. The results can be used to reconstruct missing symmetric regions on 3D models.



*Figure 2.14.* Estimating symmetry using rigid geometry and extrapolating regions of matched symmetry

In a recent work, Akbar, Hayat, Haq and Bajwa (2014) developed a technique to detect bilateral symmetry plane on a digital image using scale invariant feature transform(SIFT).

The method estimated centroid of objects using the SIFT features and subsequently determine pairs of points using their gradient features with respect to the plane passing through the centroid. This method was iterative and was an approximate method.

### **2.3 Asymmetry Measurement in Clinical and Pathological Studies**

In the preceding sections, several methods developed to measure symmetry were discussed. One of the important areas with direct implication for computational symmetry measurement is the clinical and pathological analyses. The three primary sectors of such analyses can be grouped under (1) spinal deformations, i.e., scoliosis (2) brain image processing and (3) facial image analyses. Images in 2D/3D space generated from various techniques such as surface topography, magnetic resonance imaging (MRI), positron emission topography (PET), etc. serve as the primary input for symmetry analyses.

Detecting asymmetry, especially trunk deformations of a human body, at clinical settings involve evaluation of posture at standing and sitting conditions, gait, range of motions, examination of musculoskeletal system, muscular strength and relative alignment of body parts (Kowalski, Kotwicki, & Siwik, 2013). One of the methods used in evaluating body posture is photogrammetry (Nowotny, Gaździk, Zawieska, & Podlasik, 2002; Tokarczyk & Mazur, 2006). This method uses electromagnetic radiation in a wide range of wave lengths to provide imaging and physical measurements. Raster-stereography method produces fringes projected on human body and the raster image of this object can be captured to automatically analyze the body posture. Other less technologically advanced devices such as scoliometer and digital inclinometer can help to measure spine rotation

and spinal mobility at a preliminary level without 3D visualizations (Kowalski et al., 2013).

Scoliosis conditions relate to 3D deviation of the spine that results in asymmetric distribution of the trunk volume. Cobb angle measurement is the gold standard procedure to quantify scoliosis through radiographic techniques. Some of the non-radiological instruments detecting scoliosis are Optronic Torsograph (Dawson et al., 1993), computer optical topography (Sarnadskiy, Vilberger, & Fomichev, 2002), raster stereography (Goldberg, Moore, Fogarty, & Dowling, 2001), laser Doppler (Berg et al., 2002) and ultrasound (Letts, Quanbury, Gouw, Kolsun, & Letts, 1988) techniques. Capturing the surface topography in hunched and stance positions proved to increase the sensitivity of the Cobb angle detection using optical devices (De Sèze, Randriaminahisoa, Gaunelle, de Korvin, & Mazaux, 2013; Faro, Marks, Pawelek, & Newton, 2004). Another novel surface topography system capable of producing 3D spine measurements was developed by Liu et al. (2013). The system used electromagnetic markers and a handheld laser scanner to construct a 3D surface topography from spine scans.

Brain pathology detection using 2D and 3D medical imagery is another research area where symmetry analysis and segmentation are being explored. In neuro research, for example, nearly 200 normal brain MRIs had been studied collectively with relation to age and gender to contribute to the normative database (Amunts, Jäncke, Mohlberg, Steinmetz, & Zilles, 2000). Brain images captured from variety of modalities (MR, CT, PET, SPECT, CTP and MRP) serve crucial role in the diagnosis of anatomical, functional and physiological information. Morphologically, a normal human brain is not perfectly

symmetrical and hence for any algorithm detecting asymmetry the tolerance to normal asymmetry is critical. Systematic analysis of relationship between asymmetry and pathology is key for computer-aided diagnosis (Liu, 2009).

Contrary to brain, the human body shape changes frequently and is very time-sensitive. Relationship between symmetry and health aspects was investigated and reported. While the actual health conditions did not show any strong association with asymmetry, the perceived health had shown a positive correlation with facial symmetry (Rhodes et al., 2001). Lack of symmetry in structure is considered a reflection of accumulated errors and stress on the body. It has been reported that environmental impacts accumulating on the body since birth is expected to monotonically decrease the symmetry through the life span (Murray & Lopez, 1997). Changes in bodily symmetry across development have been little studied, especially in early development stages. A study across childhood reported that symmetry increased with age (Wilson et al., 1996). A generic framework to estimate asymmetry in human structures such as brain, breast, face and limbs possessing mirror symmetry was discussed in (Liu, 2009).

Importance of assessing the symmetry of torso, face and brain and its implications on clinical studies were discussed in this section. The most common pathological condition associated with torso is scoliosis. Though there are several indices available for scoliosis, the inter and intra-rater reliability are poor due to the need for numerous manual landmark identifications (Seoud, Dansereau, Labelle, & Cheriet, 2012). Besides, the radio-graphical acquisition techniques are considered harmful if proper measures are not followed and motivate the need for a new approach that is rapid and less-harmful.

## **2.4 Summary of Limitations in the Existing Techniques/Approaches**

The provided survey of literature indicates that all of the methods found in the literature are (i) landmark-dependent and/or (ii) need human intervention at various steps of the processing. The match symmetry method requires componentized measurements such as arm length, etc. The object symmetry approaches typically use indirect steps such as transforming the object representation into other spaces such as Hough, Fourier, etc. Those techniques that are direct also rely on manual landmarks. Furthermore, the existing techniques were not developed considering the needs to characterize symmetry in a 3D human torso. Some of the techniques are limited to 2D space, which introduces error due to the plane of the photo and are not applicable for 3D data clouds. In addition, several techniques are valid for objects that feature geometric uniformity such as parallel lines, grids, etc., and are not applicable for contours that are non-uniform in the 3D space, such as the human torso. It has been established that characterizing asymmetry using bilateral traits is not sufficient to detect or diagnose clinical conditions such as scoliosis. Hence, there is a need for a technique that can estimate symmetry for a non-uniform 3D volume, and is robust to natural posture, and is computationally less-complex, and is less dependent of anatomical landmarks and human intervention.

## **CHAPTER III**

### **Methodology**

The primary objectives of this research are,

- (i) To develop a novel method to estimate the degree of asymmetry in 3D human body and that can primarily serve as a characterization and evaluation tool
- (ii) To estimate the degree of twist in the transverse plane and tilt present in the coronal plane of a torso to measure the torso deformity in the skeletal structure
- (iii) Validate the developed method by comparing with manual ratings of field experts

To achieve these objectives, the following steps were devised and conducted (see Figure-3.1 for data sampling procedure and Figure-3.2 for schematic representation of the processes), accordingly,

- (a) Data sampling and pre-processing of the digital model
- (b) Defining the pose and orientation of the model with reference to the principal axes



- (c) Developing an algorithm that allows the torso data to be sliced in the transverse plane, i.e., to make cross sections of the torso, and determine a line of bifurcation that equi-divides each cross-section in the sagittal direction
- (d) Develop an algorithm that determines shape variations in the bifurcated cross sections, and estimate a numerical index of asymmetry
- (e) Develop an algorithm to estimate twist and tilt in the torso
- (f) Validate the method using a known geometry and further validate the estimated index of asymmetry and twist by comparing with expert ratings of the 3D torso

### **3.1 Data sampling**

The CAESAR (Civilian American and European Surface Anthropometric Resource) database served as the primary data source for the 3D scans. A 3D scan, also referred as, digital model in this study is defined as the data cloud obtained by scanning the surface of a human subject using 3D scanning techniques (The 3D body scanner, n.d). The surface of the scanned object is digitized as data points represented in the Cartesian space. The CAESAR database is a repository of 3D anthropometric survey carried out in countries like the USA, Canada, Netherlands and Italy. Subjects were scanned using two scanners, i.e., Cyberware and Vitronic, to generate 3D digital representations. Before obtaining the scans, 72 landmarks were marked with stickers on the subjects by experts (Robinette, Blackwell, Daanen, Boehmer, & Fleming, 2002). Thus, the 3D scans contain the marked landmarks with their associated Cartesian positions. These 3D scans can be visualized as points, wireframes, and/or triangulated surfaces with the help of Polyworks software. Samples in CAESAR study were based on stratified sampling method. Strata used were Age (3 groups), Gender (2 groups) and Ethnicity (3 groups). In the North America (USA

and Canada), 12 locations were chosen to collect the sample subjects and the number of samples collected were 2375. Further information about CAESAR can be obtained from <http://www.humanics-es.com/CAESARvol1.pdf>.

Thirty digital human representations (a.k.a. 3D scans) were chosen from the database using a stratified random sampling technique. Fifteen male samples and the same number of female samples were selected and used. The sample size of 30 was determined to meet the large-sample requirement of parametric statistical tests. The chosen samples follow a broad distribution of weights (see Figure 3.1). The selection procedure was carried out with the aid of SPSS V19.0 software tool.

### **3.1.1. Data Characteristics.**

The subjects used in this study were US civilian adults. The weight distribution and the number of samples falling under each stratum are shown in Figure 3.1.

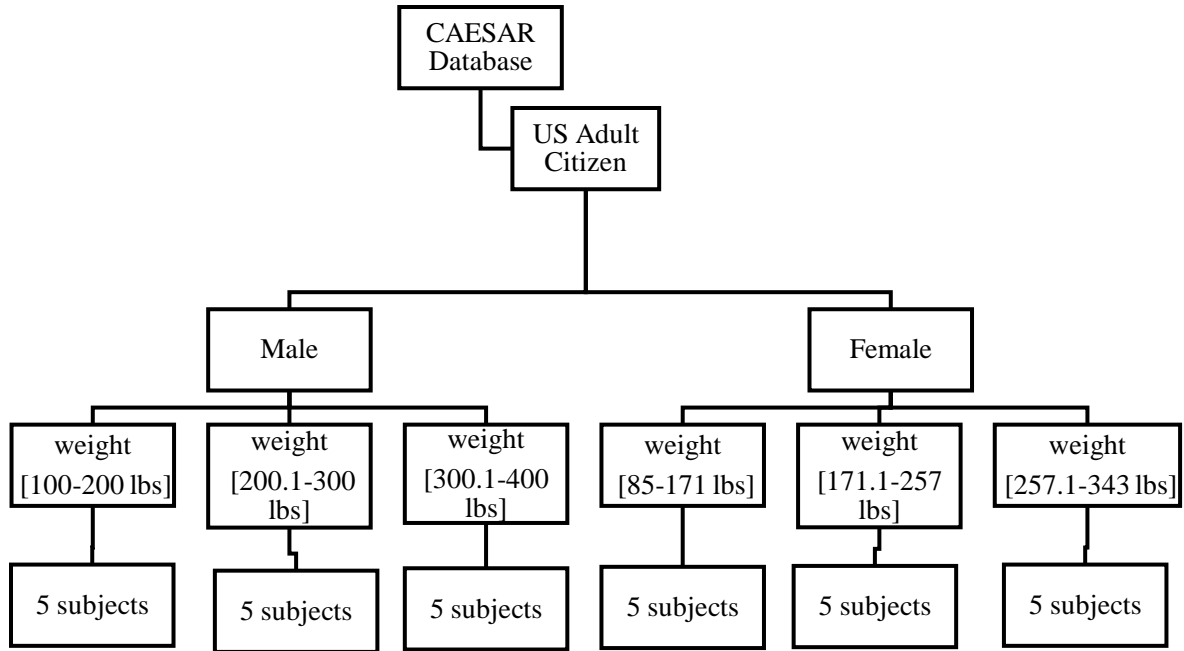


Figure 3.1. Schematic representation of the sample selection

### 3.1.2. Pre-processing of the Data Models.

The selected 3D scans (with a native format of *.ply*) from CAESAR database were imported into the Polyworks<sup>®</sup> CAD utility. The CAESAR scans by default have 72 landmarks. Planes parallel to the ground were inserted in the scan at the Cervicale, Crotch and Axilla landmarks to extract the torso region. The extracted regions were cleaned off of the landmarks and holes filled in using the in-built Polyworks filling tools. The Cartesian locations of the landmarks, however, were retained for computations involved in twist and tilt estimations (described in Section 3.5). Figure- 3.3 shows the positioning of selected landmarks used in various processes in this research. Landmarks were used to define the torso region, but, can be completely user-defined. The rest of the landmarks were used in the computation of torso tilt and twist.

Except the torso region of the scans, the rest (i.e., the lower body, the head and the upper limbs) were excluded (see Figure-3.4). The torso, here, was defined as the upper part of the body from the Cervicale to the Crotch-level, and with hands removed at Axilla point posterior left and right. A sample torso model is shown in Figure-3.4(b).

### 3.2 Defining Orientation of the Torso

The CAESAR scans were made with the subjects being in their natural standing pose. For this study, the extracted torsos were needed to be aligned to a global reference frame such that the orientation of the front/back, left/right and top/bottom can be defined (see Appendix-A). The global reference frame was chosen to be the principal axes at the origin in  $\mathbb{R}^3$  space. The Eigen vectors of the global axes are given as,

$$\begin{bmatrix} 1 & 0 & 0 \\ 0 & 1 & 0 \\ 0 & 0 & 1 \end{bmatrix}$$

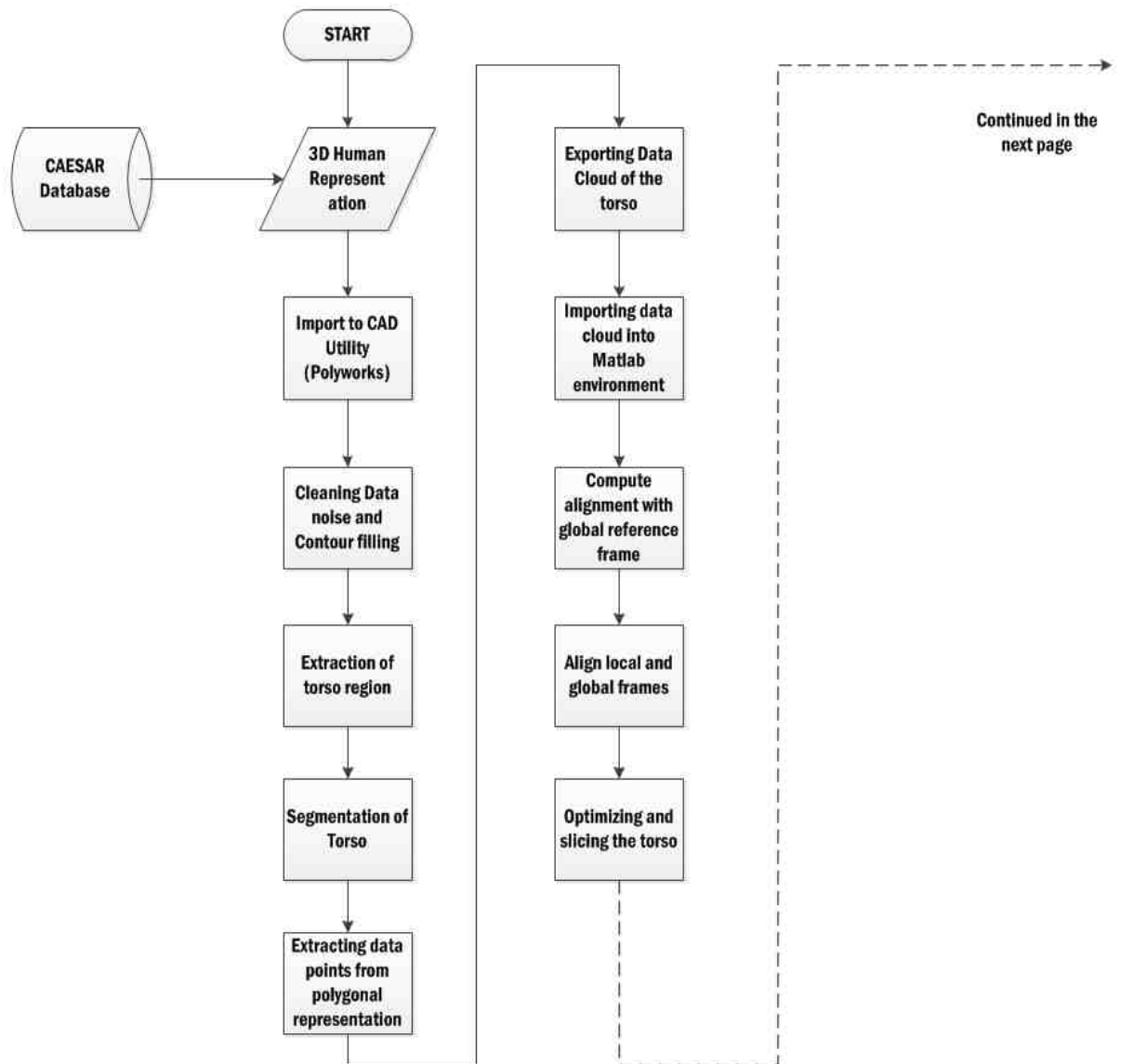
The torsos are essentially a cloud of 3D data points in the  $\mathbb{R}^3$  space, with each point represented by x, y and z positions. To have the individual torsos centered at the origin of  $\mathbb{R}^3$  space, their x, y and z positions were mean-corrected, i.e., each x-position was subtracted by the mean value of all the x-positions for a given torso, and likewise for the y and z positions with their corresponding means. The Eigen vectors of the 3D torso were then computed using standard principal component analyses technique (Cambell and Atchey, 1981; Paquet, Rioux, Murching, Naveen, & Tabatabai, 2000; Shilane, Min, Kazhdan & Funkhouser, 2004), and the angle of those vectors from the origin were estimated. The torso scans were rotated through these angles such that the rotated object had its reference frame aligned to the global frame. The rotation of the 3D object was performed using the following rotation matrices in their respective axes,

$$\text{Rotation in Z} = \begin{bmatrix} \cos(\theta_z) & \sin(\theta_z) & 0 \\ -\sin(\theta_z) & \cos(\theta_z) & 0 \\ 0 & 0 & 1 \end{bmatrix}$$

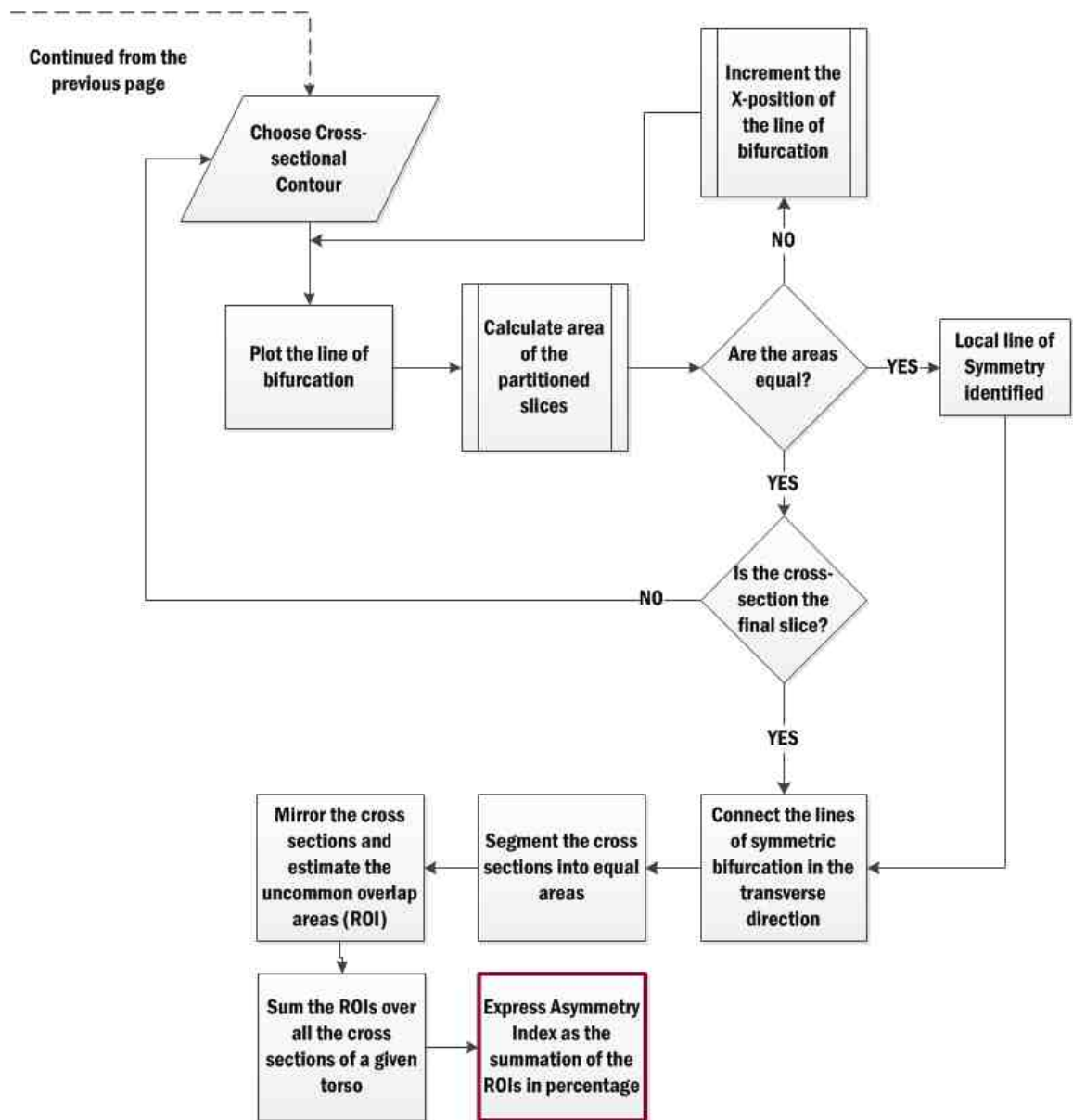
$$\text{Rotation in Y} = \begin{bmatrix} \cos(\theta_y) & 0 & \sin(\theta_y) \\ 0 & 1 & 0 \\ -\sin(\theta_y) & 0 & \cos(\theta_y) \end{bmatrix}$$

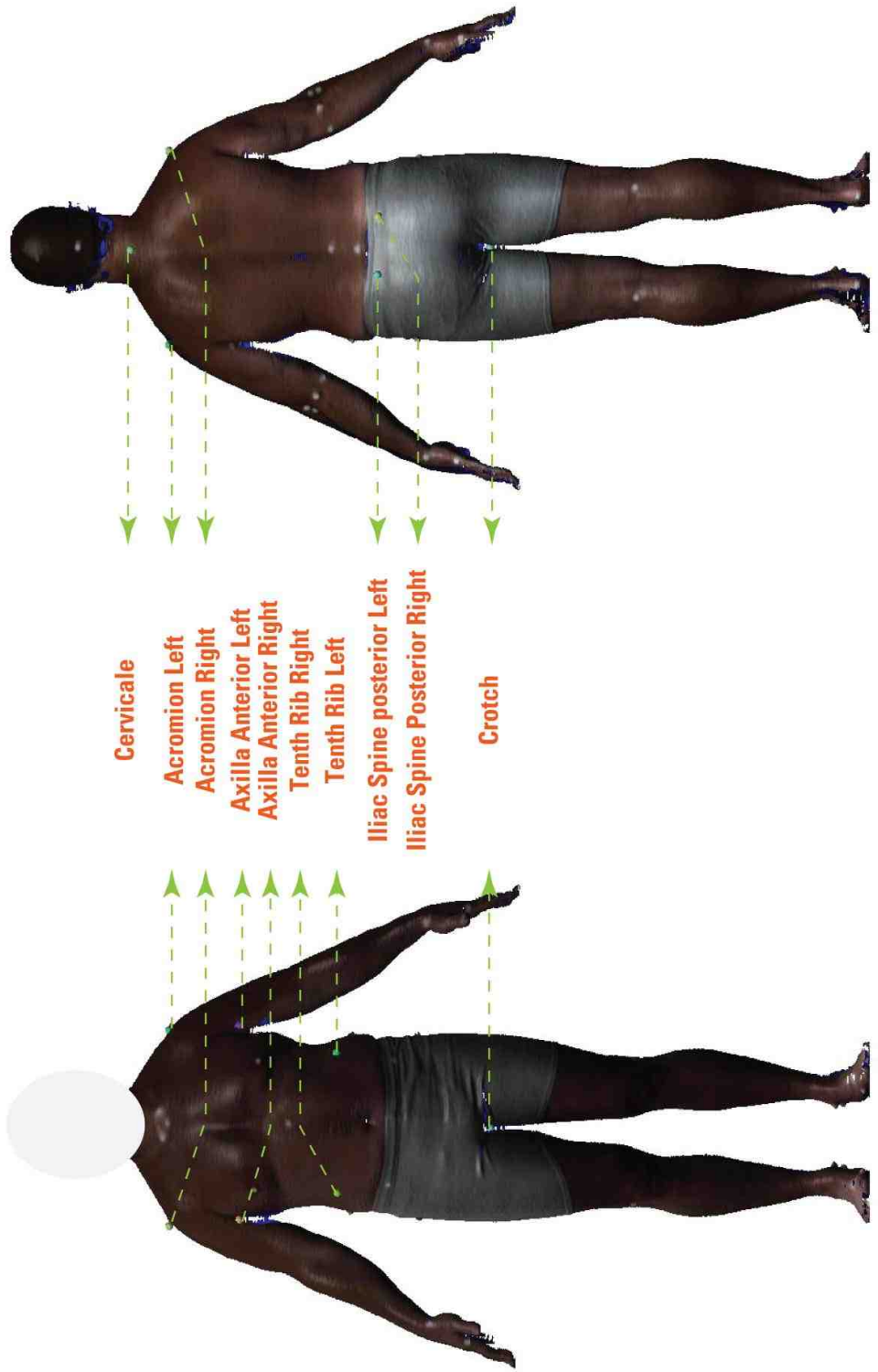
$$\text{Rotation in X} = \begin{bmatrix} 1 & 0 & 0 \\ 0 & \cos(\theta_x) & \sin(\theta_x) \\ 0 & -\sin(\theta_x) & \cos(\theta_x) \end{bmatrix}$$

where,  $\theta_z$  is the angle between the z-Eigen vector of the global coordinates and the z-Eigen vector in the local coordinates,  $\theta_y$  is the angle between the y-Eigen vector of the global coordinates and the y-Eigen vector in the local coordinates, and  $\theta_x$  is the angle between the x-Eigen vector of the global coordinates and the x-Eigen vector in the local coordinates. The rotation was performed sequentially for the three principal axes, and the rotated 3D torso was obtained with principal axes aligned to the global frame. Figure-3.5 shows the schematic of the sequence of operations. The Eigen vector in the x, y and z-directions define the right/left, front/back and top/bottom orientations of the torso, respectively (see Figure-3.5).



*Figure 3.2.* Schematic representation of the processes of orientation of the torso, extraction of the cross sections, estimating the local plane of symmetry and computing the asymmetry index





**Cervicale**

**Acromion Left**

**Acromion Right**

**Axilla Anterior Left**

**Axilla Anterior Right**

**Tenth Rib Right**

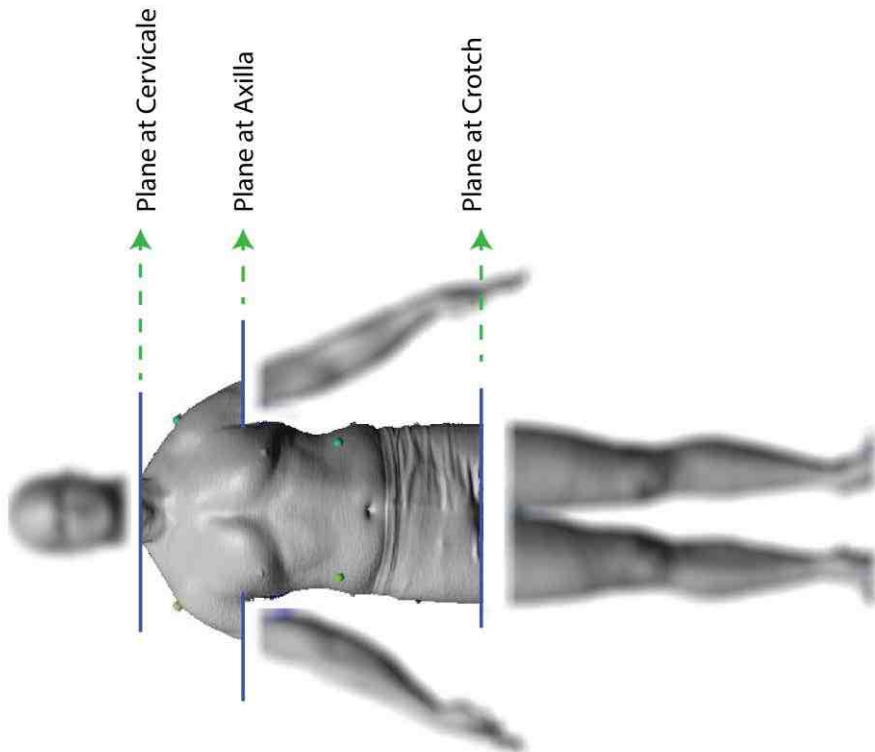
**Tenth Rib Left**

**Iliac Spine posterior Left**

**Iliac Spine Posterior Right**

**Crotch**





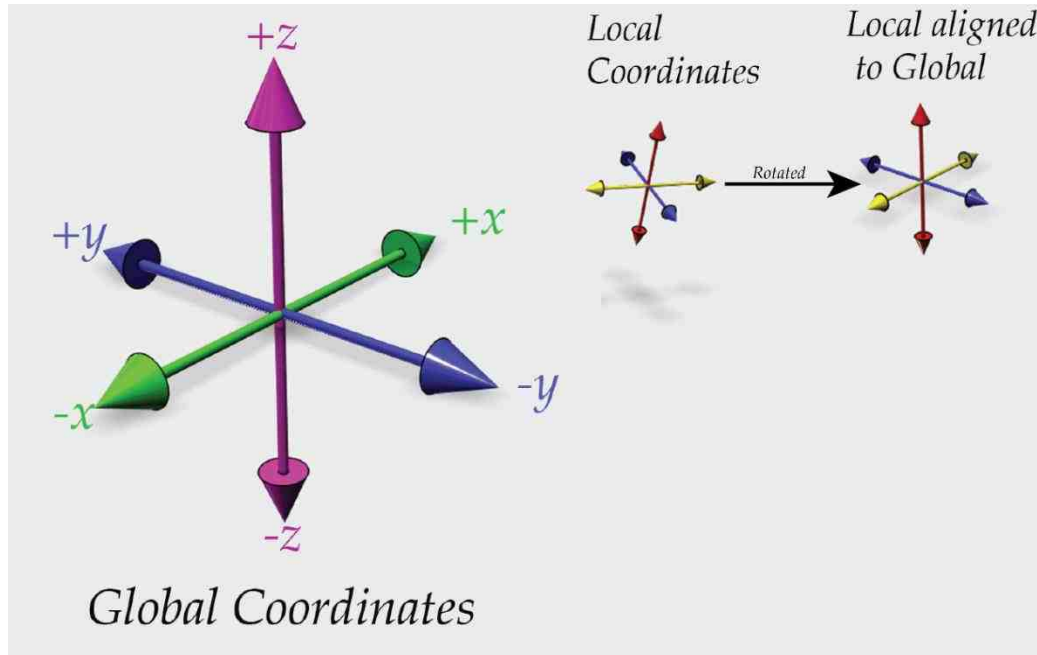


Figure 3.5. Schematic of the process of axes orientation and alignment. The local coordinate axes are rotated to align them with the global axes shown on the most left

### 3.3 Determining the Line of Symmetry

The next step involves developing a method to determine the line of symmetry for the entire torso. The technique used in this research was to subdivide the 3D torso into several numbers of 2D slices, and individual planes of bifurcation (termed as local line of symmetry) determined for each of the slice. Subsequently, the lines of bifurcation were linked along the slices in the z-direction to determine a global surface that divides the 3D volume into two equal halves (termed as the global surface of symmetry). Within each slice, the line of symmetry was computed using an iterative process where a sliding line gradually moves at the rate of 2 mm along the principal axes defining the right/left direction, and computing the area of the right and left halves of the cross section along the sliding locations. Figure-3.6 shows the schematic of the sliding line dividing a cross section into two halves. As the sliding line moves from right to left on the cross section, it

divides the cross section into two closed curves. The area of one of the closed curves was compared against the total area of the cross section to determine if that closed surface represents half of the total area. The location at which the area of the closed surface becomes equal to half of the total area was considered the local line of symmetry for that cross section.

### 3.3.1 Computing the Area of Closed Surface.

To determine the area under the closed surface, which is the cross-section here, Green's theorem was used (see Equation 1). If  $C$  be a positively oriented, piecewise-smooth, simple closed surface bounding the region  $D$ , then if  $P$  and  $Q$  are functions with continuous partial derivatives in an open region that contains  $D$ , then

$$\oint_C P(x, y)dx + Q(x, y)dy = \iint_D \left( \frac{\partial Q}{\partial x} - \frac{\partial P}{\partial y} \right) dx dy \quad (1)$$

This theorem allows determining the area of a closed contour using its line integral, i.e., integrating the contour along the perimeter to determine its area (Riley, Hobson, & Bence, 2006). In discrete domain, the Equation-1 translates into Equation-2,

$$\text{Area of closed surface } D = \frac{1}{2} \times |x_n dy_n - y_n dx_n| \quad (2)$$

where,  $x_n$  and  $y_n$  are the discrete values of the functions  $P$  and  $Q$ , and  $dx_n$  and  $dy_n$  are their differential values. In this research,  $x_n$  and  $y_n$  represents the Cartesian positions ( $x$  and  $y$ ) of data points in a cross section.

### 3.3.2 Estimating the Plane of Symmetry.

Numerical implementation of Green's theorem to determine the local line of symmetry is given in the following code snippet. The individual lines of symmetry across all the slices were linked to determine the global line of symmetry.

---

#### Algorithm to implement Green's theorem to determine the line of symmetry in 2D

---

Estimate span of the cross section to determine the bounds for the sliding line movement

Initialize sliding line

Increment sliding line to form closed surface

$$\text{Area of closed surface} = \frac{1}{2} \times |x_n dy_n - y_n dx_n|$$

while ((area of closed surface - 1/2 x total area) > 0.001\*)

    increment sliding line location

Finalize sliding line location

Define the location to be the line of symmetry

---

\* the tolerance value can be set to a much smaller number at the expense of computational intensity. Here, 0.001 was chosen heuristically.

### 3.4 Estimating the Asymmetry Index

For each cross section, the mid line divides the section into two equal halves based on their areas. However, there is a possibility that the areas are distributed into differing shapes, i.e., the contour of the two halves need not be identical, thereby causing asymmetry. To estimate this shape asymmetry, one half of the cross-section was mirrored on the other half, and the uncommon areas were estimated. In the Figure 3.6, *A* represents the right side and *B* represents the left half. The region of interest (ROI) was defined as

the areas that were not covered after reflection (Figure 3.6-right). This process was repeated for all the cross-sections in a given torso. Mathematically, this ROI is defined as,

$$ROI = A \cup B - A \cap B \quad (3)$$

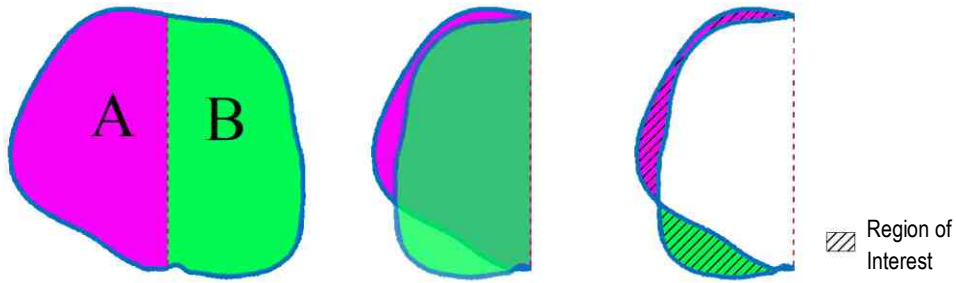


Figure 3.6. Computing the ROI. A typical Cross-section (left) was mirrored (middle), and the area corresponding to the region of interest (right) was computed

After calculating the ROI for the individual slices, the *Asymmetry Index* was defined as the proportion of the total ROI to the cumulative half-area of the slices, given as,

$$\text{Asymmetry Index (\%)} = \frac{\sum_{i=1}^n \text{Area of ROI}_i}{\sum_{i=1}^n (\text{Area of slice}_i * 0.5)} \times 100 \quad (4)$$

Where,  $i$  is the slice number and  $n$  is the total number of slices in a torso.

### 3.4.1 Estimating Deviance from the Principal Axis.

The principal axis in the z-direction passes through a point (possibly centroid) of each cross section. The shortest Euclidean distance between that point and the local line of

symmetry marks the deviance between the two measures. The mean distance was then computed from the individual deviances obtained from each of the cross sections.

### **3.5 Estimating the Degree of Twist and Tilt in Torso**

To determine the effective twist present in torso, Cartesian locations of six specific anthropometric locations were used. The following landmarks were chosen and line segments connecting the corresponding left and right landmarks were plotted,

1. Iliac Spine posterior right (ISPR),
2. Iliac Spine posterior left (ISPL),
3. Acromion right (ACR),
4. Acromion left (ACL),
5. Right tenth rib (RTR), and
6. Left tenth rib (LTR)

The relative angles between these line segments in the transverse projection were computed (see Figure 3.7). The angle between,

- (a) the line segments connecting ACR and ACL, and the ISPL and ISPR determined the overall twist in the torso
- (b) the line segment connecting ACR and ACL, and RTR and LTR determined the twist in the upper torso
- (c) the line segment connecting RTR and RTL, and ISPR and ISPL determined the twist in the lower torso

Likewise, the relative angle between the line segments connecting ACR and ACL, and ISPR and ISPL computed in the coronal plane (frontal plane) was computed as the tilt present in torso.

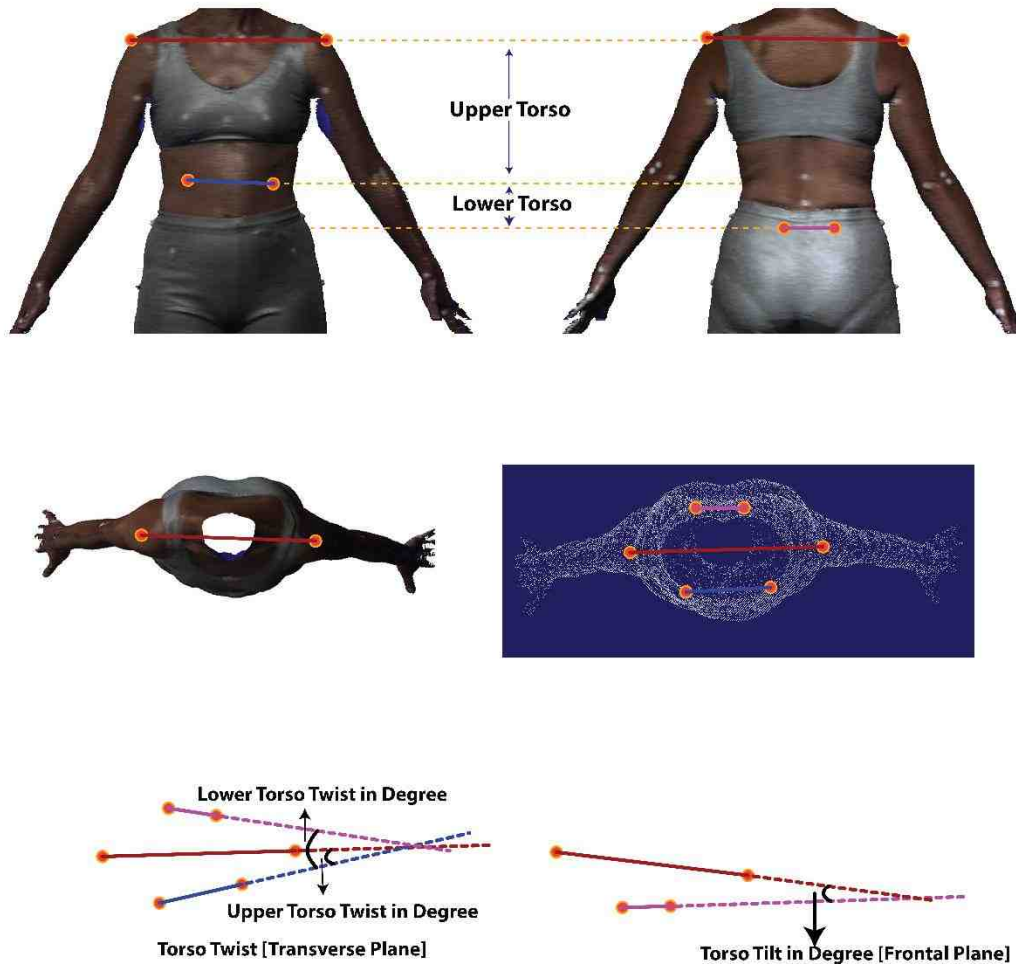


*Figure 3.7.* Torso landmarks for Twist and Tilt computation; Top row: Definition of upper and lower torso; Middle row: Top view of torso with connected landmark lines; Bottom row: Angle calculation for torso and tilt.

The developed methods were applied for the 30 subjects and their respective asymmetry index, deviance from the principal axis, torso twist (Upper, Lower and Overall) and torso

tilt values were computed. All the computations were performed using Matlab 2015b software.

### **3.6 Validation of the Developed Method**

In order to validate the developed measure whether it can rate a symmetric object to be “symmetric” and an asymmetric object as “asymmetric with a certain degree”, the following two approaches were taken,

- 1) Measuring the symmetry of a known geometry - a 3D cylinder was used in this case. This portion ensures validity of the algorithm to its applicability to a symmetric object.
- 2) Comparison with field expert ratings and the developed measure

Hereafter, the developed measure would be referred as *objective ratings* and the ratings from field experts as *subjective ratings*.

#### **3.6.1 Known Geometry Validation.**

A 3D cylinder model comprised of 10 slices was chosen to perform this validation (see Figure-3.8). The dimensions are arbitrary units. Using the developed technique, the local planes of symmetry were computed. Subsequently, the 3D plane of symmetry and the asymmetry index were estimated.



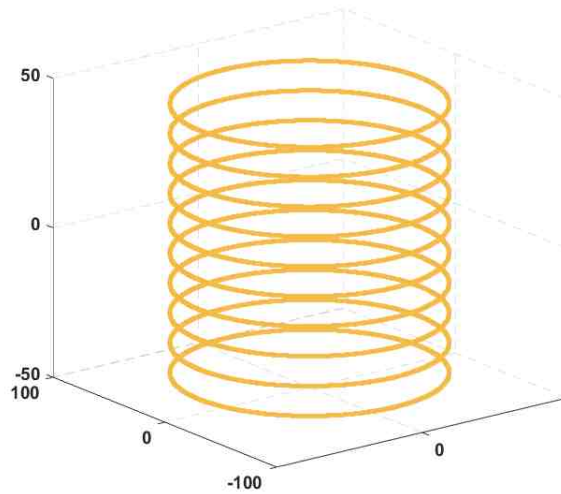


*Figure 3.8.* Cross-section of a 3D cylinder CAD model

### **3.6.2 Subjective Evaluation.**

To further validate the developed method for its efficiency in characterizing asymmetry, a subjective evaluation protocol was developed. While the objective ratings can be applied to various fields such as apparel, rehabilitation, medical therapy and physiology, the current survey was conducted with field experts in apparel domain. Three faculty experts rated each subject for their asymmetry and twist present in the torso. The evaluators were presented with four representative images of each subject comprising the top, side, front and back views (see Figure-3.9). And, all the thirty subjects were rated in a 4-point Likert scale with the following definition,

- 1- Not at all
- 2- Slightly visible
- 3- Moderate
- 4- High

The subject images were randomized in their presentation to the evaluators to avoid any bias. The survey was IRB approved and designed using the Qualtrics software and distributed digitally to collect the blind-folded responses of the evaluators.

Subsequently, inter-rater reliability was calculated using the intra-class correlation coefficient. Inter-rater reliability calculates the tendency of agreement found among the raters (Shrout and Fleiss, 1979). And, finally, the subjective ratings were tested for their correlations with the objective ratings to complete the validation process.



*Figure 3.9.* Sample Images of a female subject presented for subjective ratings by apparel experts

## **CHAPTER IV**

### **Results**

The analyses results are presented in this chapter under eight sections, i.e., (i) Descriptive statistics of the sample population (ii) preprocessing the torso (iii) optimizing the number of slices to be extracted per torso, (iv) estimated asymmetry index (AI) for the each subject in the sample population, (v) estimated twist and tilt for the samples, (vi) computed deviance from the principal axis, (vii) validation of the developed method, and (viii) the correlation between weight and AI.

#### **4.1 Descriptive Statistics of the Sample Population**

The total number of subjects used in this study was 30, with 15 male and 15 female subjects. The average age of the male subjects was 37.4 years with a range of 23 to 59 years. Similarly, the average age of the female subjects was 39.5 years with a range of 19 to 65 years. The average weight of the male subjects was 245.44 pounds with a range of 154.32 to 344.93 pounds. For the female subjects, the average weight was 195.47 with a range of 103.61 to 344.93 pounds.

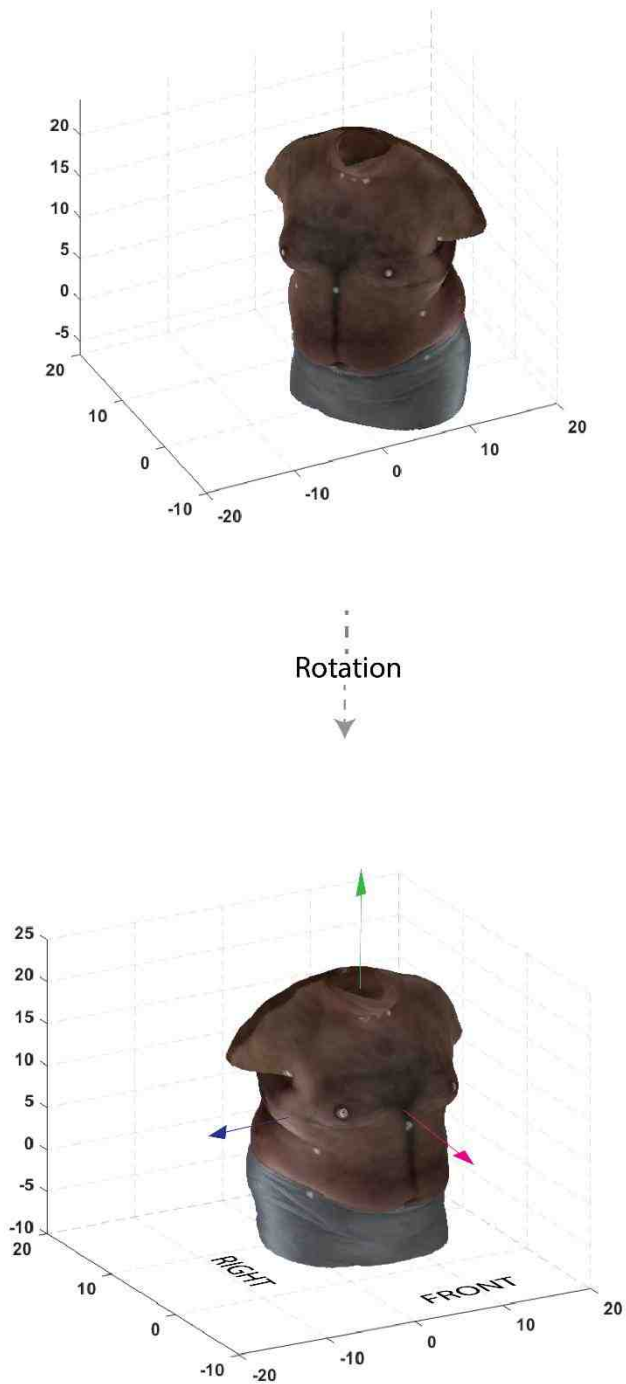
## 4.2 Preprocessing of the Torso

Figure 4.1 shows a sample illustration of the torso rotation process (described in section 3.2). The raw data of the torso region (in the *.ply* format) were imported into the Matlab environment, and their principal axes estimated. The difference in the angles of the axes with the global reference axes (see Section 3.2) were used to guide the rotation such that the local axes of the torsos and the global axes were aligned to each other.

## 4.3 Optimization of Cross-sections Extracted Per Torso

As described in Section-3.3, each torso model was sliced in the transverse plane to obtain multiple cross-sections and the line of symmetry computed for each of the slices.

However, there was no predefined relationship between the number of slices per torso and the accuracy gain. To determine the optimal number of slices needed to compute the AI, each torso was sliced between 10 and 50 slices with an increment of 5 slices, and the AI computed. With increasing number of slices, the numerical accuracy of AI improved (see Figure-4.2). It was heuristically determined that a gain less than 0.25% was insignificant, given the additional computational load experienced with the number of slices. For the male subjects, 30 slices were found to be optimal and for females, 25 slices were set to be optimal.



*Figure 4.1.* Illustration of the rotation and aligning process. The torso on the top panel was subjected to rotation in all the three principal axes such that the final orientation is in alignment with the global reference frames. The oriented torso was used to define the sides (front, back, right and left).

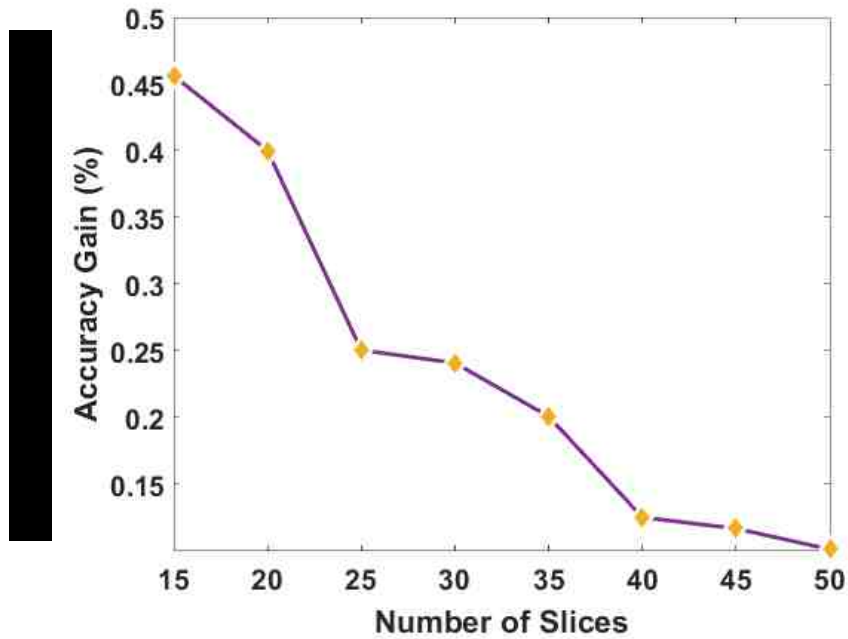
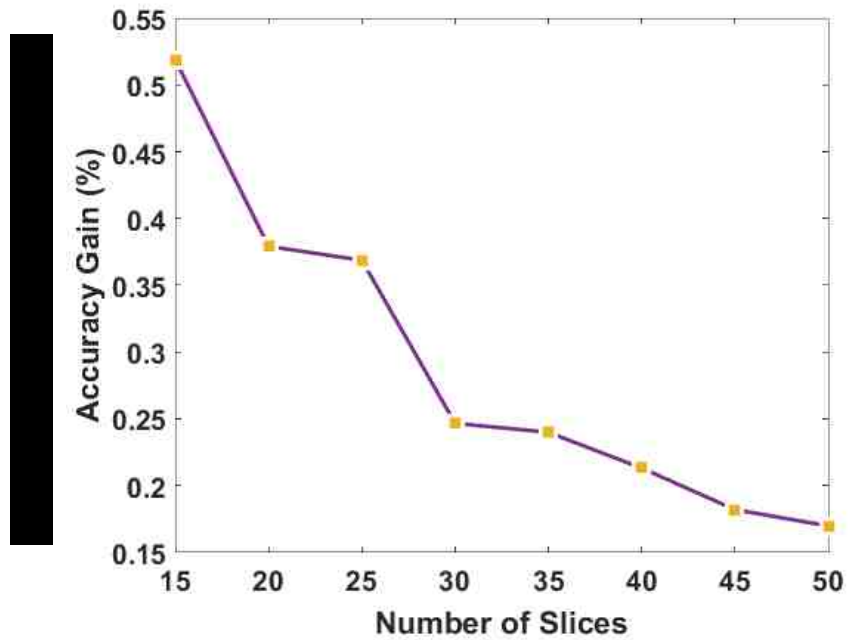
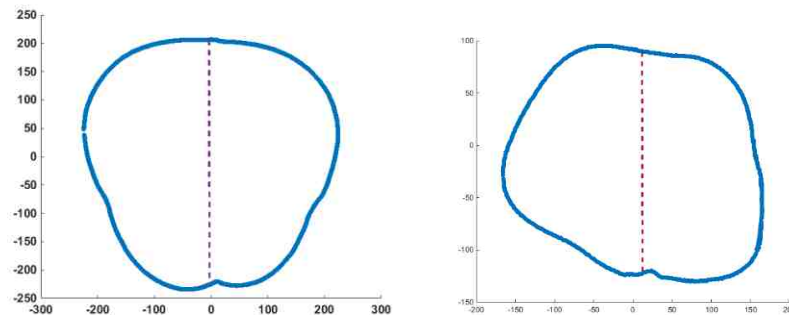


Figure 4.2. Plot shows the number of slices per torso and the improvement in the values of the estimated AI. Top panel was for the male torso models and the bottom panel corresponds to the female torso models. The value corresponding to 15 slices in the plot shows the difference in AI estimated from 10 slices.

## 4.4 Estimation of Asymmetry Index

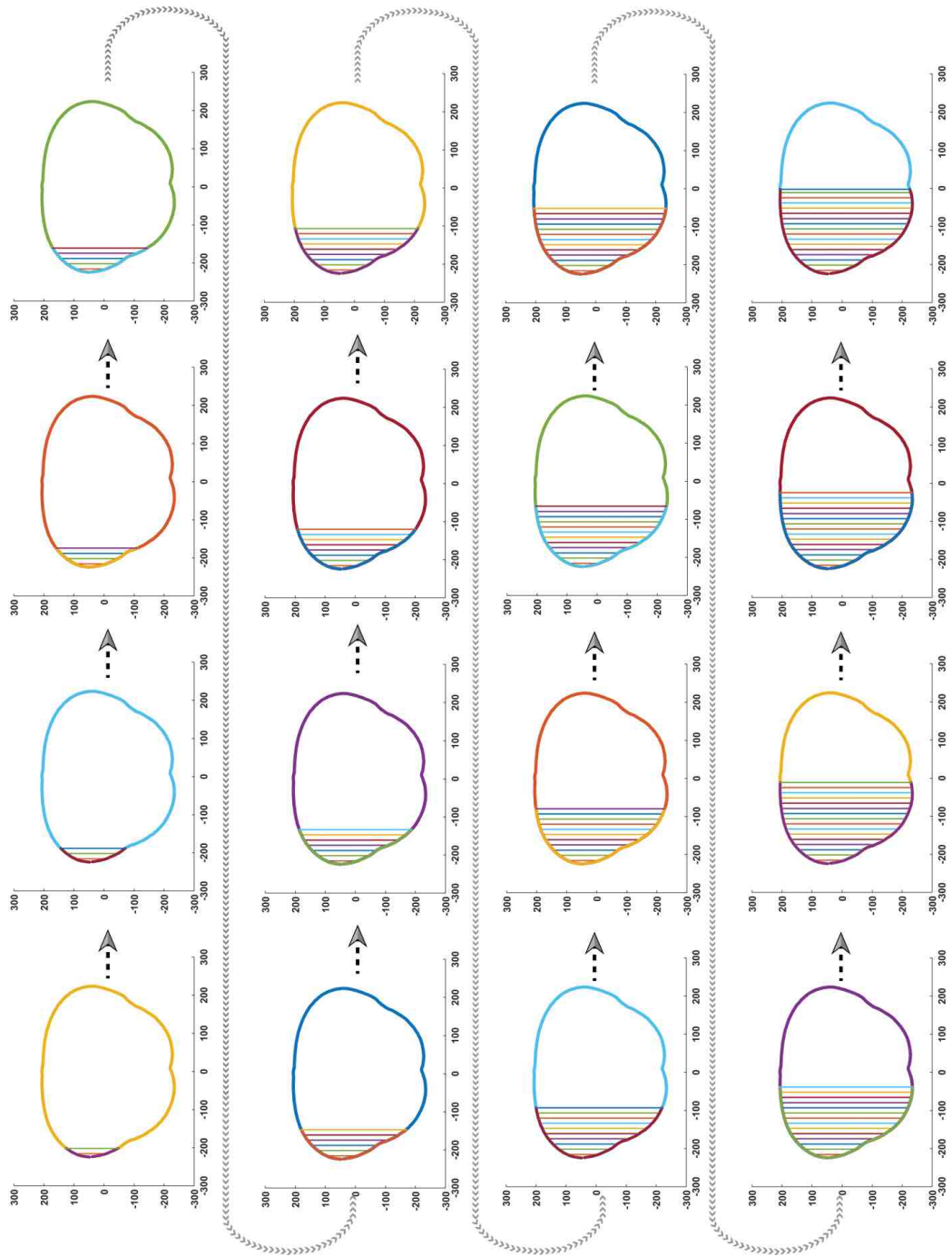
### 4.4.1 Estimating the local and global lines of symmetry.

Figure 4.3 shows the local plane of symmetry of a typical cross section extracted from a male and a scoliosis affected female subject. The sliding plane (described in section 3.3) divides the cross section progressively. The location at which the plane divides the cross section into two equal halves was registered as the local plane of symmetry. Figure-4.4 shows the progression of the sliding plane over a typical cross section. Its stepping factor for the sliding plane is shown here with a coarse resolution. The local plane of symmetry was estimated, likewise, for all the cross sections. Figure-4.6 and 4.7 show the lines of symmetry overlapped for all the slices.

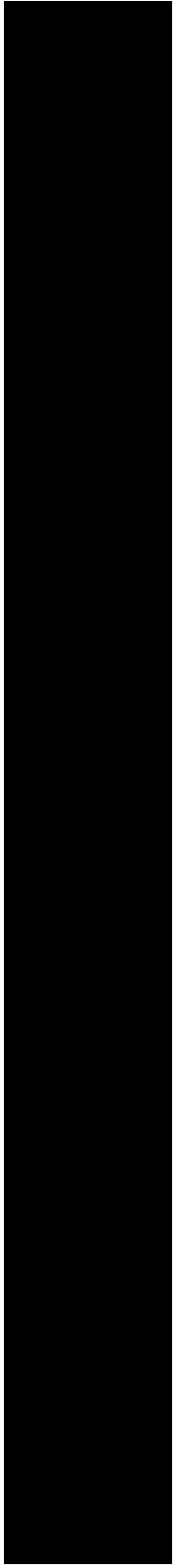
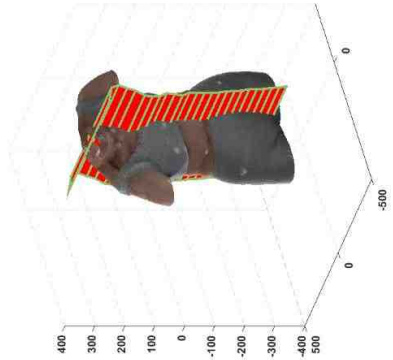
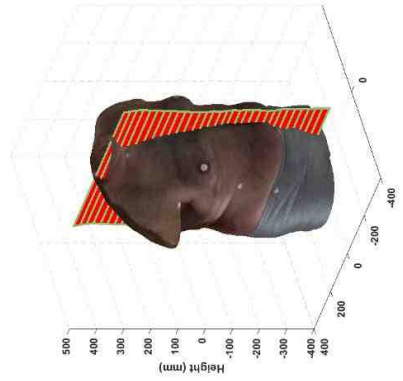
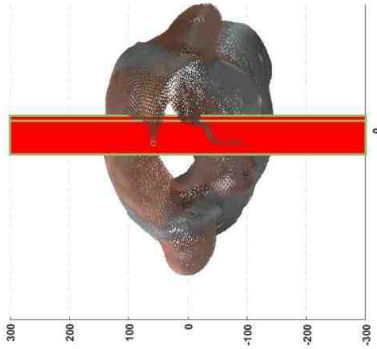
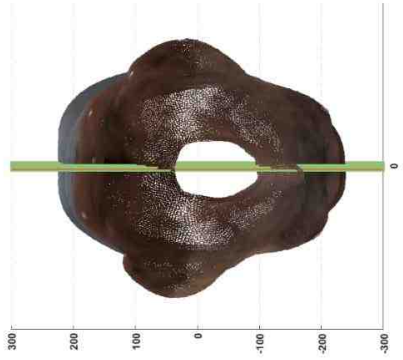
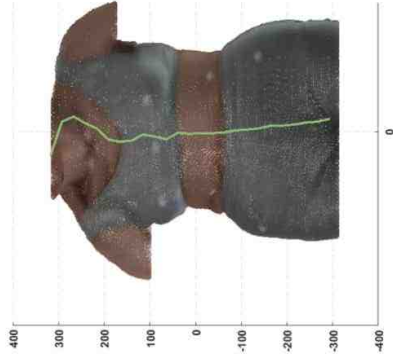
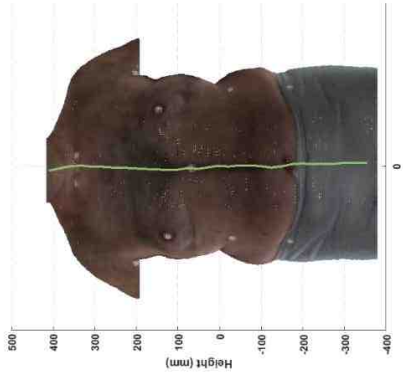


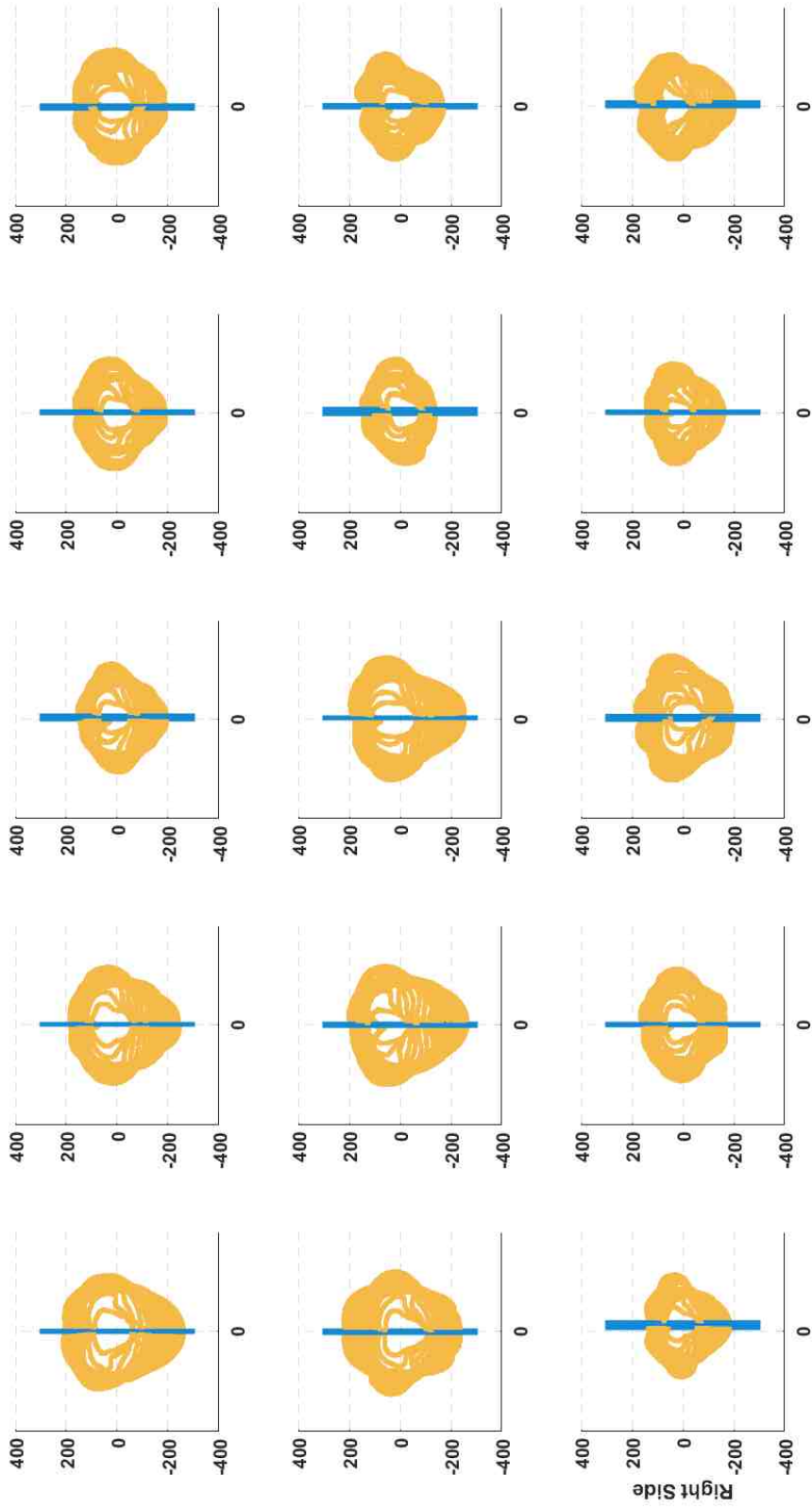
*Figure 4.3.* Typical cross sections and the local line of symmetry is shown. The left panel was from a male subject torso with less asymmetry and the right panel shows a cross section from a female subject model affected by scoliosis. It is visibly distinguishable and the shapes are not evenly distributed.

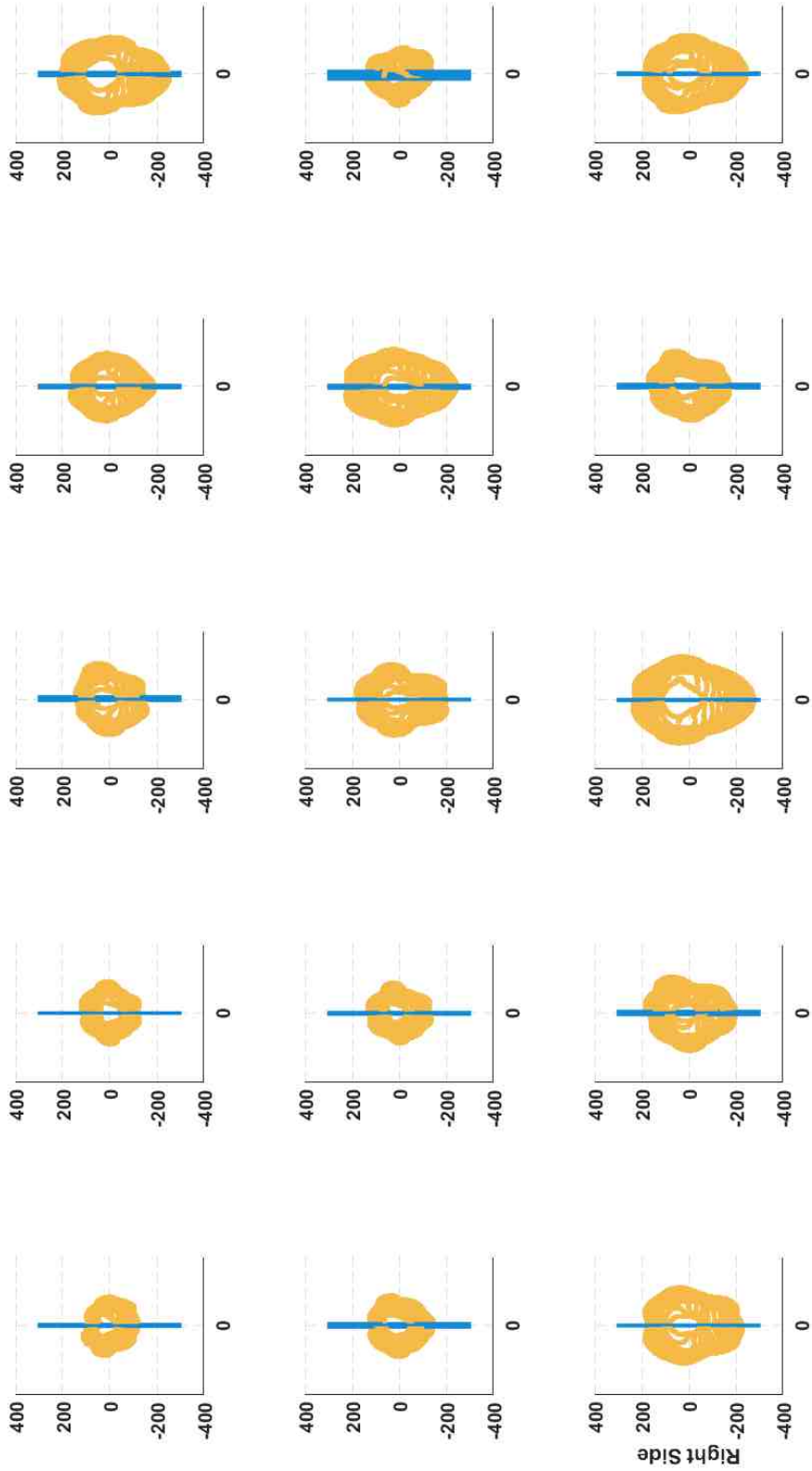




*Figure 4.4.* Schematic representation of the sliding plane on a typical cross section is shown. The area of the closed contour formed by the sliding plane in conjunction with the surface contour was computed at each step and compared with the overall area of the cross section to determine the local plane of symmetry. The progression is shown with a coarse resolution here.

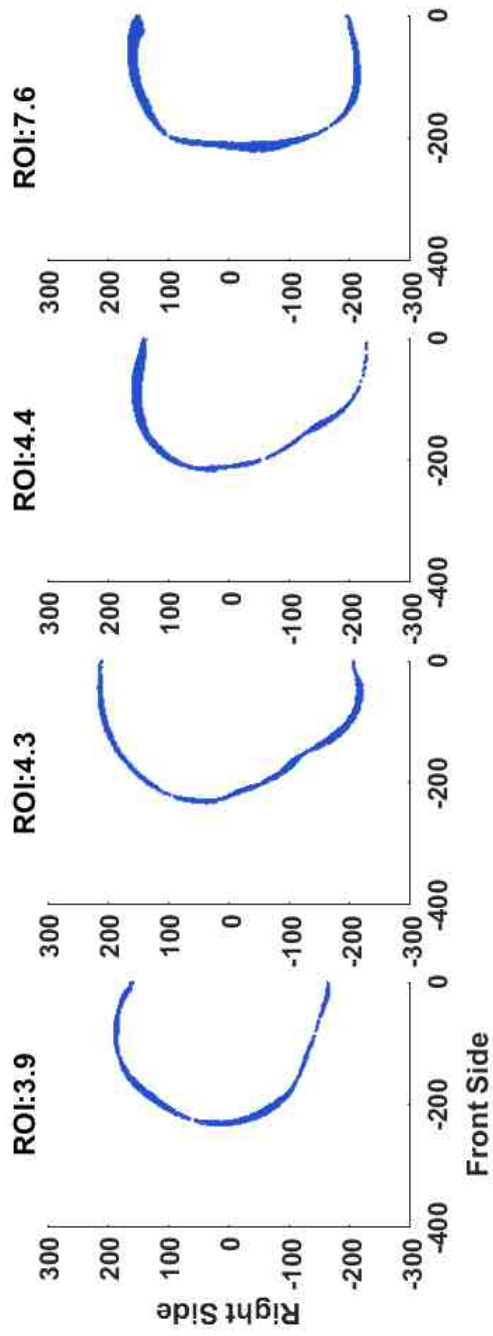
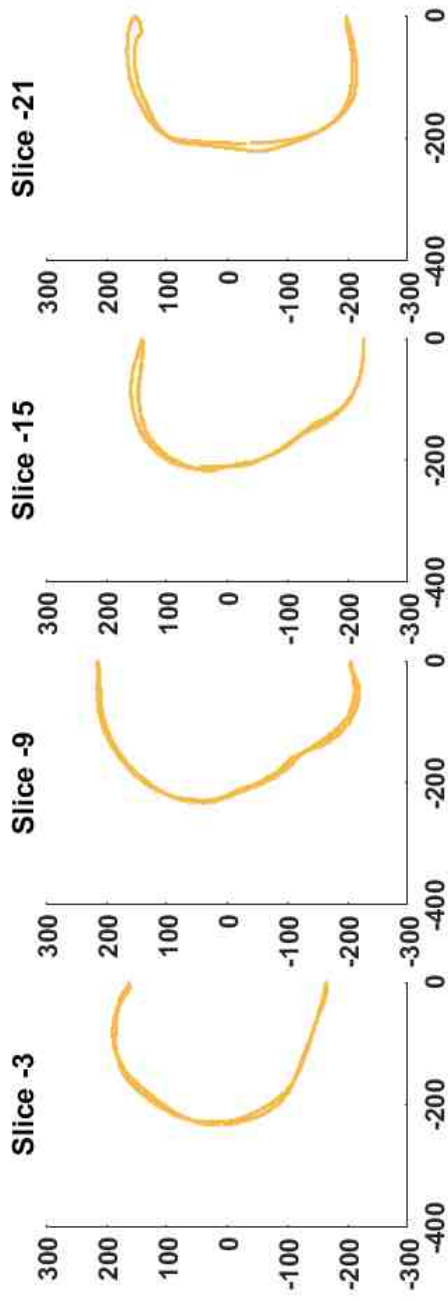






Front Side





Front Side

#### 4.4.2 Estimation of Asymmetry Index.

Based on the number of optimal slices, each of the torso models was subjected for AI estimation. Each cross section was mirrored at the plane of local symmetry, and ROI was computed (see Figure 4.8 for illustration). Likewise, the ROIs were computed for all the slices for a given torso and the AIs were estimated. Tables -4.1 shows the computed AI for the male and female subjects, respectively. The AI ranged between 5.55 and 13.31, with a mean of 8.63, for male subjects and 4.58 to 24.92 for the female subjects, with a mean of 8.45. For illustration, samples from the extremum are presented here (Figure 4.5), and the rest are included in the Appendix-C.

Table 4.1

#### *Asymmetry Indices of Male and Female Sample population*

| Subject | Asymmetry | Asymmetry |
|---------|-----------|-----------|
|         | Index (%) | Index (%) |
|         | Male      | Female    |
| 1       | 6.86      | 6.06      |
| 2       | 6.88      | 6.88      |
| 3       | 11.28     | 12.62     |
| 4       | 5.82      | 6.55      |
| 5       | 7.88      | 14.41     |
| 6       | 5.55      | 10.46     |
| 7       | 8.76      | 4.58      |

|           |       |       |
|-----------|-------|-------|
| <b>8</b>  | 10.84 | 4.92  |
| <b>9</b>  | 13.24 | 6.02  |
| <b>10</b> | 13.31 | 24.92 |
| <b>11</b> | 11.88 | 5     |
| <b>12</b> | 7.27  | 6.34  |
| <b>13</b> | 6.75  | 4.87  |
| <b>14</b> | 5.74  | 7.89  |
| <b>15</b> | 7.42  | 5.22  |

#### **4.5 Estimation of Torso Twist and Tilt**

Using the method described in section 3.5, the torso twist and tilt were computed. Table 4.2 and 4.3 show these measures for the male and female subjects, respectively.

Table 4.2

##### *Torso Twist and Tilt of Male Sample Population*

| <b>Subject</b> | <b>Overall Torso Twist (Deg.)</b> | <b>Upper Torso Twist (Deg.)</b> | <b>Lower Torso Twist (Deg.)</b> | <b>Torso Tilt (Deg.)</b> |
|----------------|-----------------------------------|---------------------------------|---------------------------------|--------------------------|
| <b>1</b>       | 1.13                              | 0.18                            | 1.31                            | 3.93                     |
| <b>2</b>       | 2.81                              | 1.2                             | 1.61                            | 2.97                     |
| <b>3</b>       | 6.97                              | 5.27                            | 1.71                            | 2.4                      |
| <b>4</b>       | 1.44                              | 4.2                             | 5.65                            | 0.54                     |

|           |      |      |      |      |
|-----------|------|------|------|------|
| <b>5</b>  | 5.72 | 1.79 | 3.93 | 4.36 |
| <b>6</b>  | 1.67 | 1.73 | 3.4  | 0.65 |
| <b>7</b>  | 5.35 | 2.75 | 2.6  | 0    |
| <b>8</b>  | 0.57 | 0.94 | 0.38 | 1.56 |
| <b>9</b>  | 4.06 | 2.54 | 1.52 | 3.41 |
| <b>10</b> | 0.44 | 0.78 | 0.34 | 4.88 |
| <b>11</b> | 1.67 | 0.81 | 0.86 | 5.2  |
| <b>12</b> | 5.49 | 3.41 | 2.07 | 0.95 |
| <b>13</b> | 3.31 | 4.38 | 1.08 | 9.09 |
| <b>14</b> | 3.67 | 1.45 | 2.22 | 1.98 |
| <b>15</b> | 4.12 | 1.73 | 2.4  | 2.19 |

The maximum degree of rotation of the torso for the male subjects was  $6.97^\circ$  and the minimum was  $0.44^\circ$ , with an average overall twist of  $3.23^\circ$ , upper torso twist of  $2.21^\circ$  and lower torso twist of  $2.07^\circ$ . The upper torso twist exceeded the lower torso twist for 7 subjects. Similarly, the minimum torso tilt was  $0^\circ$  and the maximum was  $9.09^\circ$ . The average tilt observed in the male data set was  $2.94^\circ$ .



Table 4.3

*Torso Twist and Tilt of Female Sample Population*

| <b>Subject</b> | <b>Overall Torso Twist (Degree)</b> | <b>Upper Torso Twist (Degree)</b> | <b>Lower Torso Twist (Degree)</b> | <b>Torso Tilt (Degree)</b> |
|----------------|-------------------------------------|-----------------------------------|-----------------------------------|----------------------------|
|                | 2.45                                | 1.48                              | 0.97                              | 0.65                       |
| <b>1</b>       | 0.27                                | 2.62                              | 2.35                              | 2.37                       |
| <b>2</b>       | 1.02                                | 1.78                              | 0.76                              | 0.56                       |
| <b>3</b>       | 2.22                                | 2.10                              | 0.12                              | 0.99                       |
| <b>4</b>       | 5.40                                | 2.38                              | 3.02                              | 8.28                       |
| <b>5</b>       | 4.86                                | 1.16                              | 3.70                              | 6.09                       |
| <b>6</b>       | 0.45                                | 1.44                              | 1.00                              | 0.79                       |
| <b>7</b>       | 0.55                                | 0.02                              | 0.57                              | 0.60                       |
| <b>8</b>       | 0.85                                | 1.64                              | 0.79                              | 2.05                       |
| <b>9</b>       | 9.70                                | 6.83                              | 2.87                              | 10.46                      |
| <b>10</b>      | 0.70                                | 1.79                              | 1.10                              | 0.58                       |
| <b>11</b>      | 0.66                                | 0.01                              | 0.66                              | 1.84                       |
| <b>12</b>      | 3.82                                | 2.40                              | 1.42                              | 0.26                       |
| <b>13</b>      | 4.66                                | 4.33                              | 9.00                              | 1.22                       |
| <b>14</b>      | 0.75                                | -NA-                              | -NA-                              | 1.66                       |
| <b>15</b>      | 4.12                                | 1.73                              | 2.40                              | 2.19                       |

The maximum degree of rotation of the torso for the female subjects was 9.69 ° and the minimum was 0.26°, with an average overall twist of 2.55 °, upper torso twist of 2.14°

and lower torso twist of 2.02°. The upper and lower twists were computed for 14 subjects due to missing landmark at the tenth rib for one subject. The upper torso twist exceeded the lower torso twist for 7 subjects. Similarly, the minimum torso tilt was 0.25° and the maximum was 10.45°. The average tilt observed in the female data set was 2.55°.

#### 4.6 Estimation of Deviance from the Principal Axis

To compare the deviance of the local line of symmetry from the principal axis in the z-direction, the shortest Euclidean distance between them was computed for each slice. The mean absolute deviance for each torso was then computed (see Table 4.4).

Table 4.4

*Deviance from the principal axis*

| Subject | Deviance Range (mm) | Deviance Range (mm) - |
|---------|---------------------|-----------------------|
|         | - Male              | Female                |
| 1       | 14.11               | 18.06                 |
| 2       | 10.82               | 7.77                  |
| 3       | 27.13               | 30.34                 |
| 4       | 16.99               | 21.28                 |
| 5       | 23.85               | 27.43                 |
| 6       | 19.86               | 29.85                 |
| 7       | 18.58               | 17.15                 |
| 8       | 12.05               | 9.86                  |
| 9       | 33.94               | 25.05                 |
| 10      | 19.71               | 60.79                 |
| 11      | 37.04               | 9.11                  |
| 12      | 14.13               | 27.74                 |
| 13      | 28.36               | 11.07                 |

|           |       |       |
|-----------|-------|-------|
| <b>14</b> | 14.37 | 29.59 |
| <b>15</b> | 28.39 | 15.18 |

#### 4.7 Validation of the Developed Method

The subjective evaluation comprises perception ratings of three apparel experts on the degree of asymmetry and twist for all the 30 subjects. The ratings obtained from the experts are shown in Table 4.5 . Inter-rater reliability between the three experts was calculated by the Intra-class correlation coefficient (ICC). SPSS 21.0 was used to perform the calculation. The ICC for asymmetry ratings was 0.86 and for twist was 0.67. The coefficients show that the reliability can be considered excellent for asymmetry ratings and good for twist ratings.

Table 4.5

*Mean Asymmetry and twist ratings of three experts(Likert Scale of 1to 4)*

| <b>Subject</b> | <b>Male</b>              |              | <b>Female</b>            |              |
|----------------|--------------------------|--------------|--------------------------|--------------|
|                | <b>Asymmetry Ratings</b> | <b>Twist</b> | <b>Asymmetry Ratings</b> | <b>Twist</b> |
| <b>1</b>       | 1.67                     | 1.00         | 1.33                     | 2.67         |
| <b>2</b>       | 1.67                     | 1.00         | 1.00                     | 1.67         |
| <b>3</b>       | 2.00                     | 1.33         | 1.67                     | 1.33         |
| <b>4</b>       | 1.33                     | 1.67         | 3.00                     | 2.33         |
| <b>5</b>       | 1.33                     | 1.00         | 3.33                     | 2.33         |
| <b>6</b>       | 1.67                     | 1.33         | 3.33                     | 2.00         |

|           |      |      |      |      |
|-----------|------|------|------|------|
| <b>7</b>  | 1.33 | 1.00 | 1.33 | 2.00 |
| <b>8</b>  | 2.33 | 2.00 | 1.00 | 1.00 |
| <b>9</b>  | 3.33 | 1.33 | 1.33 | 1.67 |
| <b>10</b> | 2.33 | 1.33 | 4.00 | 3.33 |
| <b>11</b> | 3.67 | 2.00 | 2.33 | 1.67 |
| <b>12</b> | 1.33 | 1.00 | 1.33 | 1.33 |
| <b>13</b> | 2.00 | 1.67 | 1.33 | 1.00 |
| <b>14</b> | 1.33 | 1.00 | 2.67 | 1.33 |
| <b>15</b> | 1.67 | 2.00 | 2.00 | 1.33 |

#### **4.7.1 Known Geometry Validation.**

The known geometry described in section 3.6.1 was processed using the developed method for validating the algorithm. Figure 4.9 shows the outcome of the validation. The global line of symmetry is a single plane passing through the centroid of the object. An estimated asymmetry of '0.0e-12' shows that the object is perfectly symmetric, as expected.

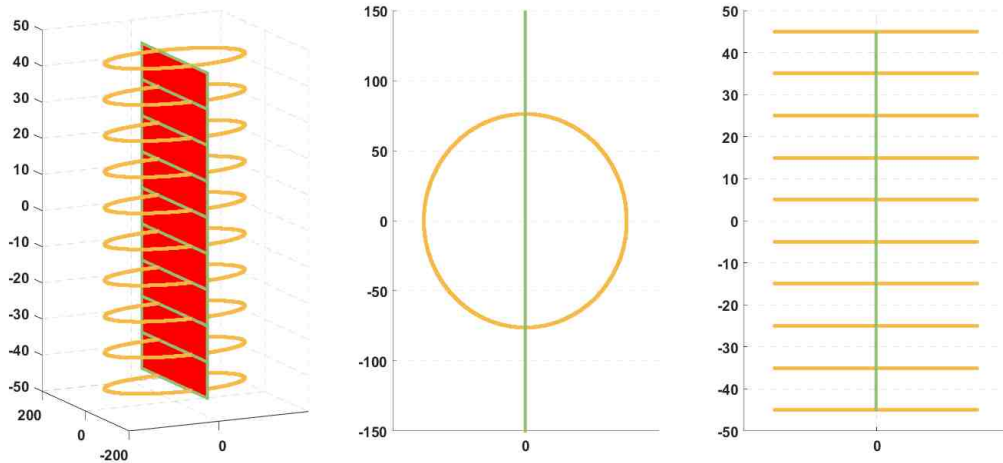


Figure 4.9. The global plane of asymmetry on the known geometry is a single plane that runs through the centroid of the object.

#### 4.7.2 Validation by Comparison With Subjective Expert Ratings.

The following hypotheses were tested that compares the statistical correlations between the developed objective measure and subjective ratings for the AI and twist in order to validate the developed method.

$H_0^1$ : *There is no significant correlation between  $AI_{Obj}$  and  $AI_{Sub}$*

$H_1^1$ : *There is a significant correlation between  $AI_{Obj}$  and  $AI_{Sub}$*

$H_0^2$ : *There is no significant correlation between  $TT_{Obj}$  and  $TT_{Sub}$*

$H_1^2$ : *There is a significant correlation between  $TT_{Obj}$  and  $TT_{Sub}$*

Where,

- a.  $AI_{Obj}$  - Asymmetry Index by the developed method
- b.  $AI_{Sub}$  - Asymmetry Index by experts

- c.  $TT_{Obj}$  – Overall Torso Twist by the developed method
- d.  $TT_{Sub}$  - Torso Twist by experts

Pearson correlation was calculated to test the hypotheses, and the results showed that there is a significant correlation between the objective and subjective values for asymmetry, with a coefficient of 0.72 (p-value = 0.0001, alpha = 0.05). The strong positive relationship between the objective asymmetry index and subjective asymmetry ratings clearly shows that the developed method characterizes asymmetry as perceived by the raters. On the contrary, the correlation between the  $TorsoTwist_{Obj}$  and  $TorsoTwist_{sub}$  was 0.245, with no significant relationship. No significant relationship between the objective and subjective evaluation for torso twist shows that the perceived twist was different than estimated. This contradiction could be due to the obscuring nature of the torso surface on the deformity at skeletal level. This can be further substantiated by the result showing a significant negative relationship ( $r = -0.46$ ) between weight and subjective twist ratings. When the weight increases, the subjective torso twist ratings decreases, in the sense, skeletal deformations might have been obscured by the muscular nature of the body. When the subject is less in weight and with a twist in the torso, it might have been visually trivial to rate and is in agreement with the negative correlation trend. Since the torso twist in this study was calculated using bone landmarks, the calculated measures are mathematically valid.

#### 4.8 Relationship between Variables.

The following six variables were tested for their correlations among each other,

- a. Weight
- b.  $AI_{Obj}$  - Asymmetry Index by the developed method
- c.  $AI_{Sub}$  - Asymmetry Index by experts
- d.  $TT_{Obj}$  – Overall Torso Twist by the developed method
- e.  $TT_{Sub}$  - Torso Twist by experts
- f. Tilt – Torso tilt by the developed method

The Pearson correlation was calculated to test the relationship between several objectively calculated variables. Results (see Figure 4.10) showed that there is no significant relationship between weight and  $AI_{Obj} / AI_{Sub}$ . Between the objective asymmetry index and overall torso twist, there is a strong significant positive relationship with a correlation value of 0.6 (p-value =0.0001, alpha = 0.05). This shows that the torso asymmetry on the sagittal plane is associated with the torso twist on the transverse plane. Since the relationship is positive, the asymmetry of the torso would increase with increase in torso twist, and vice versa. Similarly, there was a strong significant relationship between objective asymmetry index and torso tilt ( $r = 0.67$ , P-value = 0.0001, alpha = 0.05). The result shows that the asymmetry in the torso is positively related with the torso tilt, which characterizes the bend of the body. Thus, the degree of asymmetry increases with increasing bend in the body. Finally, the correlation between torso twist and torso tilt was 0.47 and it was significant with p-value of 0.009 (alpha = 0.05). It is clear, that the torso twist and tilt are positively related; however, the strength of the

relationship is moderate compared to the magnitude of other variables. The scale to interpret the strength of relationship between the variables was based on the guidelines of Cohen (1988), a commonly used source found in the literature.

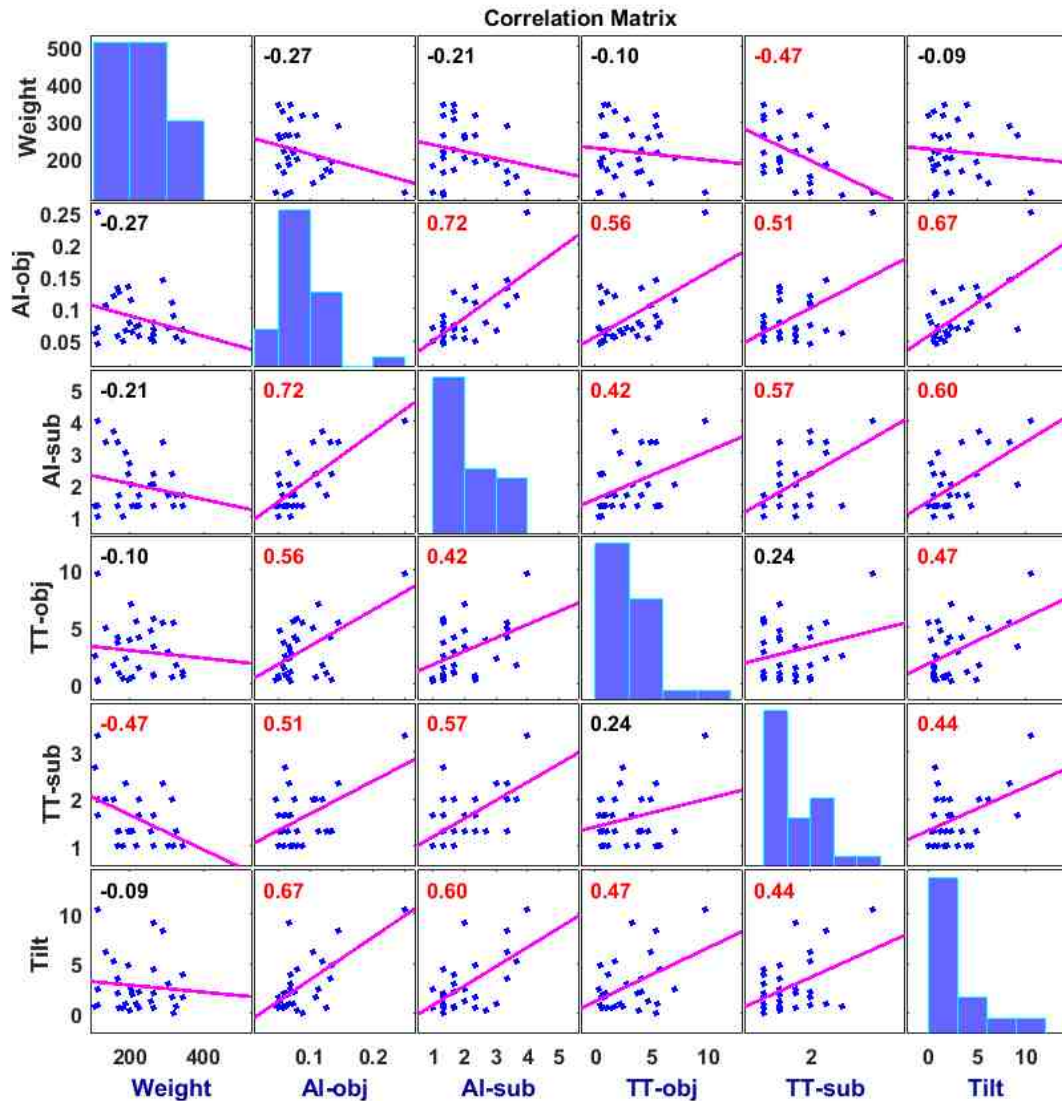


Figure 4.10. Relationship between the six variables – Weight, AI-obj, AI-sub, TT-obj, TT-sub and Tilt. The numbers within each panel shows the corresponding correlation values (red colored numbers are significant at an alpha of 0.05).



## **CHAPTER V**

### **Discussions**

Asymmetry has been agreed, consensually, as a phenomenon prevailing in human torso. However, its estimate is remaining largely subjective due to lack of reliable objective methods. In this research, a novel method to estimate the degree of asymmetry in a human torso was developed and validated. This method used digital representations of human torsos obtained from a repository (CAESAR) of 3D scans, and is a surface topography-based technique that detects local plane of symmetry in 2D cross sections and links them across the entire volume to estimate the global plane of symmetry in 3D space. The line of symmetry was estimated independent of anatomical landmark references. However, the entire 3D torso was corrected for its orientation using a global frame of reference in the Cartesian space before the cross sections were extracted. Area of the cross section was the parameter on which the local line of symmetry was estimated. Alternatively, the local plane of symmetry could be computed using Euclidean distance from the extremum as a parameter. Nevertheless, that would be a 1D parameter and is relatively sensitive to contour deviations in cross sections when compared to a 2D measure, such as the area. Another approach to compute the

global plane of symmetry would be to use the principal axes themselves as a guiding plane that divides the torso. This method may be quite trivial and computationally less expensive, but would lack the spatial resolution needed for several medical applications such as scoliosis recovery, i.e., it may not be able to provide localized degree of symmetry and how it propagates across the torso. Another approach could be to use the principal axes on the 2D cross sections as the local plane of symmetry. However, it is prone to errors due to physiological variations and requires human intervention to ascertain the correct orientation (see Figure-5.1).

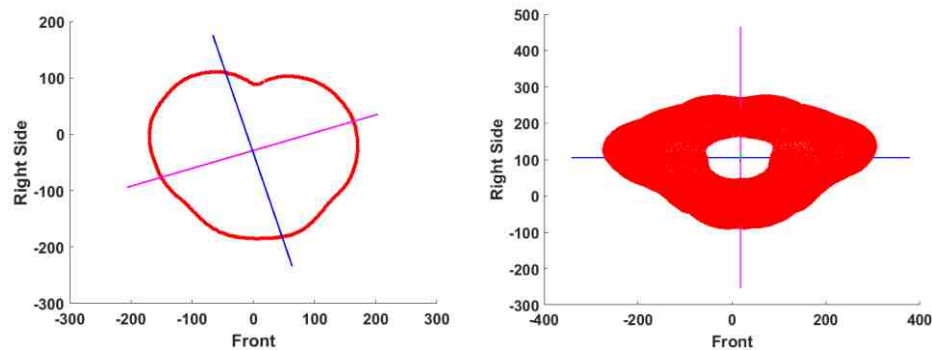


*Figure 5.1.* (Left) shows the principal axes obtained from an individual cross section and (right) shows the principal axes estimated for the entire 3D object. The 3D principal axes predicts the orientation with minimal errors.

The presented method has been optimized to capture adequate spatial information along the torso via the varied slice densities, and is relatively robust to several scan errors.

Subsequently, torso twist and tilt were also calculated by measuring the angles in skeletal structures using landmarks installed on the subjects before scanning. This method allows analysis of human torso at two characteristic levels, i.e., the asymmetry at the surface

topology and the twist/tilt at the skeletal conformations. Subsequent sections of this chapter discuss, (i) the generalizability of the developed method, (ii) key characteristics obtained from the analyses and (iii) the importance and applicability of the method to the fields of apparel and medical/rehabilitation.

### **5.1 Generalizability of the Method**

In the present study, the plane of symmetry was computed in the sagittal plane. The technique, however, is general and can be applied to other planes including transverse and coronal directions. Furthermore, the method is less constrained in terms of the definition of what comprises a torso. In this work, torso was defined to be extended from cervicale to crotch. However, depending on the application, the torso region can be redefined, say for example, from cervicale to trochanter landmark. Likewise, though the definition of orientation was based on the principal axes of the torso, it can be heuristically defined by a researcher or a user based on their application. The rest of the asymmetry computation is modular, following the orientation definitions, and is not dependent on any particular orientation.

The technique of computing the cross sectional area was based on the Green's theorem. It uses a line integral to compute the area of a closed surface. This is advantageous in cases where the 3D representation is a surface contour rather than a filled volume, such as in the present case where the scanner captures 3D surface topography alone. If the cross section happens to be a mesh rather than a contour, other methods of triangulations can be employed to compute the area, but at the expense of computational intensity. The present method is particularly advantageous in terms of its simplicity and robustness, and

is based on strong mathematical techniques. Furthermore, the technique is not dependent on the type of image capturing system. If a 3D object cloud can be represented in terms of its Cartesian positions, the technique would allow us to compute its asymmetry.

This study used specific numbers of cross sections for the male and female populations, i.e., 30 slices for the male subjects and 25 for the females. The number of slices was varied from 10 to 50 per torso model and was optimized for the acquired numerical accuracy of the AI. It was heuristically determined to optimize for an accuracy gain of 0.25%. But, if an application demands additional accuracy, the number of slices can be increased trivially. While setting the number of slices constant for a population normalizes any bias due to varying torso heights, an alternative approach could be to use a preset number of slices per unit height. For example, it could be set as 2 slices per inch of the torso height. This would allow us to estimate AI under a constant slice density.

## **5.2 Characteristics of the Findings**

### **5.2.1 Findings of the Objective measure.**

One of the major findings is that the lower bound of the AI in the sample population was around 4%, with a maximum of ~25% for a scoliosis patient. The lower bound supports the consensus on anthropometric asymmetry being ubiquitous in humans. For the male subjects, the lower bound was 5% and for females, it was 4%. Another key finding is the de-correlation between weight and asymmetry in the torso. This finding is contradictory to what was reported by Manning (1995) using bilateral traits. In his report, bilateral traits such as ear height, wrist, length of second digit and length of fifth digit were measured for 31 adult males and 39 adult females to estimate asymmetry. Results from his study

showed that there was a positive relationship between mean asymmetry and body weight for female adults, meaning that light females were more symmetric than heavy females. On the other hand, males showed a negative relationship between asymmetry and body weight, meaning that heavy males were more symmetric than light males. These results denote a key difference on the influence of the method of computing asymmetry, and shows that torso asymmetry is not identical to bilateral asymmetry. In the present study, no relationship was found between the weight, and torso twist and tilt measures. Based on the findings, it appears that weight may not be an influencing factor on torso asymmetry.

The twist computed in this study was based on the landmarks projected on the transverse plane, and the tilt was estimated from the projections on the coronal plane. These two components put together forms the twist vector in the 3D space. However, resolving it into 2D twist and tilt provides additional spatial information. And, it is trivial to compute these measures based on ground reference or any other specific global coordinate system.

The computed twist and tilt of the torso shows that twist and tilt are present to certain degree even in human subjects who were perceived to appear without deformations in the torso region. And, there were strong correlations between AI and twist, AI and tilt, and twist and tilt. It can be asserted that these three variables are to some extent influencing each other, and when computed together can adequately capture the characteristic of deformation in a human torso, even in extreme cases such as scoliosis.

In this method, the local line of symmetry was computed iteratively and then progressively linked in the third dimension. The progression of the global plane of symmetry in the transverse axis can serve as a fingerprint of asymmetry for a given

subject. The visual representation of this plane can serve as a proxy to ascertain symmetry or asymmetry of a human torso. For example, the path length of the plane would be minimal for a subject being symmetric, and would display larger variance in its path length if the subject is highly asymmetric.

### **5.2.2 Findings on the Validation.**

Comparing the computed values of AI and torso twist with the subjective ratings of three apparel field experts showed good correlation between the objective and subjective methods. The subjective ratings were tested for their inter-rater reliability using the standard intra-class correlation (ICC) on a scale of 0 to 1, with 1 being highly reliable. The ICC for asymmetry rating was 0.86 and was 0.67 for the twist ratings. According to Fleiss (1981), and Cicchetti and Sparrow (1981), values 0.6 to 0.74 are considered 'good' and values greater than 0.74 are considered 'excellent'. Thus, the reliability obtained for both asymmetry and twist are high and falls in the category of good and excellent. Finally, the correlation of the developed method was computed between the AI and the subjective asymmetry ratings. And, a significant correlation was found between the computed and manual ratings. On the contrary, the correlation between overall torso twist and torso ratings was found not to be significant. Typically, the twist and tilt deformations are at the skeletal level and often obscured by muscular structures. Since the raters were presented only with a surface representation of the torso without any landmark information, the perceived twist and tilt were based purely on the surface topography, excluding the skeletal information. This might be a possible reason for the lack of significance between the two methods.

### **5.3 Applicability of the Method**

The developed method has potential to be applied in various fields for multiple purposes. The method is suitable for both 2D and 3D surfaces and can compute asymmetry as long as a closed contour can be formed. For research domains, the methods can serve as an evaluation tool and also as a means to test hypotheses pertaining to asymmetry. Two major fields of application are discussed here, i.e., (i) apparel and (ii) medicine/rehabilitation. In case of apparel, the method serves as an evaluation tool to quantify asymmetry and in the latter case can be applied to test rehabilitation results.

#### **5.3.1 Application to Apparel Field.**

Dress forms are used extensively in apparel domain to creating patterns, fit evaluation/alteration, size grading, draping and for visual merchandising. Generally, the dress forms for apparel industry are created using anthropometric surveys as the basis (Chan and Peng, 2014). Varying shapes of dress forms are created to represent typical population, special population and partial body shapes. It is claimed that these dress forms are symmetrical, and manufactures develop the forms by creating an imaginary symmetry line (why your clothes don't fit, 2001). For instance, Alvanon is a dress form manufacturing company that creates mannequin from 3D body scans. In the creation process, subsequent to the scan acquisition, the 3D digital form is adjusted for symmetry and balance to ensure symmetry in the final dress form. There could be certain in-house practices to ensure symmetry, but, no standard objective methods are employed in assessing symmetry in the final form. Using the presented method, symmetry in the dress forms can be trivially measured and corrected for. Also, if dress forms are created for

individuals to develop custom clothing, and are based on their 3D scans, the deviance of the final dress form and the individual can be compared using the present method.

Similar to dress forms, fit models are extensively used in the apparel field during prototype development and evaluation. They serve as live mannequins. One of the primary features demanded for an apparel fit model is symmetry, along-side a well-proportioned and balanced body structure (True Model Management, n.d). Symmetry in the body and face was also studied for attractiveness, and people with symmetrical face and body were considered attractive. These requirements are quite common in the fashion advertisement industry. Companies often prefer their fit model, both for production and advertisement, to be balanced and symmetrical to maximize the rate of attractiveness. It is evident that symmetrical body is more than a desired criterion to serve as a fit model, and the developed method has potential to aid model agencies and the apparel industry to evaluate symmetry in their models.

Additionally, standard sizing charts are based on anthropometrical body measurement data, and it is assumed that the human body is highly symmetrical. Traditional pattern making too uses the same assumption. However, this widely used assumption has never been hypothetically tested - specifically on the torso region. The developed method could possibly be used in validating the assumption on symmetry, and can offer new ways to improve pattern adjustments objectively, in case the assumption appears violated. There is a potential possibility that the classification of body shapes can be resolved further based on the degree of symmetry/asymmetry.



Finally, apparel experts are quite familiar with the inconsistencies of fit induced by asymmetry in various body parts. Fit mapping is one of the well-known and established methods to quantify fit of any product human wear. Fit mapping score might be affected by asymmetry of a given body. The relationship between fit-mapping score and asymmetry has never been explored thus far, and the developed method can serve as a means to such a study. Perhaps, it is even possible to derive an adjustment coefficient to correct the influence of asymmetry on apparel fit.

### **5.3.2 Application to Medicine/Rehabilitation.**

Asymmetry in torso can be caused by deformity in the regions of thorax, pelvis and/or shoulder, fat accumulation, weight change and muscle growth. One such pathology that combines deformations in more than one region is scoliosis. It is a pathological condition in which deformation of spine prevails in the lateral deviation and axial rotation of the vertebrae. Due to the deformation, noticeable range of tilt and asymmetries in the region of shoulder, scapula, waist and hip becomes unavoidable. Typically, the scoliosis is detected by radiographic information and its severity is determined by Cobb angles estimated from X-ray images. Besides initial diagnosis, patients have to periodically undergo X-ray examination, typically once every six months. Due to the nature of repeated radiation, subjects are susceptible to health risks and may even lead to DNA mutation and cancer. Thus, there is a need to quantify scoliosis-induced asymmetry using a non-invasive method entailing the reduction of radiation exposure (Liu, 2013). The developed method can serve as a potential alternative to the existing approach and meet the requirement of non-invasiveness towards measuring asymmetry in scoliosis patients.

It is noteworthy that the technique does not require any harmful radiation scanning components.

Scoliosis patients often express concerns about their external appearance, and studies found that their appearance are not only affecting their social attendant but also depriving them psychologically (Dickson, 1999). The existing clinical standard method does not quantify the torso surface in the 3D space. Rather, X-rays of 2D spine images are used to quantify the scoliosis, and the whole 3D body surface is often neglected. This further limits the estimation of torso rotations. With the newly developed method, twist and tilt of the whole torso is also characterized providing a more holistic approach to study deformation in the torso region. Thus, in general, the developed method might help quantifying asymmetry, twist and tilt in scoliosis patients using 3D surface and skeletal structure without introducing any harmful ionizing radiations. This technique can possibly be applied to classify severity of deformation due to scoliosis.

Currently, in the United States, certain states governments require screening of public school children to detect scoliosis in its very early stage. The developed method can be easily implemented to collect the scans at schools and then the scans can be processed later for quantification. This drastically reduces the time and effort compared to the existing methods. Besides, tracking the level of changes in the indices for children across different time period can be a very convenient metric.

Another potential application of this method is to measure the efficiency of surgical procedures performed on scoliosis patients. Patients' appearance scores can be calculated in the pre and post-surgical instances to measure the improvements in symmetry and

torso appearance. Likewise, efficacy of scoliosis braces in increasing the degree of symmetry can be studied using the developed method. There is no known surface method that calculates asymmetry, torso twist and tilt with braces mounted on the subjects. Thus this method can potentially be used in evaluating torso appearance with braces. Similarly, the improvements in asymmetry, twist and tilt due to rehabilitation and/or physical therapy can be estimated using the developed method.

Another potential area of application for the developed method would be in evaluating the body asymmetry for professional body builders. In Mr.Olympia, symmetry of the body is considered as one of the important criteria for participation and securing a winning position in the competition. Currently, symmetry is being visually inspected or with primary linear measurements, and participants do not have a rapid measurement method to validate their symmetry as they prepare for the competition. The developed method can be potentially used for the purposes of evaluating symmetry across training and participation.

## **CHAPTER VI**

### **Conclusions**

A general assumption about human body is that it is bilaterally symmetric. And, this assumption has lead researchers look for a single plane that divides a human body volumetrically. In reality, human body is a three dimensional object and it needs to be perfectly symmetric for such a plane to exist. However, majority of human body shapes exhibit asymmetry at different degrees. While it is possible to obtain a close approximation of a single plane to volumetrically divide the torso into two halves, it can be accomplished only by compromising the local variations in the symmetry that may be key characteristics for several applications.

Asymmetry of human body is an important measure that is being used largely subjectively in the field of medicine and design. Objective measures such as Cobb-angle require invasive scanning aided by X-rays. Any user-centered product that makes use of whole body measurements should consider asymmetry as a criterion in the design process. So far, asymmetry in human body has been measured by estimating differential linear measurement of bilateral traits. However, the characteristics of asymmetry can be better understood and be useful for clinicians and designers if it is quantified by considering the whole 3D surface. Thus, the primary objectives of this research are,

- (i) To develop a novel non-invasive method for estimating the rate of asymmetry in the 3d human torso to serve as a characteristic and evaluation tool
- (ii) To develop a system for quantifying an estimated degree of asymmetry using surface structure and skeletal structure of the torso
- (iii) To estimate the degree of twist in the transverse plane and tilt present in the coronal plane of a torso

## **6.1 Summary**

In this work, a novel method was developed to quantify the degree of asymmetry in human torso. Digitized representations of human body were sampled from a repository and the torso regions were extracted using a software utility. The developed method uses cross-sections of the torso to progressively estimate the asymmetry of the whole body. Furthermore, the study estimated the degree of twist and tilt in human torso. The twist and tilt were calculated by using the bone landmarks. Put together, the study quantifies asymmetry in the body by taking into consideration both the body surface and the skeletal structure. Asymmetry index was derived from the whole body surface and the twist and tilt were derived from anatomical landmarks structure. Additionally, the developed method is a non-invasive technique and relatively safer to use repeatedly. These methods provide a better understanding of torso deformity in all the three dimensions. Based on the developed method, the asymmetry index calculated for both male and female shows that both gender have asymmetry of 7% on an average. With a minimum asymmetry of ~5%, it appears no human body is symmetric in this representative population. Body asymmetry/symmetry is a key measurement in the field of growth development. Using this new measure, characteristics of growth in terms of symmetry can be easily studied

and tracked. Similarly, in the field of medicine, the method can be used for various evaluations. One of the key applications of this method is the quantification of torso deformity due to scoliosis. This method can provide valuable insights and information for clinicians working with scoliosis patients. In the field of design, this method could serve as an asymmetry measuring tool and products can be developed considering the asymmetry as an additional coefficient. Besides, the nature of bodily changes due to ageing can be tracked using this measure. Along with the bilateral trait asymmetry, torso asymmetry would be helpful understanding the nature of human body anthropometry.

## **6.2 Future Recommendations**

- 1) A sample population of scoliosis patients with mild to severe deformation can be evaluated using this new method, and correlations with existing measures such as the Cobb angle can be estimated. This would allow validating the method as a potential alternative to the existing invasive methods.
- 2) In the current work, subjective evaluation ratings were obtained from apparel experts alone. Ratings from experts in medicine/physiology can be obtained to increase the specificity of the findings for respective application domains.
- 3) Furthermore, the relationship between gait asymmetry and torso asymmetry could be tested and it can provide insights to the field of biomechanics.
- 4) The influence of asymmetry in the range of motion and daily activities is an additional area to be explored.
- 5) Possibilities to estimate twist and tilt based on surface deformity instead of planted landmarks have to be explored.

## REFERENCES

- Abdel Fatah, E. E., Shirley, N. R., Mahfouz, M. R., & Auerbach, B. M. (2012). A three-dimensional analysis of bilateral directional asymmetry in the human clavicle. *American Journal of Physical Anthropology*, *149*(4), 547–559.  
<http://doi.org/10.1002/ajpa.22156>
- Akbar, H., Hayat, K., Haq, N. ul, & Bajwa, U. I. (2014). Bilateral symmetry detection on the basis of Scale Invariant Feature Transform. *PloS One*, *9*(8), e103561.  
<http://doi.org/10.1371/journal.pone.0103561>
- Al-Eisa, E., Egan, D., & Wassersug, R. (2004). Fluctuating asymmetry and low back pain. *Evolution and Human Behavior*, *25*(1), 31–37.  
[http://doi.org/10.1016/S1090-5138\(03\)00081-3](http://doi.org/10.1016/S1090-5138(03)00081-3)
- Amunts, K., Jäncke, L., Mohlberg, H., Steinmetz, H., & Zilles, K. (2000). Interhemispheric asymmetry of the human motor cortex related to handedness and gender. *Neuropsychologia*, *38*(3), 304–312. [http://doi.org/10.1016/S0028-3932\(99\)00075-5](http://doi.org/10.1016/S0028-3932(99)00075-5)
- Arnold, F. (1844). *Handbook of Functional Anatomy* (1st ed.). Germany.
- Bashour, M. (2006). History and current concepts in the analysis of facial attractiveness. *Plastic and Reconstructive Surgery*, *118*(3), 741–756.  
<http://doi.org/10.1097/01.prs.0000233051.61512.65>
- Berg, D. C., Hill, D. D. L., Raso, V. J., Lou, E., Church, T., Moreau, M. J., & Mahood, J.

- K. (2002). Using three-dimensional difference maps to assess changes in scoliotic deformities. *Medical and Biological Engineering and Computing*, 40(3), 290–295. <http://doi.org/10.1007/BF02344210>
- Berlin, N. F., Berssenbrügge, P., Runte, C., Wermker, K., Jung, S., Kleinheinz, J., & Dirksen, D. (2014). Quantification of facial asymmetry by 2D analysis – A comparison of recent approaches. *Journal of Cranio-Maxillofacial Surgery*, 42(3), 265–271. <http://doi.org/10.1016/j.jcms.2013.07.033>
- Bokeloh, M., Berner, A., Wand, M., Seidel, H.-P., & Schilling, A. (2009). Symmetry Detection Using Feature Lines. *Computer Graphics Forum*, 28(2), 697–706. <http://doi.org/10.1111/j.1467-8659.2009.01410.x>
- Bunnell, W. P. (1984). An objective criterion for scoliosis screening. *The Journal of Bone & Joint Surgery*, 66(9), 1381-1387.
- Campbell, N. A., & Atchley, W. R. (1981). The Geometry of Canonical Variate Analysis. *Systematic Biology*, 30(3), 268–280. <http://doi.org/10.1093/sysbio/30.3.268>
- Chan, C. K., Peng, S. X., & Luximon, A. (2014). Design And Development Of An Interactive Robotic Mannequin For The Fashion Industry. *International Journal of Engineering Research & Innovation*, 5.
- Cicchetti, D. V., & Sparrow, S. A. (1981). Developing criteria for establishing interrater reliability of specific items: Applications to assessment of adaptive behavior. *American Journal of Mental Deficiency*, 86(2), 127–137.
- Cohen, J. (1988). *Statistical Power Analysis for the Behavioral Sciences*. 2nd edn. Hillsdale, New Jersey: L. Erlbaum.
- Cornelius, H., & Loy, G. (2006). Detecting Bilateral Symmetry in Perspective. In



- Conference on Computer Vision and Pattern Recognition Workshop, 2006.*  
*CVPRW '06* (pp. 191–191). <http://doi.org/10.1109/CVPRW.2006.63>
- Dawson, E. G., Kropf, M. A., Purcell, G., Kabo, J. M., Kanim, L. E., & Burt, C. (1993).  
Optoelectronic evaluation of trunk deformity in scoliosis. *Spine, 18*(3), 326–331.
- De Sèze, M., Randriaminahisoa, T., Gaunelle, A., de Korvin, G., & Mazaux, J.-M.  
(2013). Inter-observer reproducibility of back surface topography parameters  
allowing assessment of scoliotic thoracic gibbosity and comparison with two  
standard postures. *Annals of Physical and Rehabilitation Medicine, 56*(9–10),  
599–612. <http://doi.org/10.1016/j.rehab.2013.10.003>
- Denoel, C., Aguirre, M. F. I., Bianco, G., Mahaudens, P. H., Vanwijck, R., Garson, S., ...  
Debrun, A. (2009). Idiopathic scoliosis and breast asymmetry. *Journal of Plastic,  
Reconstructive & Aesthetic Surgery: JPRAS, 62*(10), 1303–1308.  
<http://doi.org/10.1016/j.bjps.2008.04.031>
- Dickson, R. A. (1999). Spinal deformity-adolescent idiopathic scoliosis: nonoperative  
treatment. *Spine, 24*(24), 2601.
- Drzał-Grabiec, J., Snela, S., Rachwał, M., Podgórska, J., & Rykała, J. (2014). Effects of  
Carrying a Backpack in an Asymmetrical Manner on the Asymmetries of the  
Trunk and Parameters Defining Lateral Flexion of the Spine. *Human Factors: The  
Journal of the Human Factors and Ergonomics Society, 0018720814546531*.
- Eder, M., Waldenfels, F. v., Swobodnik, A., Klöppel, M., Pape, A.-K., Schuster, T., ...  
Kovacs, L. (2012). Objective breast symmetry evaluation using 3-D surface  
imaging. *The Breast, 21*(2), 152–158. <http://doi.org/10.1016/j.breast.2011.07.016>
- Faro, F. D., Marks, M. C., Pawelek, J., & Newton, P. O. (2004). Evaluation of a

functional position for lateral radiograph acquisition in adolescent idiopathic scoliosis. *Spine*, 29(20), 2284–2289.

Fleiss, J. L. (1981). Balanced Incomplete Block Designs for Inter-Rater Reliability Studies. *Applied Psychological Measurement*, 5(1), 105–112.

<http://doi.org/10.1177/014662168100500115>

Fong, G. C. Y., Mak, Y. F., Swartz, B. E., Walsh, G. O., & Delgado-Escueta, A. V. (2003). Body part asymmetry in partial seizure. *Seizure*, 12(8), 606–612.

[http://doi.org/10.1016/S1059-1311\(03\)00138-9](http://doi.org/10.1016/S1059-1311(03)00138-9)

Frey, F. M., Robertson, A., & Bukoski, M. (2007). A method for quantifying rotational symmetry. *The New Phytologist*, 175(4), 785–791. <http://doi.org/10.1111/j.1469-8137.2007.02146.x>

Goldberg, C., Moore, D., Fogarty, E., & Dowling, F. (2001). Surface topography and the several components of scoliotic deformity. *Studies in Health Technology and Informatics*, 88, 67–69.

Gray, P. B., & Marlowe, F. (2002). Fluctuating asymmetry of a foraging population: the Hadza of Tanzania. *Annals of Human Biology*, 29(5), 495–501.

<http://doi.org/10.1080/03014460110112060>

Haapasalo, H., Kontulainen, S., Sievänen, H., Kannus, P., Järvinen, M., & Vuori, I.

(2000). Exercise-induced bone gain is due to enlargement in bone size without a change in volumetric bone density: a peripheral quantitative computed tomography study of the upper arms of male tennis players. *Bone*, 27(3), 351–357.

Huang, C. S., Liu, X. Q., & Chen, Y. R. (2013). Facial asymmetry index in normal young

- adults. *Orthodontics & Craniofacial Research*, 16(2), 97–104.  
<http://doi.org/10.1111/ocr.12010>
- Hume, D. K., & Montgomerie, R. (2001). Facial attractiveness signals different aspects of “quality” in women and men. *Evolution and Human Behavior: Official Journal of the Human Behavior and Evolution Society*, 22(2), 93–112.
- Jones, H. H., Priest, J. D., Hayes, W. C., Tichenor, C. C., & Nagel, D. A. (1977). Humeral hypertrophy in response to exercise. *The Journal of Bone and Joint Surgery. American Volume*, 59(2), 204–208.
- Kakarala, R., Kaliamoorthi, P., & Premachandran, V. (2013). Three-Dimensional Bilateral Symmetry Plane Estimation in the Phase Domain. In *2013 IEEE Conference on Computer Vision and Pattern Recognition (CVPR)* (pp. 249–256).  
<http://doi.org/10.1109/CVPR.2013.39>
- Keller, Y., & Shkolnisky, Y. (2004). An algebraic approach to symmetry detection. In *Proceedings of the 17th International Conference on Pattern Recognition, 2004. ICPR 2004* (Vol. 3, pp. 186–189 Vol.3).  
<http://doi.org/10.1109/ICPR.2004.1334499>
- Koehler, N., Simmons, L. W., Rhodes, G., & Peters, M. (2004). The relationship between sexual dimorphism in human faces and fluctuating asymmetry. *Proceedings of the Royal Society B: Biological Sciences*, 271(Suppl 4), S233–S236.
- Komori, M., Kawamura, S., & Ishihara, S. (2009). Averageness or symmetry: Which is more important for facial attractiveness? *Acta Psychologica*, 131(2), 136–142.  
<http://doi.org/10.1016/j.actpsy.2009.03.008>
- Kong, P. W., & De Heer, H. (2008). Anthropometric, gait and strength characteristics of

- kenyan distance runners. *Journal of Sports Science & Medicine*, 7(4), 499–504.
- Kowalski, I. M., Kotwicki, T., & Siwik, P. (2013). Analysis of diagnostic methods in trunk deformities in the developmental age. *Polish Annals of Medicine*, 20(1), 43–50. <http://doi.org/10.1016/j.poamed.2013.06.002>
- Letts, M., Quanbury, A., Gouw, G., Kolsun, W., & Letts, E. (1988). Computerized ultrasonic digitization in the measurement of spinal curvature. *Spine*, 13(10), 1106–1110.
- Li, W. H., Zhang, A. M., & Kleeman, L. (2008). Bilateral symmetry detection for real-time robotics applications. *The International Journal of Robotics Research*, 27(7), 785-814.
- Liu, S. X. (2009). Symmetry and asymmetry analysis and its implications to computer-aided diagnosis: A review of the literature. *Journal of Biomedical Informatics*, 42(6), 1056–1064. <http://doi.org/10.1016/j.jbi.2009.07.003>
- Liu, X.-C., Tassone, J. C., Thometz, J. G., Paulsen, L. C., Lyon, R. M., Marquez-Barrientos, C., ... Johnson, P. R. (2013). Development of a 3-Dimensional Back Contour Imaging System for Monitoring Scoliosis Progression in Children. *Spine Deformity*, 1(2), 102–107. <http://doi.org/10.1016/j.jspd.2012.10.006>
- Livshits, G., & Kobylansky, E. (1989). Study of genetic variance in the fluctuating asymmetry of anthropometrical traits. *Annals of Human Biology*, 16(2), 121-129.
- Maeda, M., Katsumata, A., Ariji, Y., Muramatsu, A., Yoshida, K., Goto, S., ... Ariji, E. (2006). 3D-CT evaluation of facial asymmetry in patients with maxillofacial deformities. *Oral Surgery, Oral Medicine, Oral Pathology, Oral Radiology, and Endodontics*, 102(3), 382–390. <http://doi.org/10.1016/j.tripleo.2005.10.057>

- Mancini, S., Sally, S. L., & Gurnsey, R. (2005). Detection of symmetry and anti-symmetry. *Vision Research*, *45*(16), 2145–2160.  
<http://doi.org/10.1016/j.visres.2005.02.004>
- Manning, J. T. (1995). Fluctuating asymmetry and body weight in men and women: Implications for sexual selection. *Ethology and Sociobiology*, *16*(2), 145–153.  
[http://doi.org/10.1016/0162-3095\(94\)00074-H](http://doi.org/10.1016/0162-3095(94)00074-H)
- Manning, J. T., & Pickup, L. J. (1998). Symmetry and performance in middle distance runners. *International Journal of Sports Medicine*, *19*(3), 205–209.  
<http://doi.org/10.1055/s-2007-971905>
- Manning, J. T., Scutt, D., Whitehouse, G. H., & Leinster, S. J. (1997). Breast asymmetry and phenotypic quality in women. *Evolution and Human Behavior*, *18*(4), 223–236. [http://doi.org/10.1016/S0162-3095\(97\)00002-0](http://doi.org/10.1016/S0162-3095(97)00002-0)
- Mardia, K., Bookstein, F., & Moreton, I. (2000). Statistical assessment of bilateral symmetry of shapes. *Biometrika*, *87*(2), 285–300.  
<http://doi.org/10.1093/biomet/87.2.285>
- Milne, B. J., Belsky, J., Poulton, R., Thomson, W. M., Caspi, A., & Kieser, J. (2003). Fluctuating asymmetry and physical health among young adults. *Evolution and Human Behavior*, *24*(1), 53–63. [http://doi.org/10.1016/S1090-5138\(02\)00120-4](http://doi.org/10.1016/S1090-5138(02)00120-4)
- Milner, D., Raz, S., Hel-Or, H., Keren, D., & Nevo, E. (2007). A new measure of symmetry and its application to classification of bifurcating structures. *Pattern Recognition*, *40*(8), 2237–2250. <http://doi.org/10.1016/j.patcog.2006.12.008>
- Minovic, P., Ishikawa, S., & Kato, K. (1993). Symmetry identification of a 3-D object represented by octree. *IEEE Transactions on Pattern Analysis and Machine*

- Intelligence*, 15(5), 507–514. <http://doi.org/10.1109/34.211472>
- Mitra, N. J., Guibas, L. J., & Pauly, M. (2006). Partial and approximate symmetry detection for 3D geometry. *ACM Transactions on Graphics (TOG)*, 25(3), 560–568.
- Møller, A. P. (1996). Parasitism and Developmental Instability of Hosts: A Review. *Oikos*, 77(2), 189–196. <http://doi.org/10.2307/3546057>
- Murray, C. J., & Lopez, A. D. (1997). Mortality by cause for eight regions of the world: Global Burden of Disease Study. *The Lancet*, 349(9061), 1269–1276. [http://doi.org/10.1016/S0140-6736\(96\)07493-4](http://doi.org/10.1016/S0140-6736(96)07493-4)
- Nowotny, J., Gaździk, T., Zawieska, D., & Podlasik, P. (2002). Photogrammetry: myths and reality. *Ortopedia, Traumatologia, Rehabilitacja*, 4(4), 498–502.
- O'Mara, D., & Owens, R. (1996). Measuring bilateral symmetry in digital images. In *TENCON '96. Proceedings., 1996 IEEE TENCON. Digital Signal Processing Applications* (Vol. 1, pp. 151–156 vol.1). <http://doi.org/10.1109/TENCON.1996.608740>
- Ozener, B. (2010). Fluctuating and directional asymmetry in young human males: effect of heavy working condition and socioeconomic status. *American Journal of Physical Anthropology*, 143(1), 112–120. <http://doi.org/10.1002/ajpa.21300>
- Palmer, A. R. (1994). Fluctuating asymmetry analyses: a primer. In T. A. Markow (Ed.), *Developmental Instability: Its Origins and Evolutionary Implications* (pp. 335–364). Springer Netherlands. Retrieved from [http://link.springer.com/chapter/10.1007/978-94-011-0830-0\\_26](http://link.springer.com/chapter/10.1007/978-94-011-0830-0_26)
- Paquet, E., Rioux, M., Murching, A., Naveen, T., & Tabatabai, A. (2000). Description of

- shape information for 2-D and 3-D objects. *Signal Processing: Image Communication*, 16(1–2), 103–122. [http://doi.org/10.1016/S0923-5965\(00\)00020-5](http://doi.org/10.1016/S0923-5965(00)00020-5)
- Parui, S. K., & Majumder, D. D. (1983). Symmetry analysis by computer. *Pattern Recognition*, 16(1), 63-67.
- Pierre, M. A., Zurakowski, D., Nazarian, A., Hauser-Kara, D. A., & Snyder, B. D. (2010). Assessment of the bilateral asymmetry of human femurs based on physical, densitometric, and structural rigidity characteristics. *Journal of Biomechanics*, 43(11), 2228–2236. <http://doi.org/10.1016/j.jbiomech.2010.02.032>
- Ramsay, J., Joncas, J., Gilbert, G., Trop, I., Cheriet, F., Labelle, H., & Parent, S. (2014). Is Breast Asymmetry Present in Girls with Adolescent Idiopathic Scoliosis? *Spine Deformity*, 2(5), 374–379. <http://doi.org/10.1016/j.jspd.2014.05.002>
- Reisfeld, D., Wolfson, H., & Yeshurun, Y. (1995). Context-free attentional operators: The generalized symmetry transform. *International Journal of Computer Vision*, 14(2), 119–130. <http://doi.org/10.1007/BF01418978>
- Rhodes, G., Zebrowitz, L. A., Clark, A., Kalick, S. M., Hightower, A., & McKay, R. (2001). Do facial averageness and symmetry signal health? *Evolution and Human Behavior*, 22(1), 31–46. [http://doi.org/10.1016/S1090-5138\(00\)00060-X](http://doi.org/10.1016/S1090-5138(00)00060-X)
- Rikowski, A., & Grammer, K. (1999). Human body odour, symmetry and attractiveness. *Proceedings. Biological Sciences / The Royal Society*, 266(1422), 869–874. <http://doi.org/10.1098/rspb.1999.0717>
- Riley, K. F., Hobson, M. P., & Bence, S. J. (2006). *Mathematical methods for physics and engineering: a comprehensive guide*. Cambridge University Press.

- Robinette, K. M., Blackwell, S., Daanen, H., Boehmer, M., & Fleming, S. (2002). *Civilian American and European Surface Anthropometry Resource (CAESAR), Final Report. Volume 1. Summary*. DTIC Document.
- Ruff, C. B., & Jones, H. H. (1981). Bilateral asymmetry in cortical bone of the humerus and tibia-sex and age factors. *Human Biology*, *53*(1), 69–86.
- Ruff, C., Holt, B., & Trinkaus, E. (2006). Who’s afraid of the big bad Wolff?: “Wolff’s law” and bone functional adaptation. *American Journal of Physical Anthropology*, *129*(4), 484–498. <http://doi.org/10.1002/ajpa.20371>
- Sarnadskiy, V., Vilberger, S. Y., & Fomichev, N. (2002). Motion analysis of the trunk and spine. Surface measurement using computer optical topography. *Studies in Health Technology and Informatics*, *91*, 222.
- Savriama, Y., & Klingenberg, C. P. (2011). Beyond bilateral symmetry: geometric morphometric methods for any type of symmetry. *BMC Evolutionary Biology*, *11*(1), 280. <http://doi.org/10.1186/1471-2148-11-280>
- Schell, L. M., Johnston, F. E., Smith, D. R., & Paolone, A. M. (1985). Directional asymmetry of body dimensions among white adolescents. *American Journal of Physical Anthropology*, *67*(4), 317–322. <http://doi.org/10.1002/ajpa.1330670404>
- Seoud, L., Dansereau, J., Labelle, H., & Cheriet, F. (2012). Multilevel analysis of trunk surface measurements for noninvasive assessment of scoliosis deformities. *Spine*, *37*(17), E1045-E1053.
- Shilane, P., Min, P., Kazhdan, M., & Funkhouser, T. (2004). The Princeton Shape Benchmark. In *Shape Modeling Applications, 2004. Proceedings* (pp. 167–178). <http://doi.org/10.1109/SMI.2004.1314504>



- Symmetry.(n.d). In *Merriam-Webster.com*. Retrieved April 8, 2015, from  
<http://www.merriam-webster.com/dictionary/symmetry>
- Tate, S. J., & Jared, G. E. M. (2003). Recognising symmetry in solid models. *Computer-Aided Design*, 35(7), 673–692. [http://doi.org/10.1016/S0010-4485\(02\)00093-3](http://doi.org/10.1016/S0010-4485(02)00093-3)
- The 3D Body Scanner - Introduction. (n.d.). Retrieved May 1, 2016, from  
<http://www.bodyscan.human.cornell.edu/scene0037.html>
- Tokarczyk, R., & Mazur, T. (2006). Photogrammetry-Principles of operation and application in rehabilitation. *Rehabilitacja Medyczna*, 10(4), 31–38.
- Tomkinson, G. R., Popović, N., & Martin, M. (2003). Bilateral symmetry and the competitive standard attained in elite and sub-elite sport. *Journal of Sports Sciences*, 21(3), 201–211. <http://doi.org/10.1080/0264041031000071029a>
- Townsend, G. (1987). A correlative analysis of dental crown dimensions in individuals with Down syndrome. *Human Biology*, 59(3), 537–548.
- Trivers, R., Manning, J. T., Thornhill, R., Singh, D., & McGuire, M. (1999). Jamaican Symmetry Project: long-term study of fluctuating asymmetry in rural Jamaican children. *Human Biology*, 71(3), 417–430.
- True Model Management NYC | Model Scouts. (n.d.). Retrieved April 3, 2016, from  
<https://www.modelscouts.com/blog/true-model-management-new-york>
- Weyl, H. (1952). *Symmetry*. Princeton University Press.
- why your clothes don't fit. (n.d.). Retrieved April 3, 2016, from  
<http://www.rostitchery.com/2011/09/why-your-clothes-dont-fit.html>
- Willing, R. T., Roumeliotis, G., Jenkyn, T. R., & Yazdani, A. (2013). Development and evaluation of a semi-automatic technique for determining the bilateral symmetry

plane of the facial skeleton. *Medical Engineering & Physics*, 35(12), 1843–1849.  
<http://doi.org/10.1016/j.medengphy.2013.06.006>

Wilson, J. M., & Manning, J. T. (1996). Fluctuating asymmetry and age in children: evolutionary implications for the control of developmental stability. *Journal of Human Evolution*, 30(6), 529–537. <http://doi.org/10.1006/jhev.1996.0041>

Wolanski, N. (1972). Functions of the extremities and their influence on the asymmetric structure of body in children and young persons from different environmental conditions. *Acta Med Auxol*, 23(2), 465-471.

Yip, R. K. K. (2000). A Hough transform technique for the detection of reflectional symmetry and skew-symmetry. *Pattern Recognition Letters*, 21(2), 117–130.  
[http://doi.org/10.1016/S0167-8655\(99\)00138-5](http://doi.org/10.1016/S0167-8655(99)00138-5)

Zabrodsky, H., Peleg, S., & Avnir, D. (1992). A measure of symmetry based on shape similarity. In , *1992 IEEE Computer Society Conference on Computer Vision and Pattern Recognition, 1992. Proceedings CVPR '92* (pp. 703–706).  
<http://doi.org/10.1109/CVPR.1992.223196>

Zakharov, V. M. (1989). *Future prospects for population phenogenetics*. Chur, Switzerland: Harwood Academic Pub. Zavidovique, B., & Di Gesù, V. (2007). The S-kernel: A measure of symmetry of objects. *Pattern Recognition*, 40(3), 839–852. <http://doi.org/10.1016/j.patcog.2006.04.013>

## **APPENDICES**

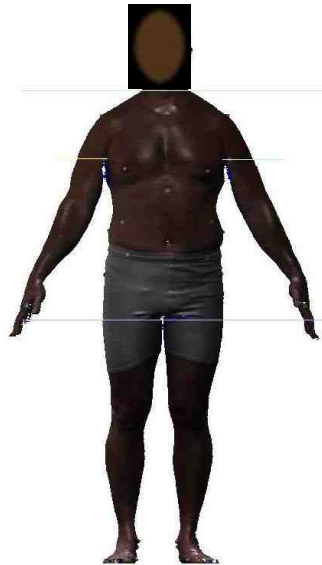
## Appendix A

### The Process of Estimating Asymmetry, in Steps

Step 1: Read the 3D scan into the Polyworks software



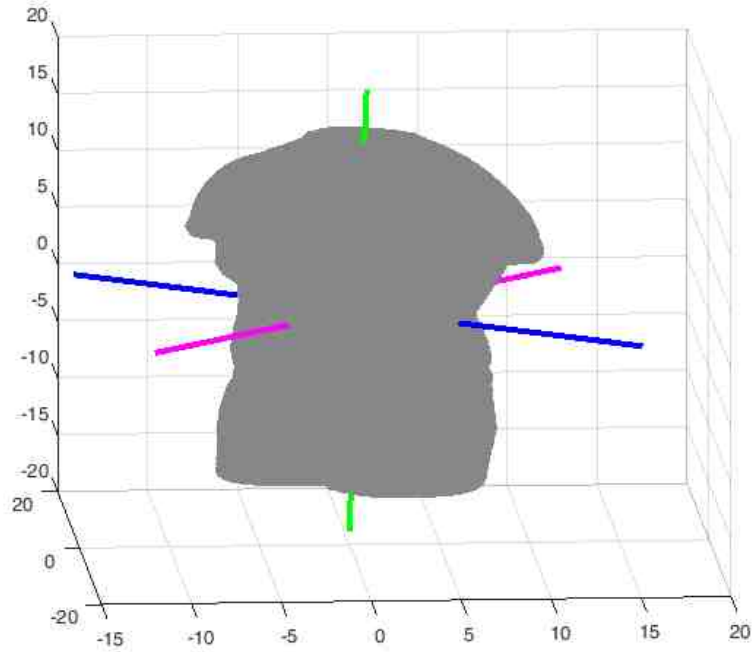
Step 2: Insert planes at the landmarks [Cervicale, crotch, Axilla] and fill any undesired holes



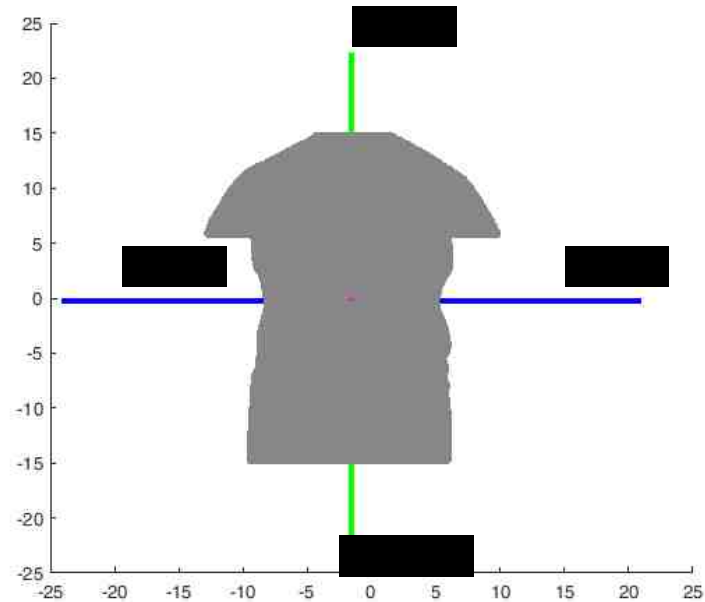
Step 3: Extract the torso region from the full body scan



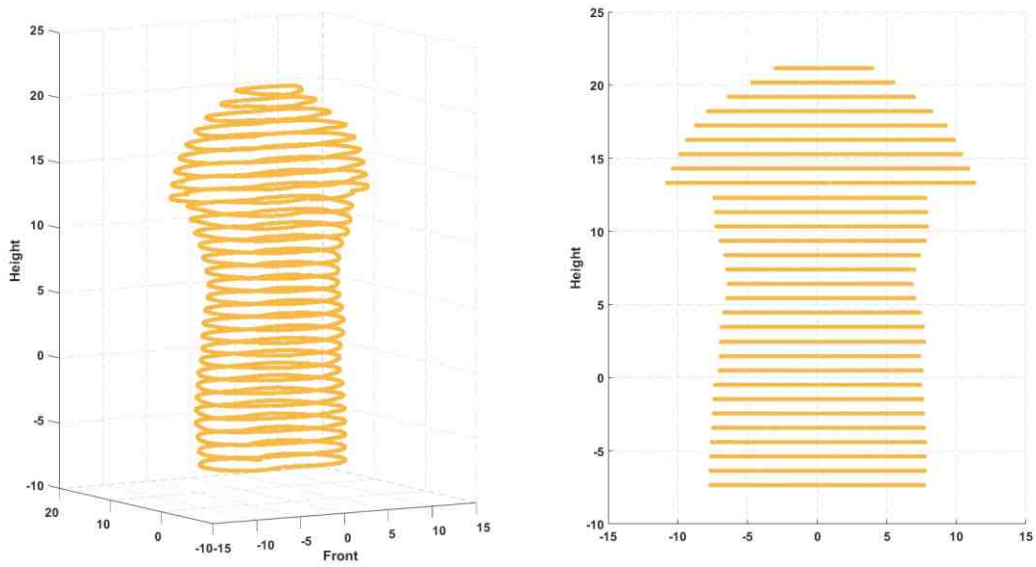
Step 4: Find the principal axes for the torso 3D cloud



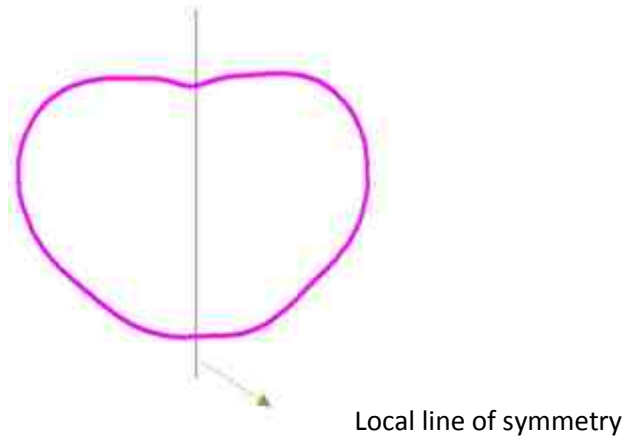
Step 5: If the principal axes determined in Step-4 are not in alignment with the global reference axes, rotate the torso cloud such that the principal axes and the global axes are aligned (see Section-3.2 for mathematical details). Define the front, back and top of the torso using the rotated principal axes as the basis. Accordingly, the first principal axis (green) defines top/bottom, the second axis (blue) defines right/left and the third axis (magenta) defines front/back.



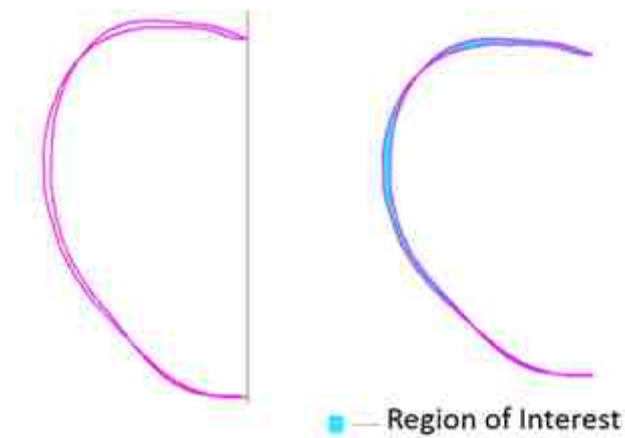
Step 6: Extract multiple cross-sections along the top-bottom axis



Step 7: For each cross-section, detect the mid line in the sagittal plane based on the area. The mid line divides the cross-section into two equal areas. The line that divides the cross-section should be perpendicular to the right-left axis.



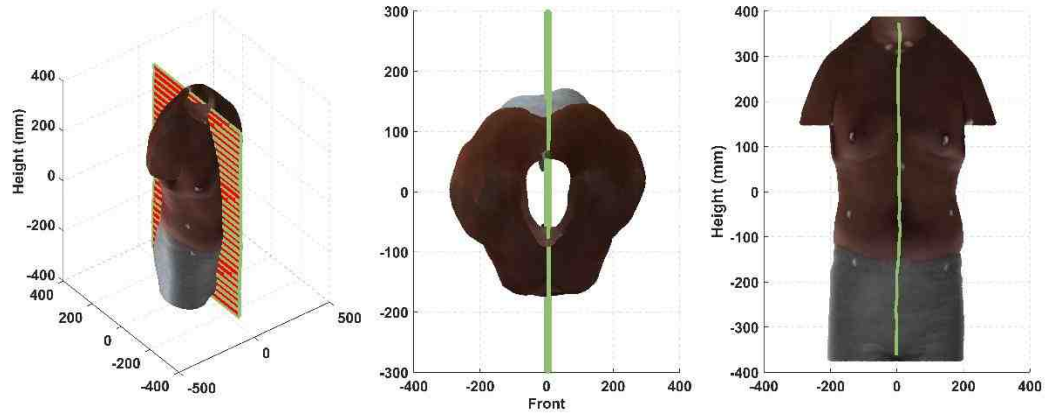
Step 8: After detecting the midline, overlay the mirrored left halve on to the right halve of the  $i^{\text{th}}$  cross-section, and estimate the non-matching areas (a.k.a. region of interest) between the two halves. Repeat the process for all the cross-section.



Step 9: Calculate the asymmetry index using the following formula.

$$\text{Asymmetry Index (\%)} = \frac{\sum_{i=1}^n \text{Area of Region Of Interest}_i}{\sum_{i=1}^n (\text{Area of slice}_i * 0.5)} \times 100$$

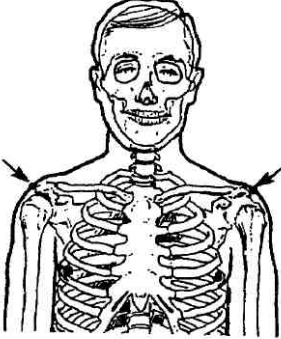
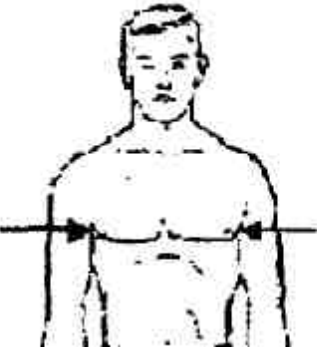
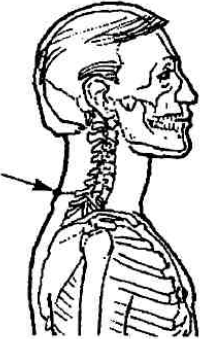
Step 10: Link the midline of each cross-section along the top-bottom axis so that a surface is formed and that is referred as the global plane/surface of symmetry.

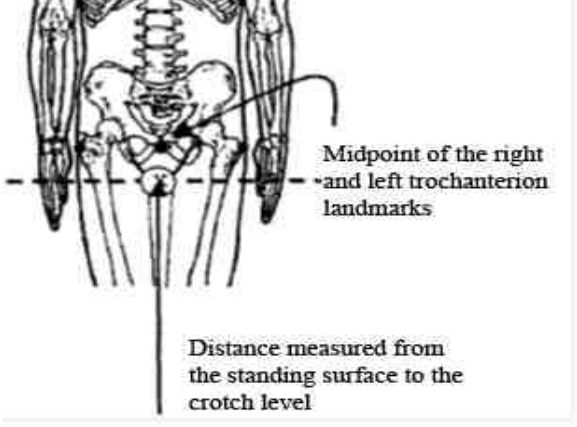
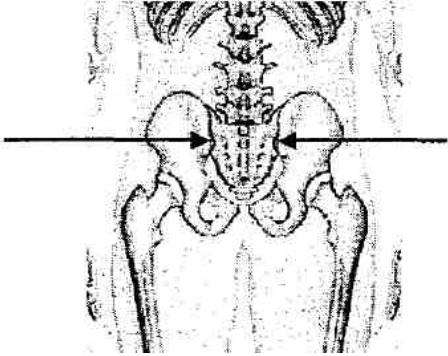
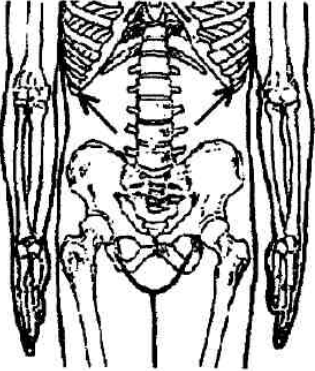




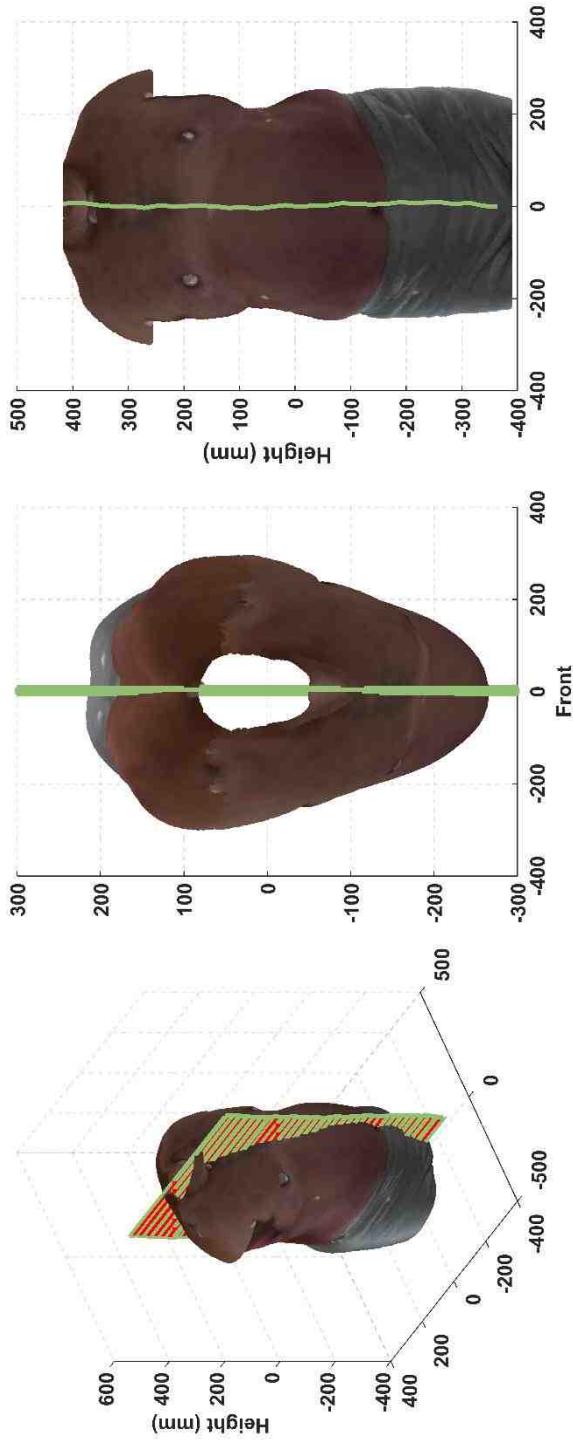
Appendix B

Definition of Landmarks [Adopted from CAESAR]

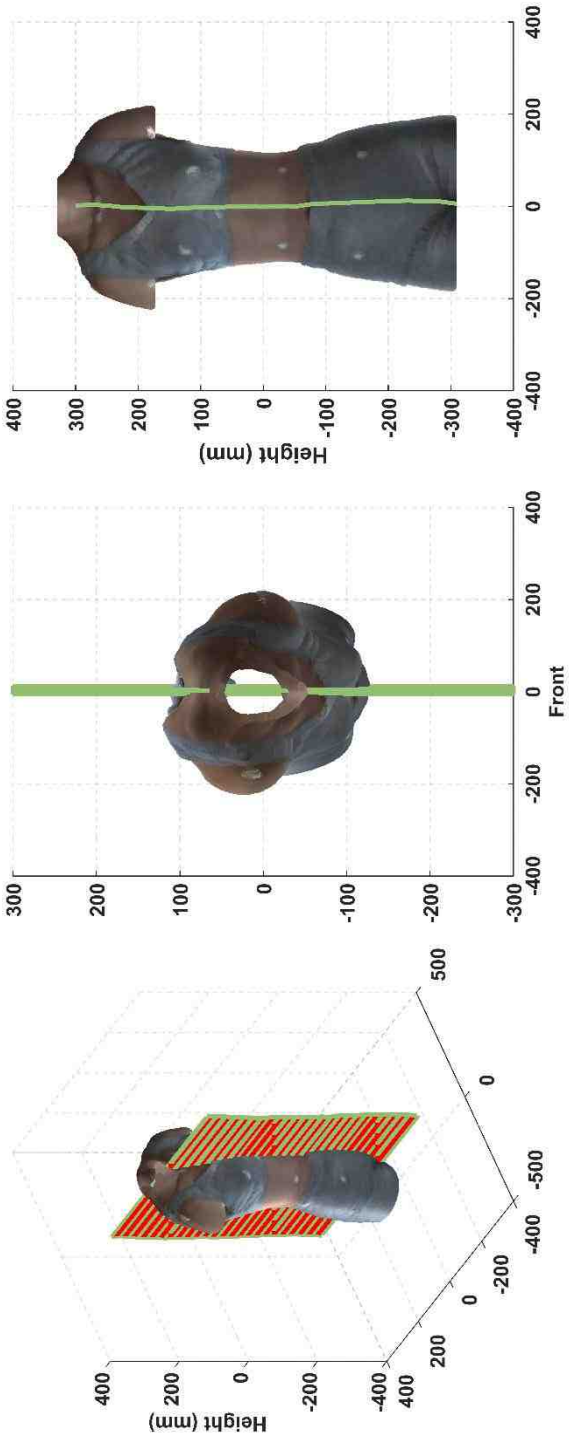
|   |  |   |
|---|--|---|
| <p>Acromion: Left and Right</p>               | <p>Most lateral point of the lateral edge of the acromial process of the scapula</p> |    |
| <p>Axilla Point, Anterior: Left and Right</p> | <p>Lowest point on the anterior axillary fold (Armpit)</p>                           |   |
| <p>Cervicale</p>                              | <p>Most prominent point of the spinous process of the seventh cervical vertebra</p>  |  |

|  |   |  |
|--|---|--|
| <p>Crotch</p>                                | <p>Point calculated midway between the right and left trochanterion landmarks at the level of crotch height</p> |    |
| <p>Iliac Spine posterior; Left and Right</p> | <p>Prominent point on the posterior superior spine of the ilium; a dimple often overlies this point</p>         |   |
| <p>Tenth Rib, Left and Right</p>             | <p>Lowest palpable point on the inferior border of the tenth rib at the bottom of the rib cage</p>              |  |

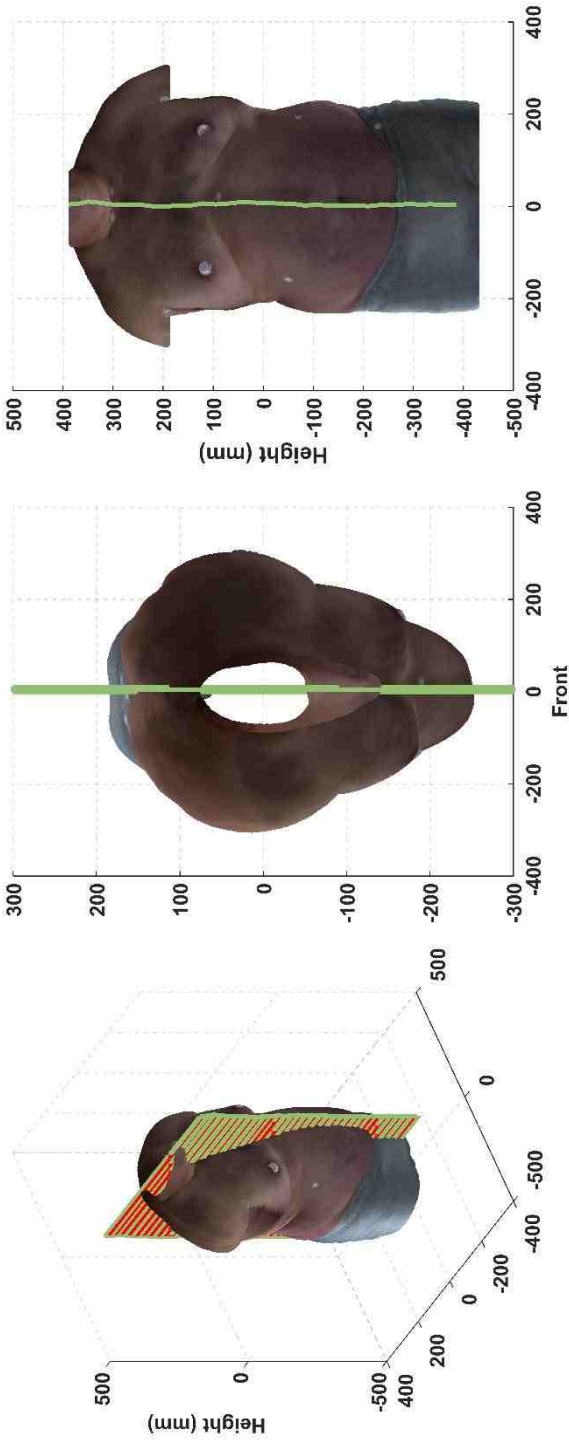
# Appendix C



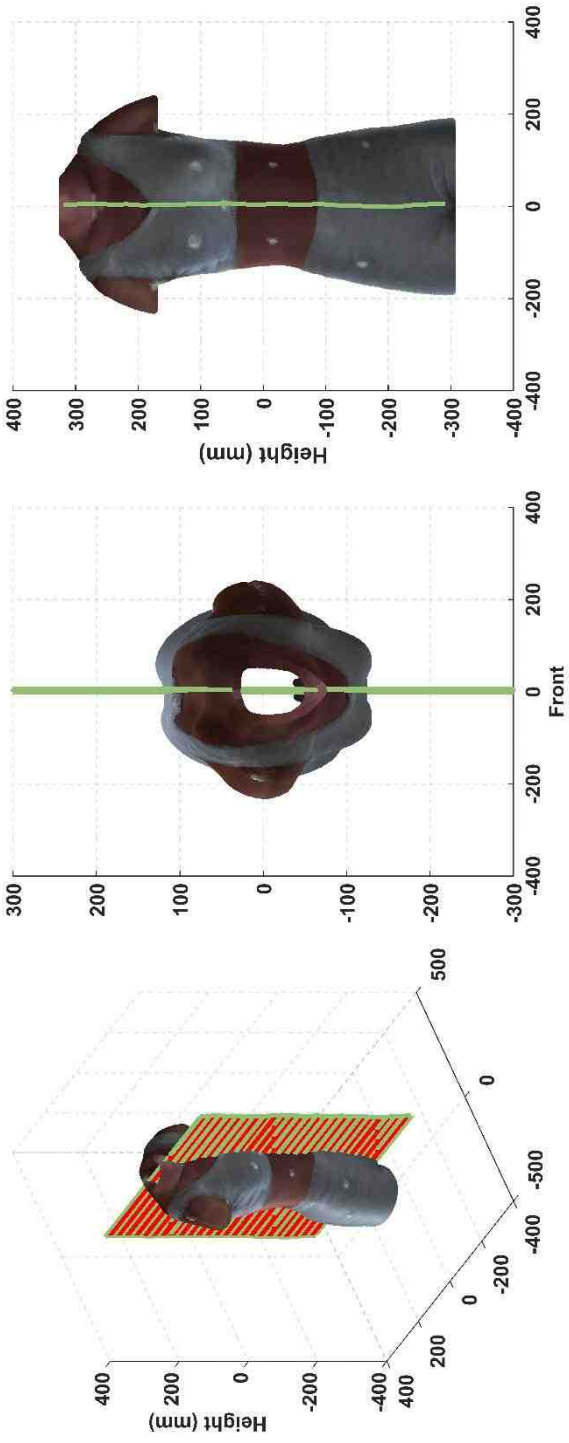
| Asymmetry Index (%) | Over all Torso Twist (degree) | Torso Tilt (degree) |
|---------------------|-------------------------------|---------------------|
| 6.86                | 1.13                          | 3.93                |



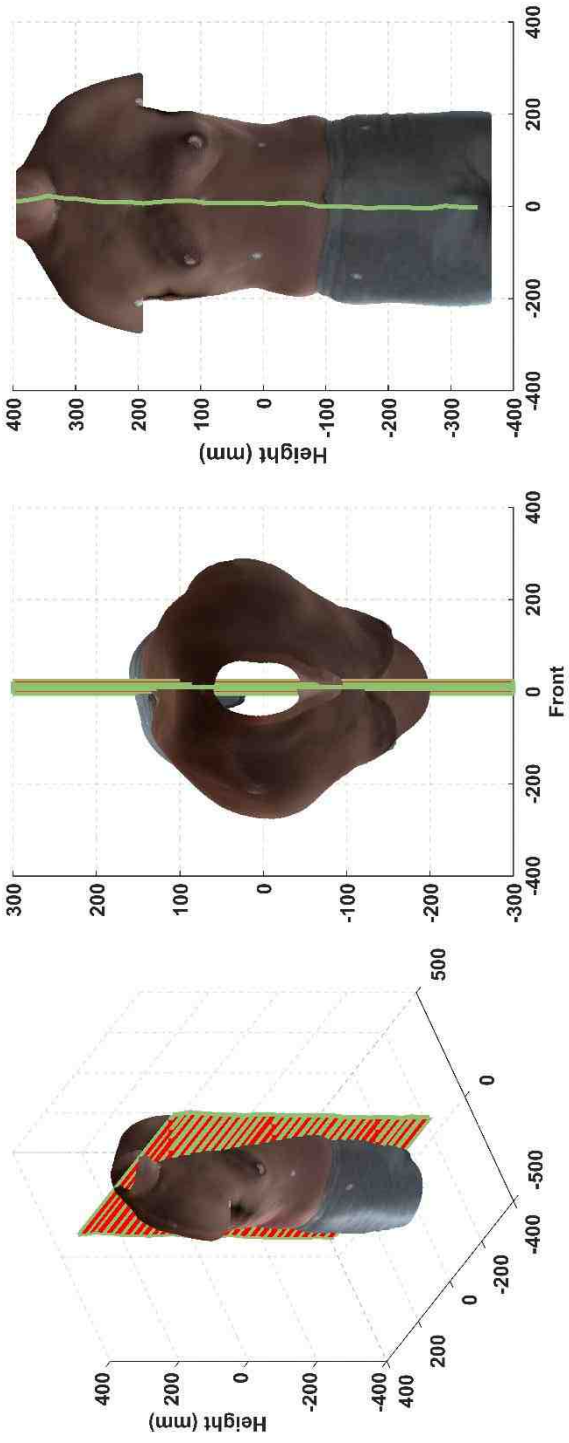
|                     |      |                               |      |                     |      |
|---------------------|------|-------------------------------|------|---------------------|------|
| Asymmetry Index (%) | 6.06 | Over all Torso Twist (degree) | 2.45 | Torso Tilt (degree) | 0.65 |
|---------------------|------|-------------------------------|------|---------------------|------|



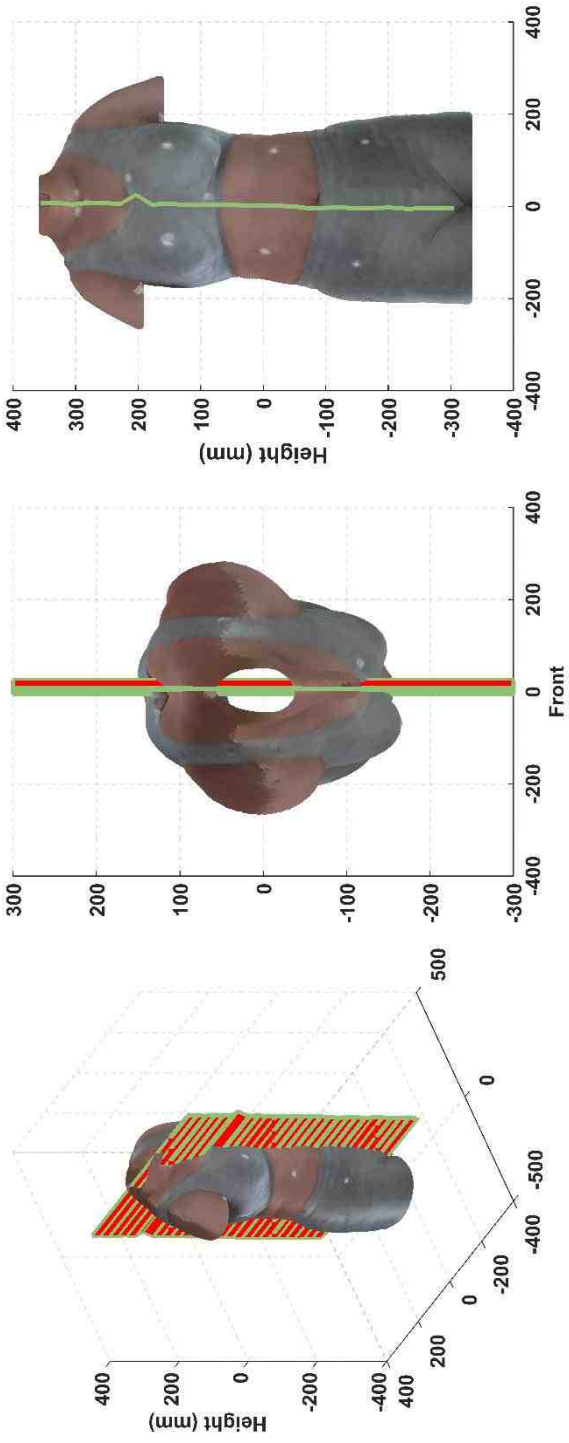
|                     |      |                               |      |                     |      |
|---------------------|------|-------------------------------|------|---------------------|------|
| Asymmetry Index (%) | 6.88 | Over all Torso Twist (degree) | 2.81 | Torso Tilt (degree) | 2.97 |
|---------------------|------|-------------------------------|------|---------------------|------|



|                     |      |                               |      |                     |      |
|---------------------|------|-------------------------------|------|---------------------|------|
| Asymmetry Index (%) | 6.88 | Over all Torso Twist (degree) | 0.27 | Torso Tilt (degree) | 2.37 |
|---------------------|------|-------------------------------|------|---------------------|------|

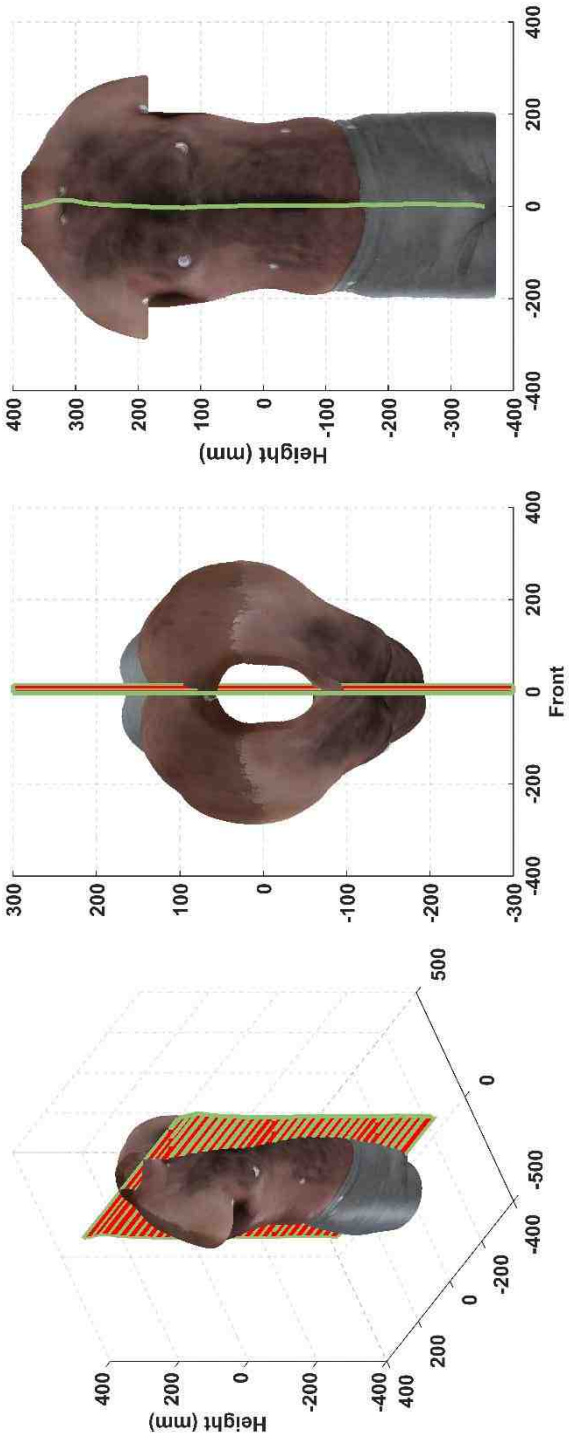


|                     |       |                               |      |                     |      |
|---------------------|-------|-------------------------------|------|---------------------|------|
| Asymmetry Index (%) | 11.28 | Over all Torso Twist (degree) | 6.97 | Torso Tilt (degree) | 2.40 |
|---------------------|-------|-------------------------------|------|---------------------|------|

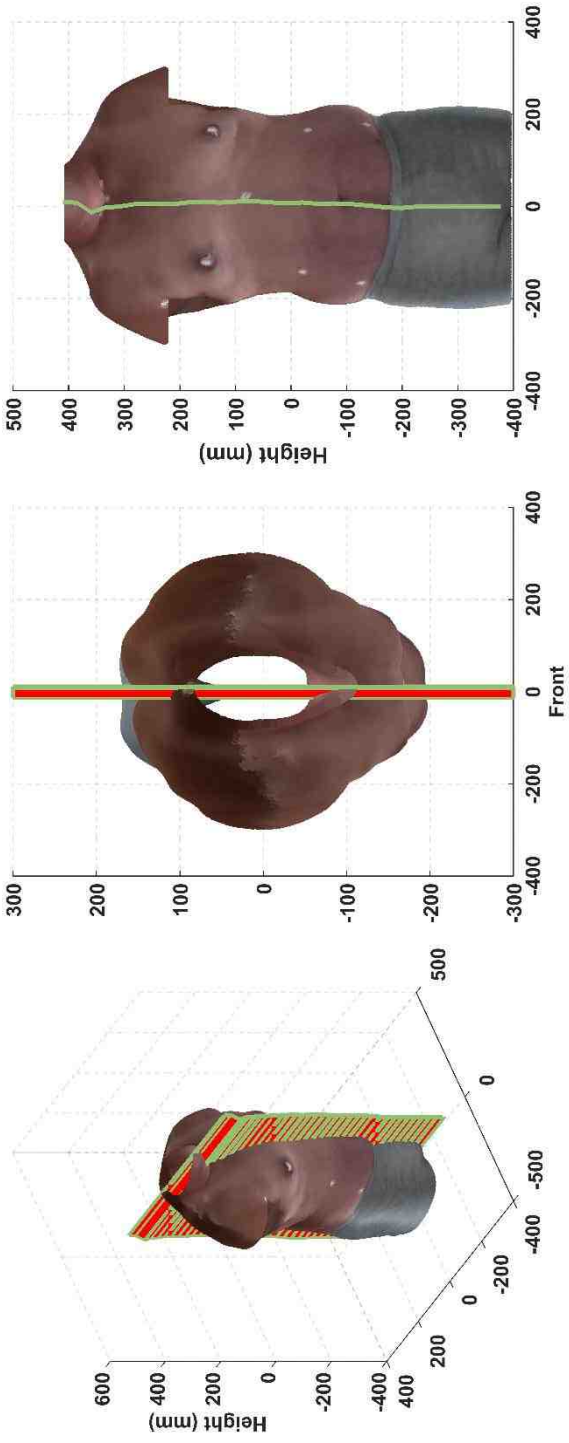


|                     |       |                               |      |                     |      |
|---------------------|-------|-------------------------------|------|---------------------|------|
| Asymmetry Index (%) | 12.62 | Over all Torso Twist (degree) | 1.02 | Torso Tilt (degree) | 0.56 |
|---------------------|-------|-------------------------------|------|---------------------|------|

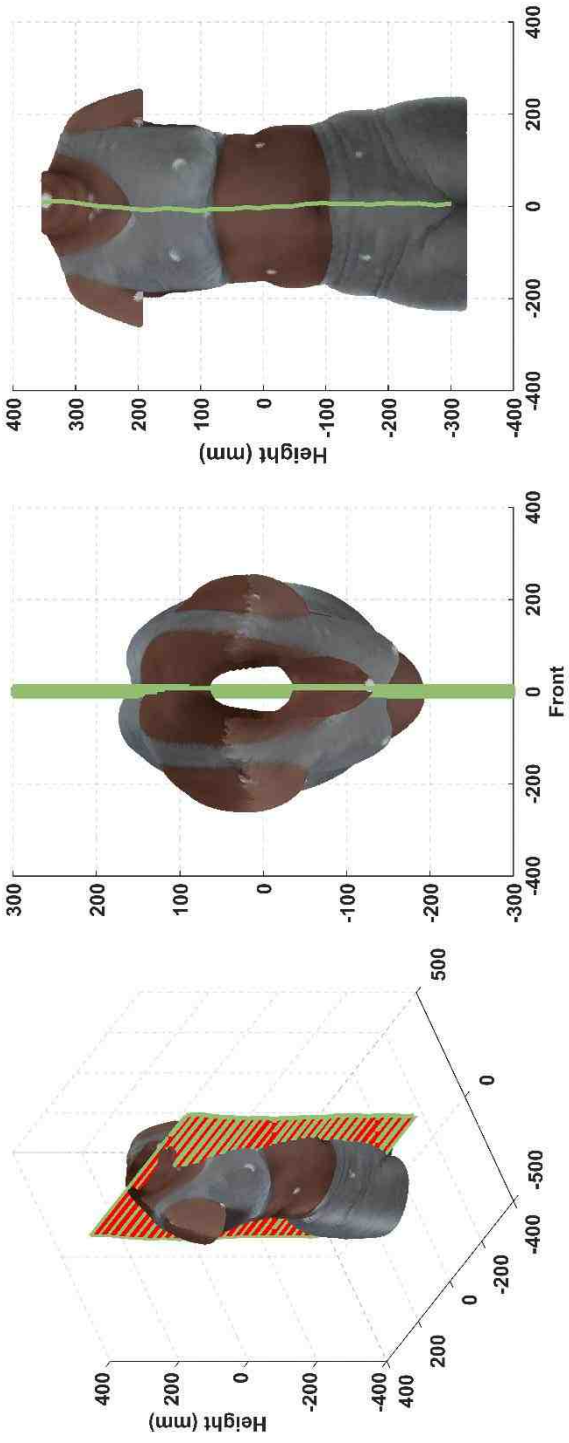




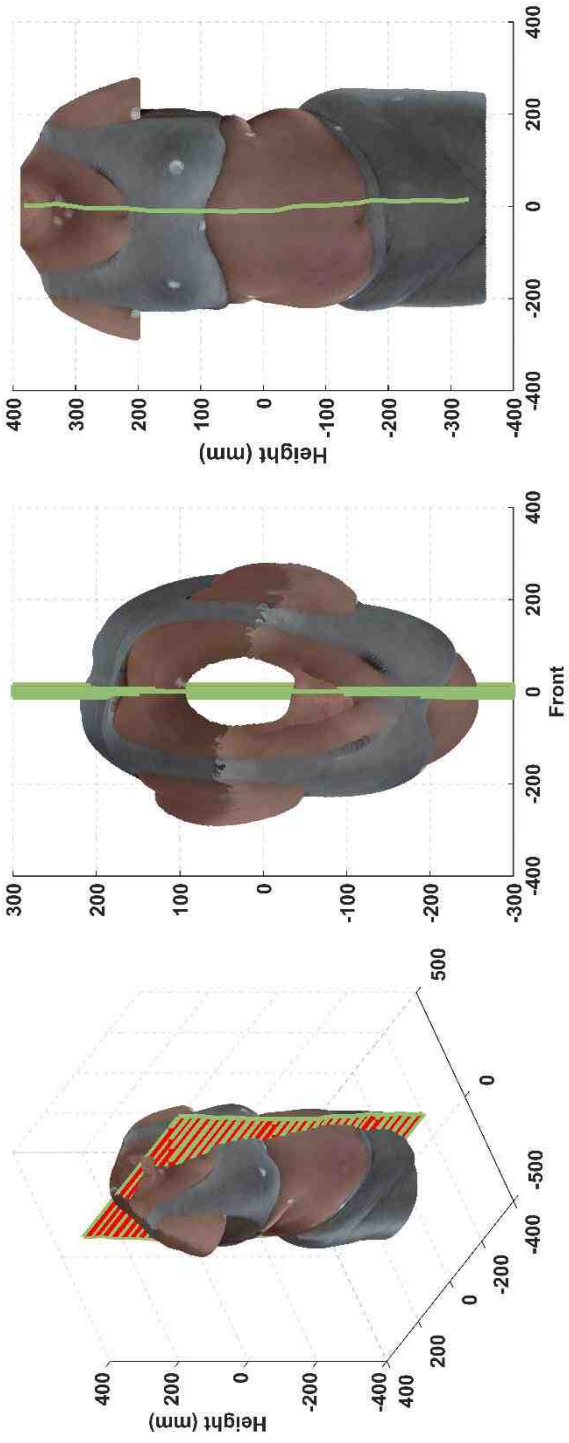
|                     |      |                               |      |                     |      |
|---------------------|------|-------------------------------|------|---------------------|------|
| Asymmetry Index (%) | 5.82 | Over all Torso Twist (degree) | 1.44 | Torso Tilt (degree) | 0.54 |
|---------------------|------|-------------------------------|------|---------------------|------|



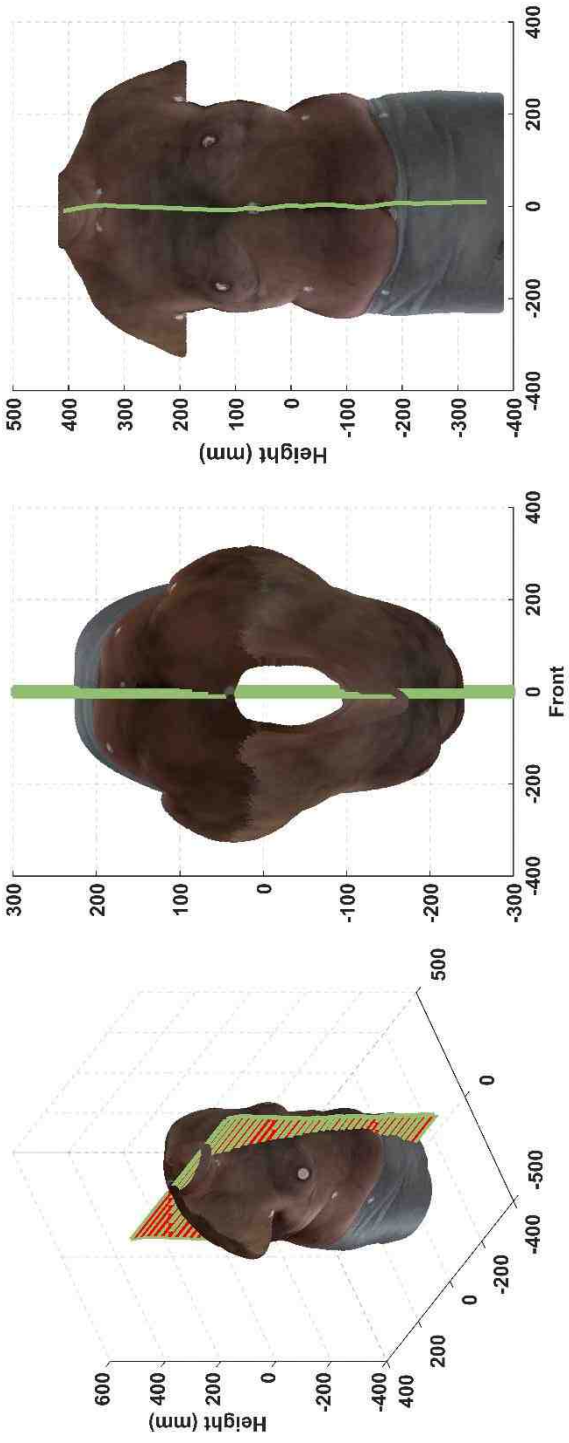
|                     |      |                               |      |                     |      |
|---------------------|------|-------------------------------|------|---------------------|------|
| Asymmetry Index (%) | 7.88 | Over all Torso Twist (degree) | 5.72 | Torso Tilt (degree) | 4.36 |
|---------------------|------|-------------------------------|------|---------------------|------|



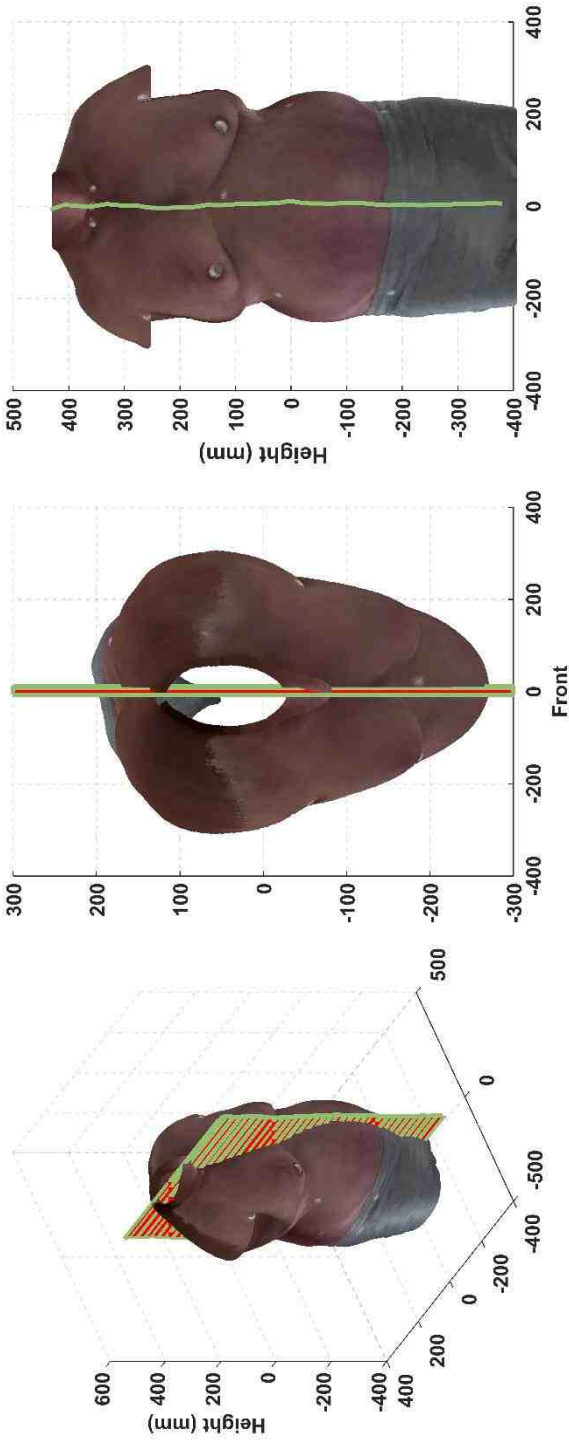
|                     |      |                               |      |                     |      |
|---------------------|------|-------------------------------|------|---------------------|------|
| Asymmetry Index (%) | 6.55 | Over all Torso Twist (degree) | 2.22 | Torso Tilt (degree) | 0.99 |
|---------------------|------|-------------------------------|------|---------------------|------|



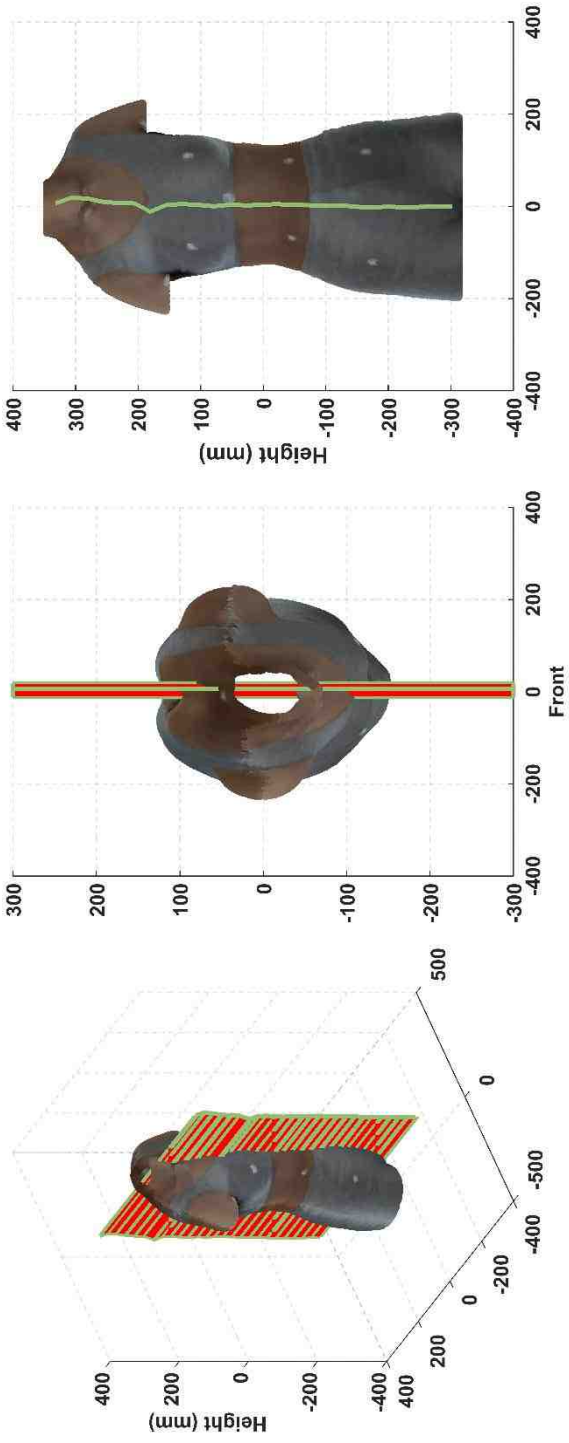
|                     |       |                               |      |                     |      |
|---------------------|-------|-------------------------------|------|---------------------|------|
| Asymmetry Index (%) | 14.41 | Over all Torso Twist (degree) | 5.40 | Torso Tilt (degree) | 8.28 |
|---------------------|-------|-------------------------------|------|---------------------|------|



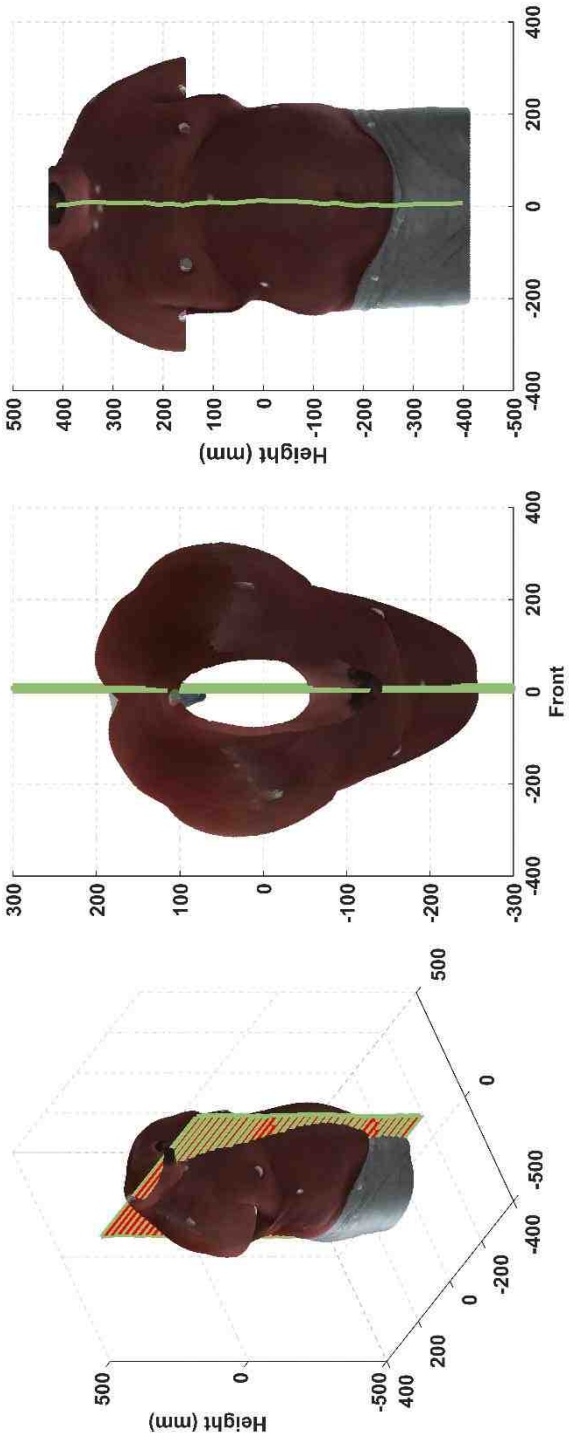
|                     |      |                               |      |                     |      |
|---------------------|------|-------------------------------|------|---------------------|------|
| Asymmetry Index (%) | 5.55 | Over all Torso Twist (degree) | 1.67 | Torso Tilt (degree) | 0.65 |
|---------------------|------|-------------------------------|------|---------------------|------|



|                     |      |                               |      |                     |      |
|---------------------|------|-------------------------------|------|---------------------|------|
| Asymmetry Index (%) | 8.76 | Over all Torso Twist (degree) | 5.35 | Torso Tilt (degree) | 0.00 |
|---------------------|------|-------------------------------|------|---------------------|------|

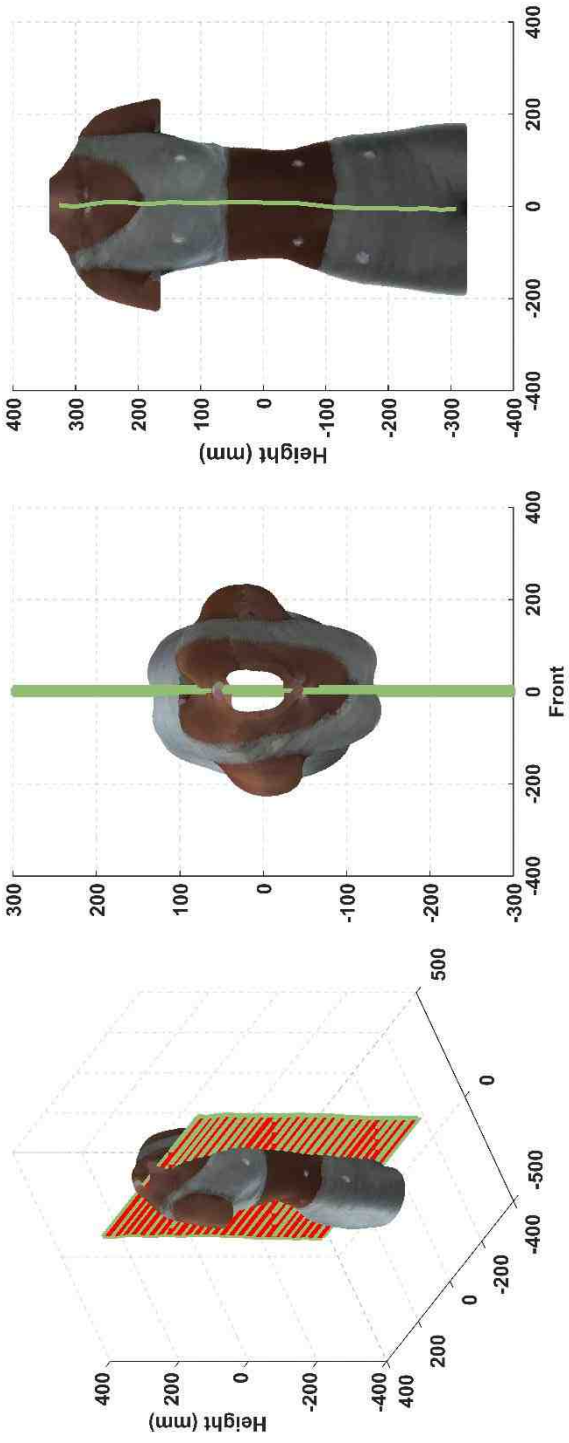


|                     |       |                               |      |                     |      |
|---------------------|-------|-------------------------------|------|---------------------|------|
| Asymmetry Index (%) | 10.46 | Over all Torso Twist (degree) | 4.86 | Torso Tilt (degree) | 6.09 |
|                     |       |                               |      |                     |      |

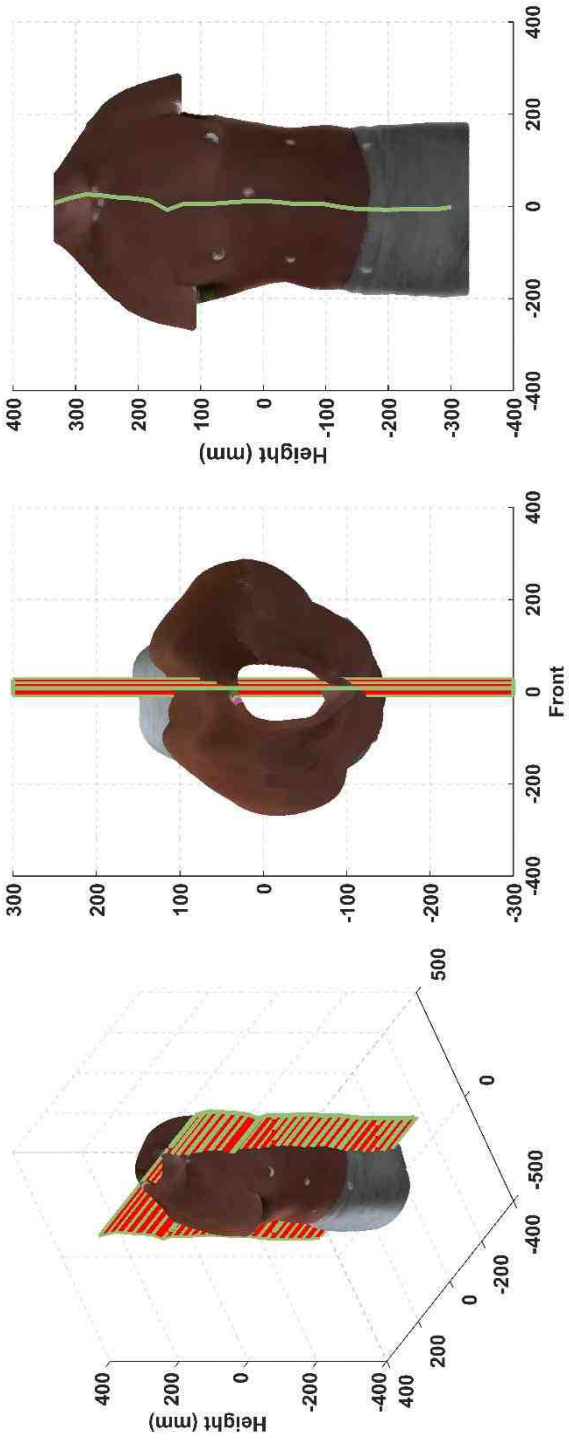


|                     |       |                               |      |                     |      |
|---------------------|-------|-------------------------------|------|---------------------|------|
| Asymmetry Index (%) | 10.84 | Over all Torso Twist (degree) | 0.57 | Torso Tilt (degree) | 1.56 |
|---------------------|-------|-------------------------------|------|---------------------|------|

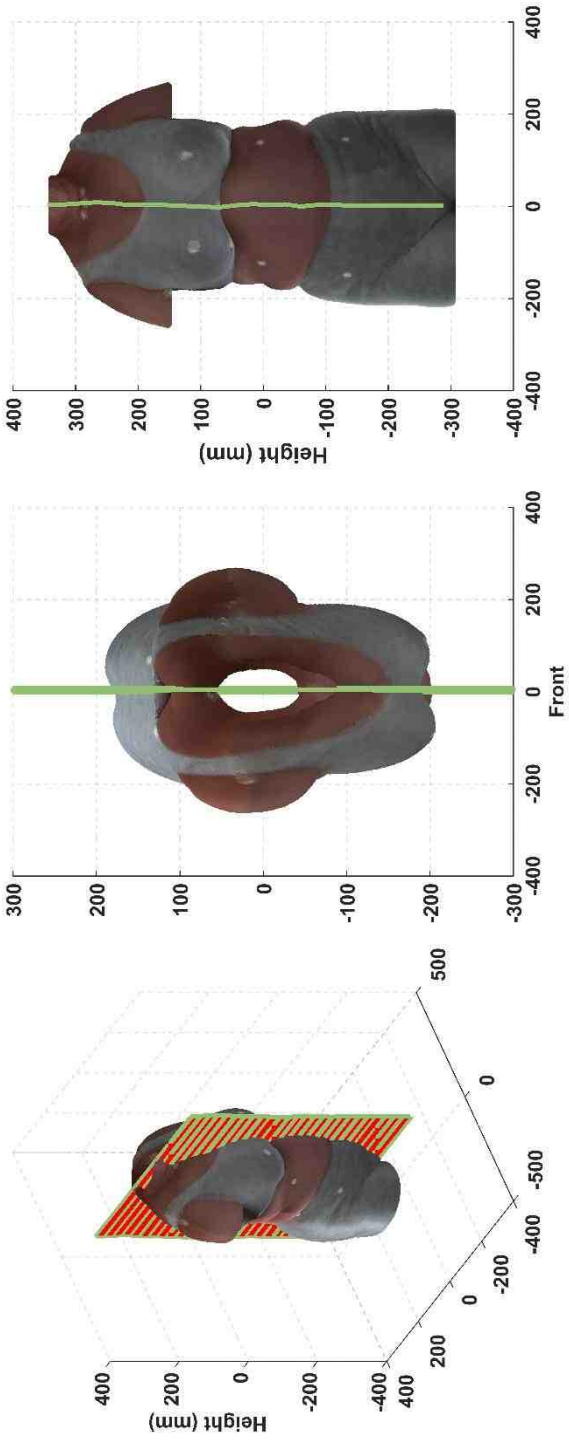




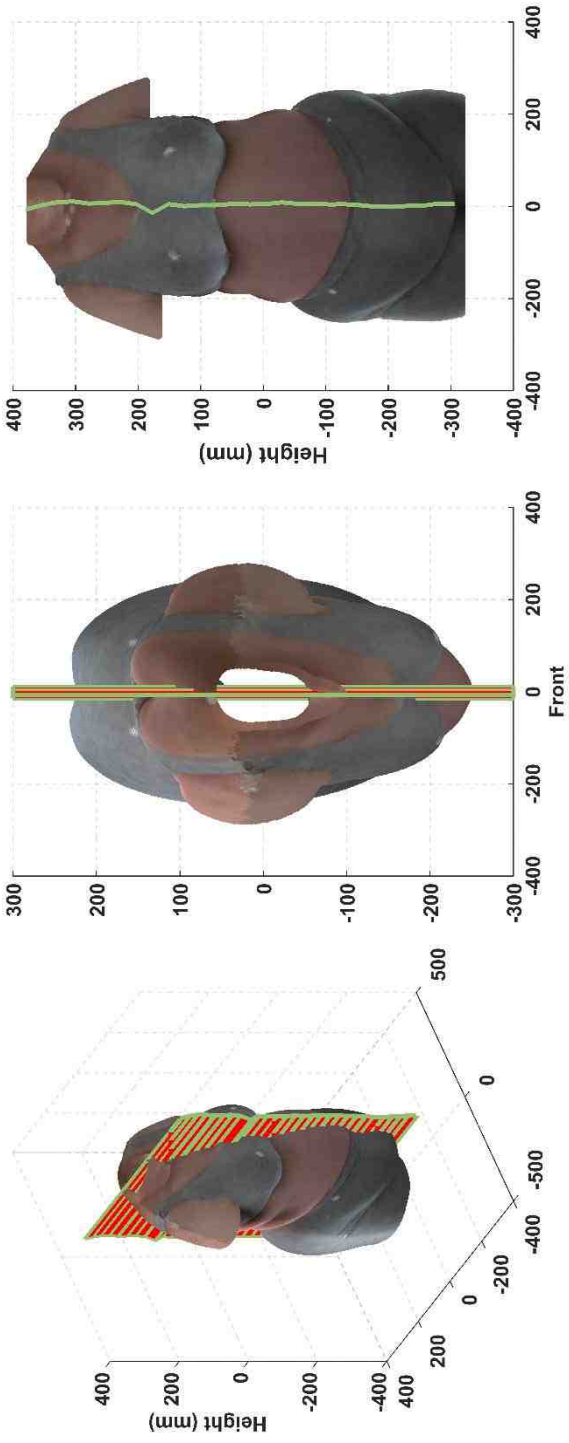
|                     |      |                               |      |                     |      |
|---------------------|------|-------------------------------|------|---------------------|------|
| Asymmetry Index (%) | 4.58 | Over all Torso Twist (degree) | 0.45 | Torso Tilt (degree) | 0.79 |
|---------------------|------|-------------------------------|------|---------------------|------|



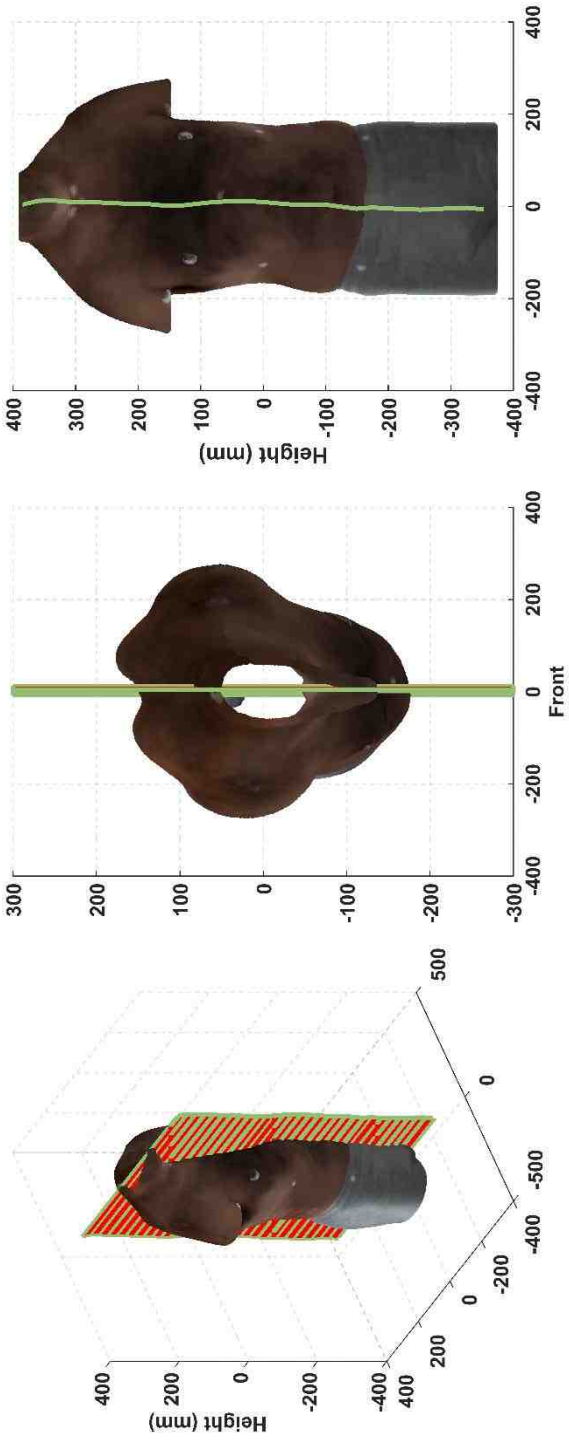
|                     |                               |                     |
|---------------------|-------------------------------|---------------------|
| Asymmetry Index (%) | Over all Torso Twist (degree) | Torso Tilt (degree) |
| 13.24               | 4.06                          | 3.41                |



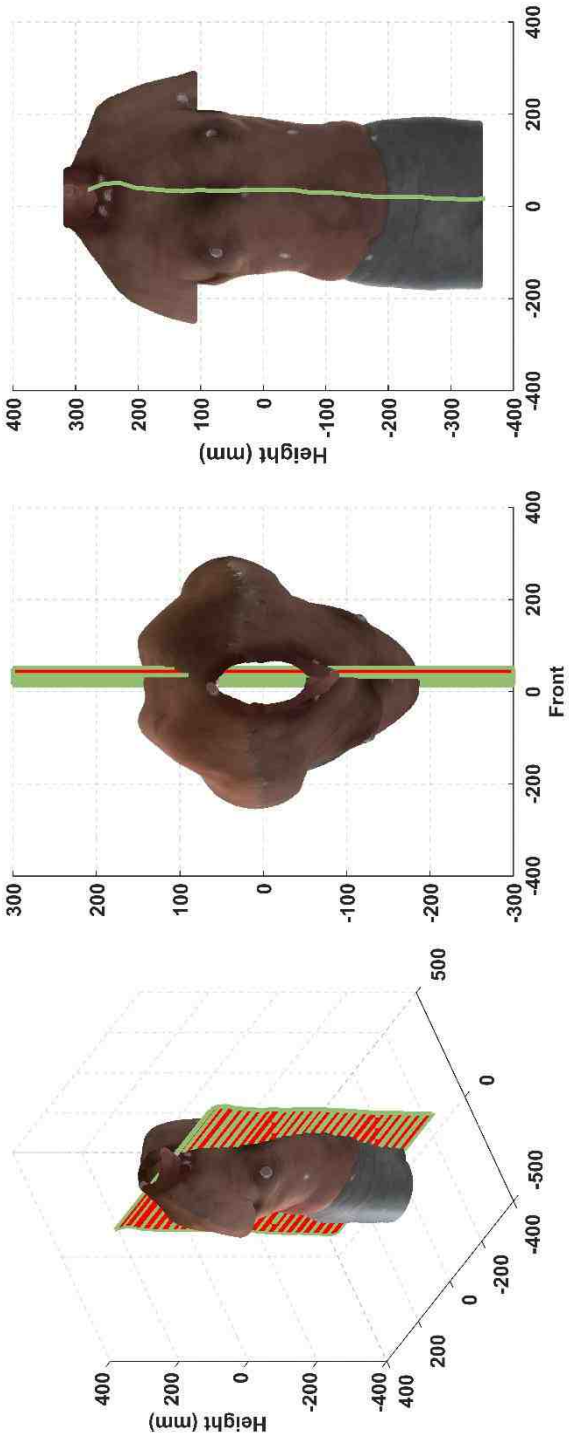
|                     |      |                               |      |                     |      |
|---------------------|------|-------------------------------|------|---------------------|------|
| Asymmetry Index (%) | 4.92 | Over all Torso Twist (degree) | 0.55 | Torso Tilt (degree) | 0.60 |
|---------------------|------|-------------------------------|------|---------------------|------|



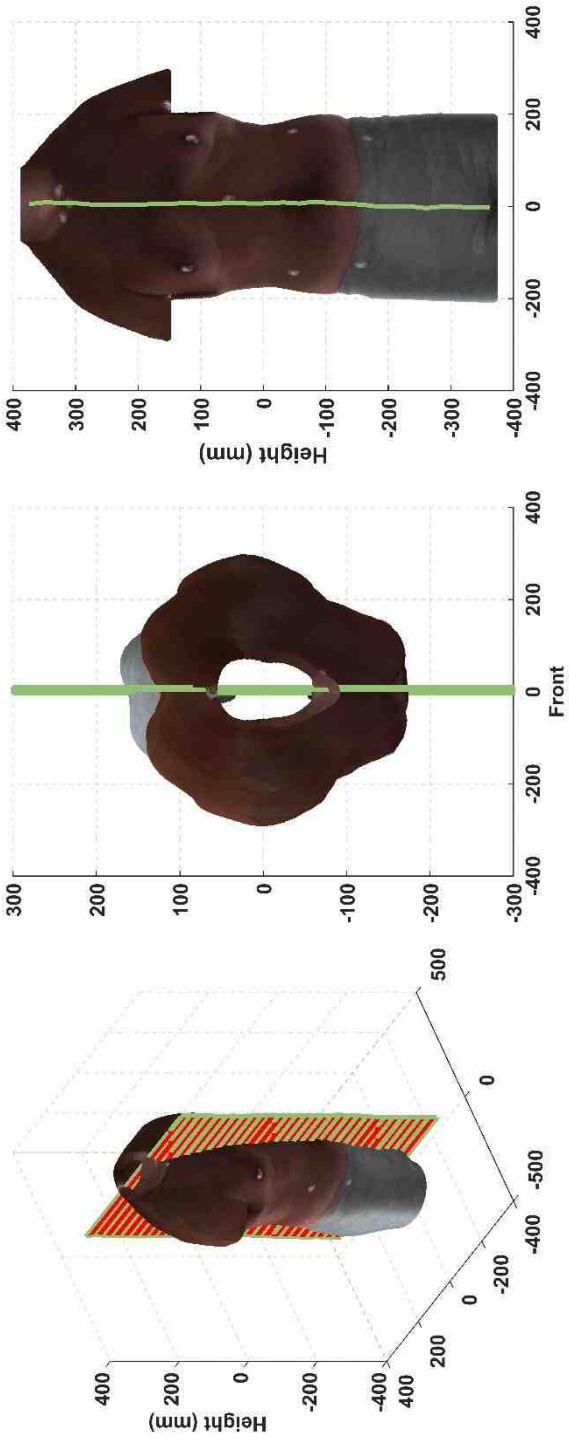
|                     |      |                               |      |                     |      |
|---------------------|------|-------------------------------|------|---------------------|------|
| Asymmetry Index (%) | 6.02 | Over all Torso Twist (degree) | 0.85 | Torso Tilt (degree) | 2.05 |
|---------------------|------|-------------------------------|------|---------------------|------|



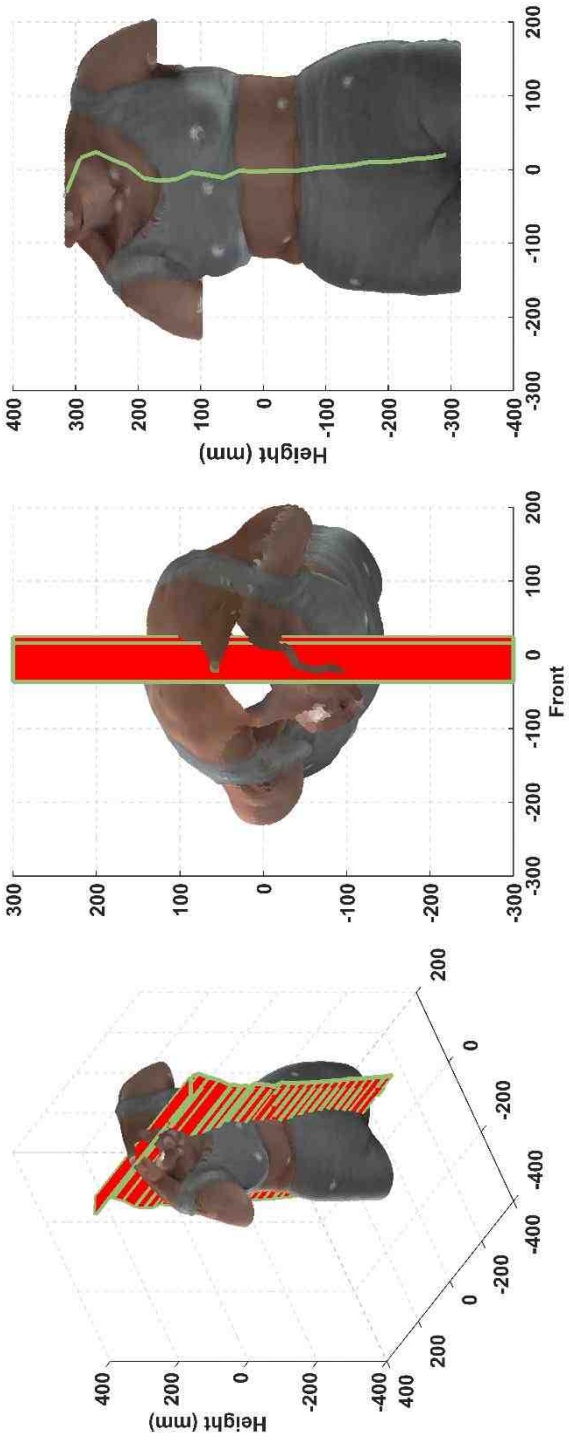
|                     |       |                               |      |                     |      |
|---------------------|-------|-------------------------------|------|---------------------|------|
| Asymmetry Index (%) | 13.31 | Over all Torso Twist (degree) | 0.44 | Torso Tilt (degree) | 4.88 |
|---------------------|-------|-------------------------------|------|---------------------|------|



|                     |       |                               |      |                     |      |
|---------------------|-------|-------------------------------|------|---------------------|------|
| Asymmetry Index (%) | 11.88 | Over all Torso Twist (degree) | 1.67 | Torso Tilt (degree) | 5.20 |
|---------------------|-------|-------------------------------|------|---------------------|------|

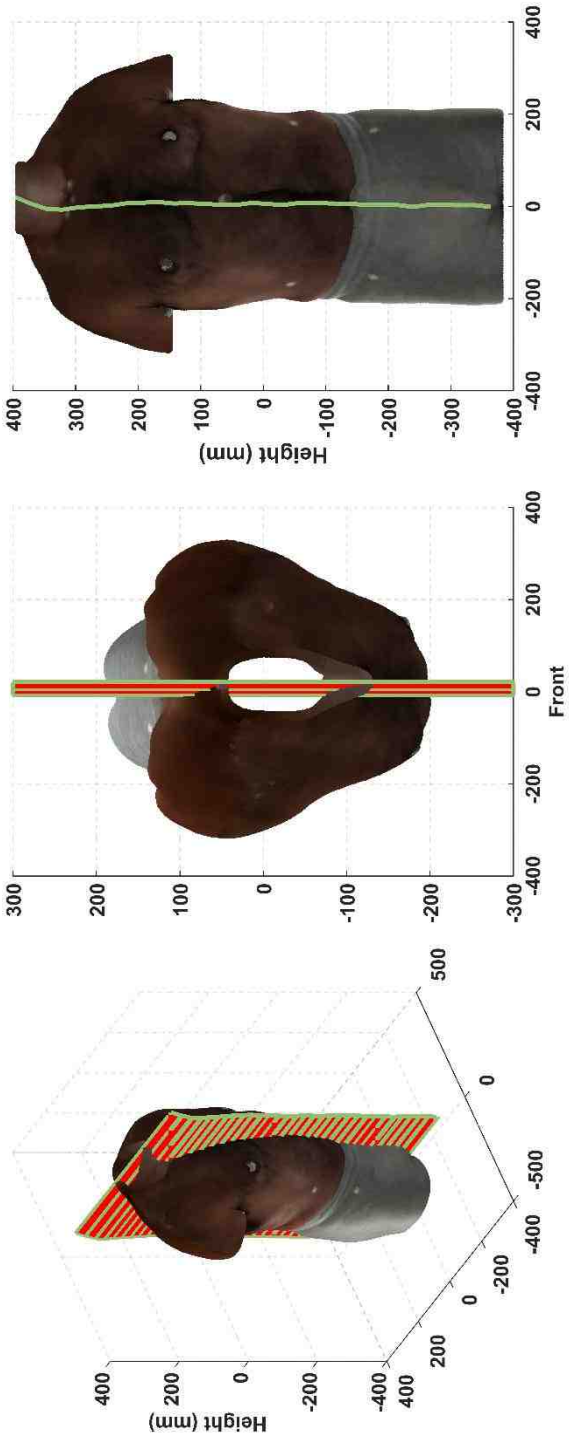


|                     |      |                               |      |                     |      |
|---------------------|------|-------------------------------|------|---------------------|------|
| Asymmetry Index (%) | 7.27 | Over all Torso Twist (degree) | 5.49 | Torso Tilt (degree) | 0.95 |
|---------------------|------|-------------------------------|------|---------------------|------|

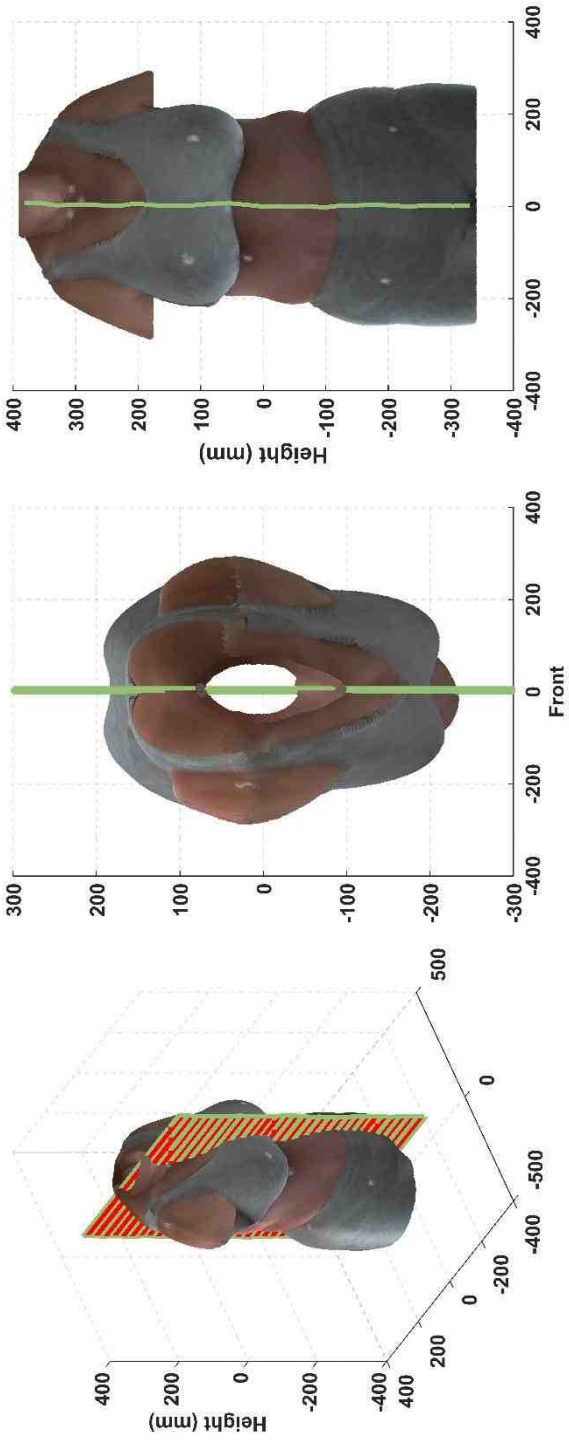


|                     |       |                               |      |                     |       |
|---------------------|-------|-------------------------------|------|---------------------|-------|
| Asymmetry Index (%) | 24.92 | Over all Torso Twist (degree) | 9.70 | Torso Tilt (degree) | 10.46 |
|---------------------|-------|-------------------------------|------|---------------------|-------|

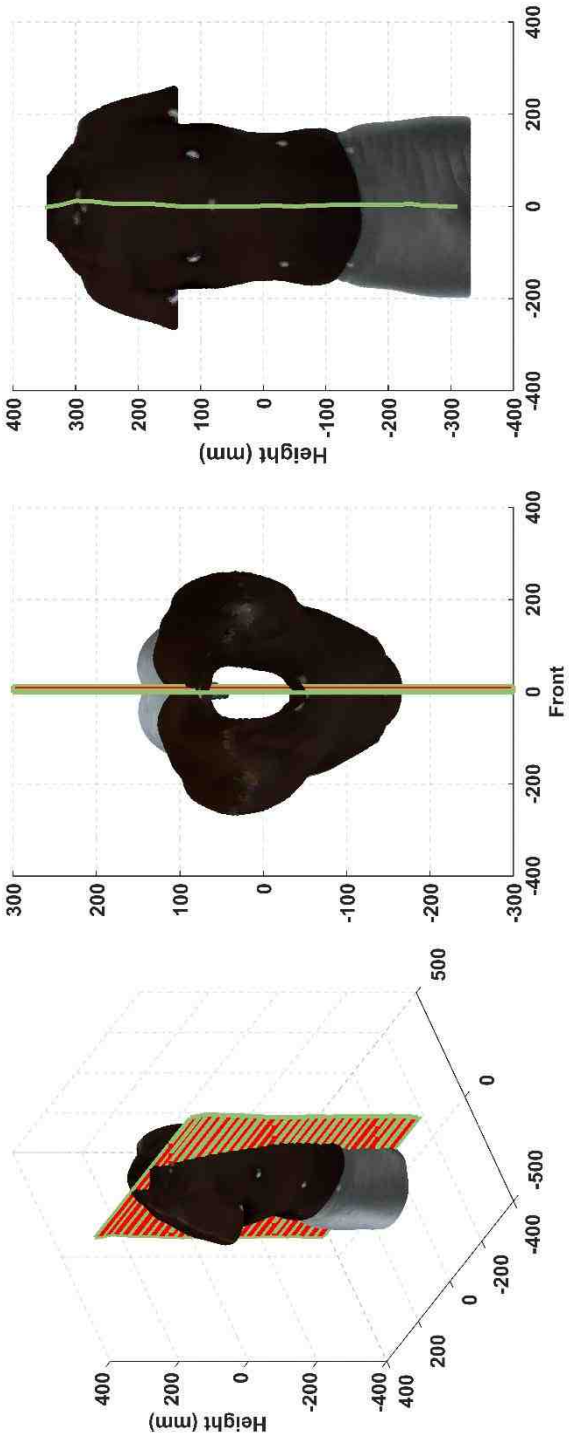




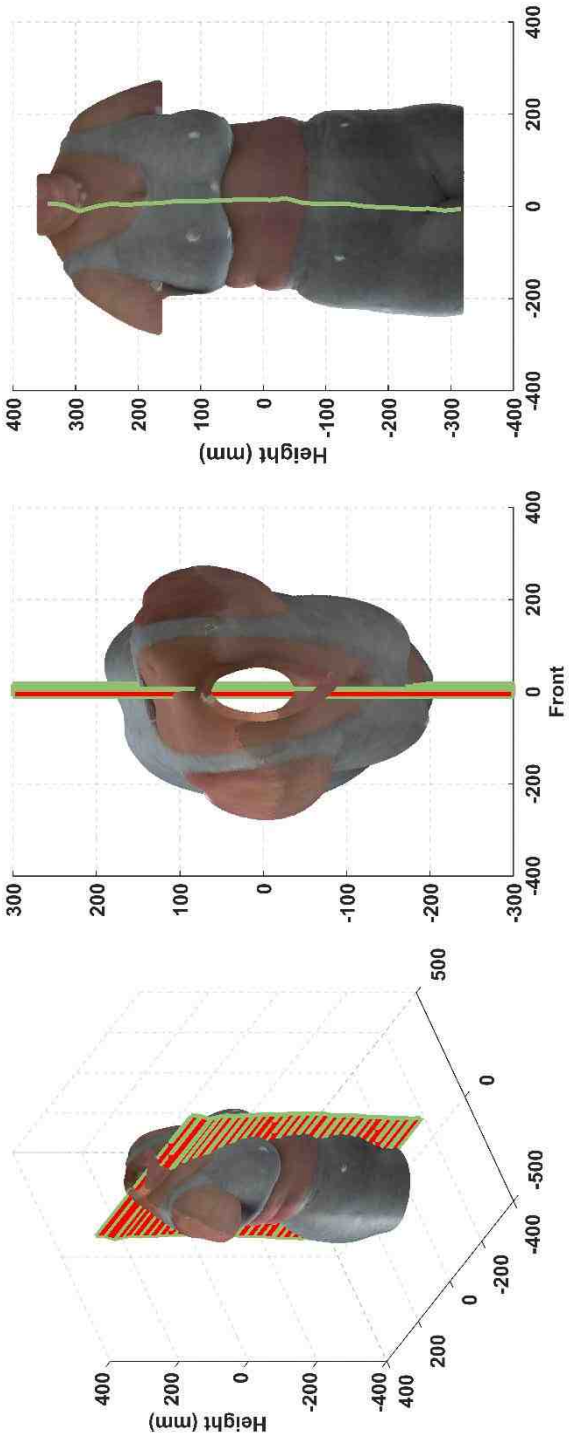
|                     |      |                               |      |                     |      |
|---------------------|------|-------------------------------|------|---------------------|------|
| Asymmetry Index (%) | 6.75 | Over all Torso Twist (degree) | 3.31 | Torso Tilt (degree) | 9.09 |
|---------------------|------|-------------------------------|------|---------------------|------|



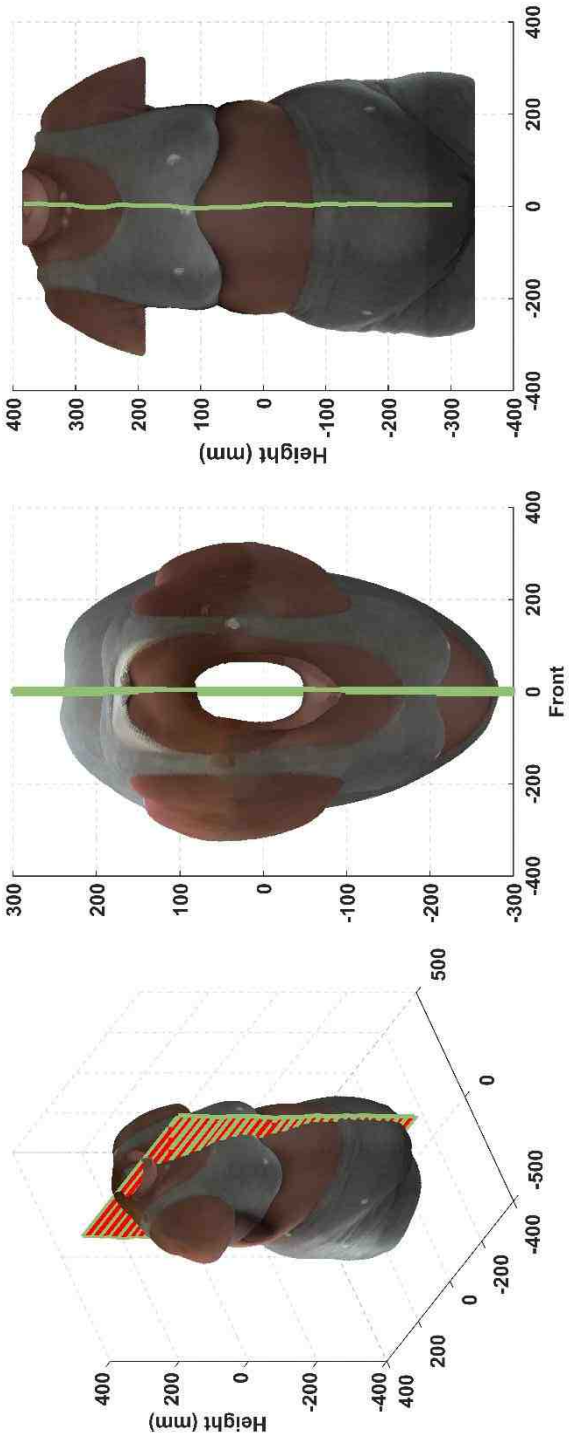
|                     |      |                               |      |                     |      |
|---------------------|------|-------------------------------|------|---------------------|------|
| Asymmetry Index (%) | 5.00 | Over all Torso Twist (degree) | 0.70 | Torso Tilt (degree) | 0.58 |
|---------------------|------|-------------------------------|------|---------------------|------|



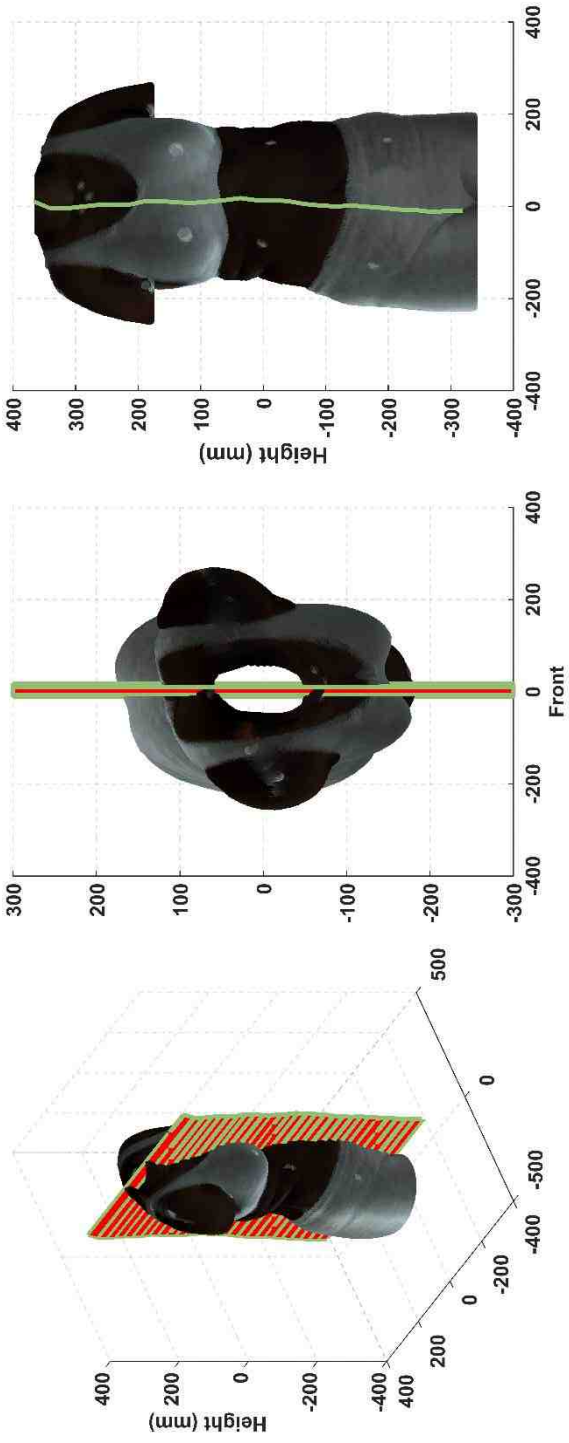
|                     |      |                               |      |                     |      |
|---------------------|------|-------------------------------|------|---------------------|------|
| Asymmetry Index (%) | 5.74 | Over all Torso Twist (degree) | 3.67 | Torso Tilt (degree) | 1.98 |
|---------------------|------|-------------------------------|------|---------------------|------|



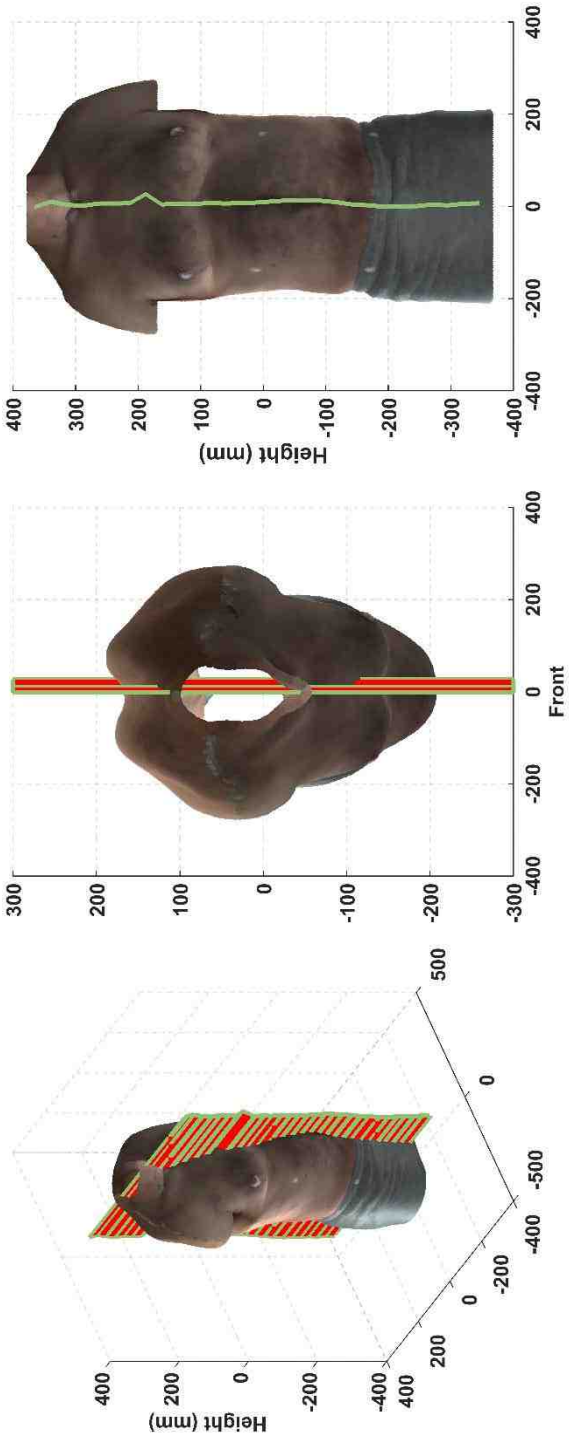
|                     |      |                               |      |                     |      |
|---------------------|------|-------------------------------|------|---------------------|------|
| Asymmetry Index (%) | 6.34 | Over all Torso Twist (degree) | 0.66 | Torso Tilt (degree) | 1.84 |
|---------------------|------|-------------------------------|------|---------------------|------|



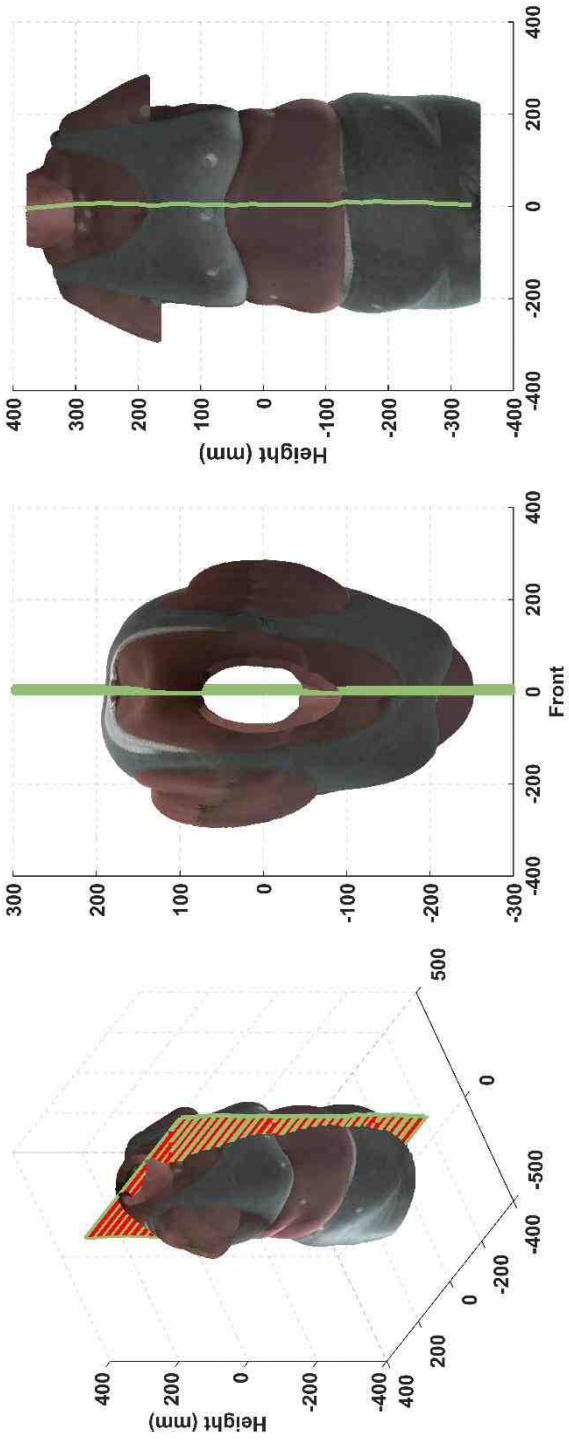
|                     |      |                               |      |                     |      |
|---------------------|------|-------------------------------|------|---------------------|------|
| Asymmetry Index (%) | 4.87 | Over all Torso Twist (degree) | 0.75 | Torso Tilt (degree) | 1.66 |
|---------------------|------|-------------------------------|------|---------------------|------|



|                     |      |                               |      |                     |      |
|---------------------|------|-------------------------------|------|---------------------|------|
| Asymmetry Index (%) | 7.89 | Over all Torso Twist (degree) | 3.82 | Torso Tilt (degree) | 0.26 |
|---------------------|------|-------------------------------|------|---------------------|------|



|                     |      |                               |      |                     |      |
|---------------------|------|-------------------------------|------|---------------------|------|
| Asymmetry Index (%) | 7.42 | Over all Torso Twist (degree) | 4.12 | Torso Tilt (degree) | 2.19 |
|                     |      |                               |      |                     |      |



|                     |      |                               |      |                     |      |
|---------------------|------|-------------------------------|------|---------------------|------|
| Asymmetry Index (%) | 5.22 | Over all Torso Twist (degree) | 4.66 | Torso Tilt (degree) | 1.22 |
|---------------------|------|-------------------------------|------|---------------------|------|



## Appendix D

### IRB Approval

#### Oklahoma State University Institutional Review Board

Date: Thursday, March 17, 2016  
IRB Application No: HE1614  
Proposal Title: Estimating symmetry/asymmetry in the human torso: A novel computational method  
Reviewed and Processed as: Exempt

Status Recommended by Reviewer(s): Approved Protocol Expires: 3/16/2019

Principal Investigator(s):

Mahendran Balasubramanian Kathleen Robinette  
433 HS  
Stillwater, OK 74078 Stillwater, OK 74078

---

The IRB application referenced above has been approved. It is the judgment of the reviewers that the rights and welfare of individuals who may be asked to participate in this study will be respected, and that the research will be conducted in a manner consistent with the IRB requirements as outlined in section 45 CFR 46.

- The final versions of any printed recruitment, consent and assent documents bearing the IRB approval stamp are attached to this letter. These are the versions that must be used during the study.

As Principal Investigator, it is your responsibility to do the following:

1. Conduct this study exactly as it has been approved. Any modifications to the research protocol must be submitted with the appropriate signatures for IRB approval. Protocol modifications requiring approval may include changes to the title, PI advisor, funding status or sponsor, subject population composition or size, recruitment, inclusion/exclusion criteria, research site, research procedures and consent/assent process or forms.
2. Submit a request for continuation if the study extends beyond the approval period. This continuation must receive IRB review and approval before the research can continue.
3. Report any adverse events to the IRB Chair promptly. Adverse events are those which are unanticipated and impact the subjects during the course of the research, and
4. Notify the IRB office in writing when your research project is complete.

Please note that approved protocols are subject to monitoring by the IRB and that the IRB office has the authority to inspect research records associated with this protocol at any time. If you have questions about the IRB procedures or need any assistance from the Board, please contact Dawnell Watkins 219 Scott Hall (phone: 405-744-5700, dawnell.watkins@okstate.edu).

Sincerely,



Hugh Crethar, Chair  
Institutional Review Board

VITA

MAHENDRAN BALASUBRAMANIAN

Candidate for the Degree of

Doctor of Philosophy

Thesis: ESTIMATING SYMMETRY/ASYMMETRY IN THE HUMAN TORSO:  
A NOVEL COMPUTATIONAL METHOD

Major Field: Human Sciences

Biographical:

Education:

Completed the requirements for the Doctor of Philosophy in Human Sciences at Oklahoma State University, Stillwater, Oklahoma in July, 2016.

Completed the requirements for the Master of Science in Apparel Design at Auburn University, Auburn, Alabama in 2009.

Completed the requirements for the Bachelor of Technology in Fashion Technology at Anna University, India in 2007.

Experience:

Graduate Research Associate, Oklahoma State University, 2012-2016

Graduate Teaching Associate, Oklahoma State University, 2013-2015

Professional Memberships: AATCC, ASTM International, Phi Kappa Phi